

การสังเคราะห์และวิเคราะห์ลักษณะอนุภาคไทเทเนียมทรงกลมกลางด้วยเทคนิคการพ่น



นาย เอกสิทธิ์ นามแก้ว

สถาบันวิทยบริการ

จุฬาลงกรณ์มหาวิทยาลัย
วิทยานิพนธ์นี้เป็นส่วนหนึ่งของการศึกษาตามหลักสูตรปริญญาวิศวกรรมศาสตรมหาบัณฑิต

สาขาวิชาวิศวกรรมเคมี ภาควิชาวิศวกรรมเคมี
คณะวิศวกรรมศาสตร์ จุฬาลงกรณ์มหาวิทยาลัย

ปีการศึกษา 2551

ลิขสิทธิ์ของจุฬาลงกรณ์มหาวิทยาลัย

SYNTHESIS AND CHARACTERIZATION OF TiO₂ HOLLOW SPHERES USING
SPRAYING TECHNIQUE




Mr. Eakasit Namkaeo

สถาบันวิทยบริการ
จุฬาลงกรณ์มหาวิทยาลัย

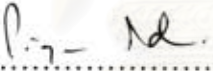
A Thesis Submitted in Partial Fulfillment of the Requirements
for the Degree of Master of Engineering Program in Chemical Engineering
Department of Chemical Engineering
Faculty of Engineering
Chulalongkorn University
Academic Year 2008
Copyright of Chulalongkorn University


Thesis Title SYNTHESIS AND CHARACTERIZATION OF TiO₂ HOLLOW
 SPHERES USING SPRAYING TECHNIQUE
By Mr. Eakasit Namkaeo
Field of Study Chemical Engineering
Advisor Akawat Sirisuk, Ph.D.

Accepted by the Faculty of Engineering, Chulalongkorn University in Partial
Fulfillment of the Requirements for the Master's Degree



.....Dean of the Faculty of Engineering
(Associate Professor Boonsom Lerdhirunwong, Dr.Ing.)

THESIS COMMITTEE


.....Chairman
(Professor Piyasarn Praserttham, Dr.Ing.)


..... Advisor
(Akawat Sirisuk, Ph.D.)


..... Examiner
(Associate Professor Tawatchai Charinpanitkul, Ph.D.)


.....External Examiner
(Soipatta Soisuwan, D.Eng.)

เอกสิทธิ์ นามแก้ว: การสังเคราะห์และวิเคราะห์ลักษณะอนุภาคไทเทเนียมทรงกลมกลวงด้วยเทคนิคการพ่น. (SYNTHESIS AND CHARACTERIZATION OF TiO₂ HOLLOW SPHERES USING SPRAYING TECHNIQUE) อ. ที่ปริกษาวิทยานิพนธ์หลัก: อ.ดร. อัครวัต ศิริสุข, 98 หน้า.

การสังเคราะห์อนุภาคไทเทเนียมทรงกลมกลวง จากสารละลายไทเทเนียมซัลเฟตด้วยวิธีการพ่น โดยนำสารละลายไทเทเนียมซัลเฟตพ่นลงบนสารละลายของสารลดแรงตึงผิวของ tween 20, polyethylene glycol และ sodium dodecyl sulfate ที่อุณหภูมิห้อง โดยศึกษาอิทธิพลของค่าเฉลี่ยของขนาดอนุภาคไทเทเนียมทรงกลมกลวง คือ อัตราการไหลของสารละลายไทเทเนียมซัลเฟต ความเข้มข้นของสารลดแรงตึงผิว ระยะทางระหว่างหัวพ่นกับผิวของของเหลวและชนิดของสารลดแรงตึงผิว วิเคราะห์เฟสของอนุภาคทรงกลมกลวงด้วย X-Ray diffractometry เพื่อพิสูจน์ว่าอนุภาคไทเทเนียมทรงกลมกลวงที่สังเคราะห์ได้อยู่ในเฟสของอนาเทส และศึกษารูปร่างและขนาดของอนุภาคไทเทเนียมทรงกลมกลวงด้วย กล้องจุลทรรศน์อิเล็กตรอนแบบส่องกราด และกล้องจุลทรรศน์อิเล็กตรอนแบบส่องผ่าน จากผลการทดลองพบว่าค่าเฉลี่ยของขนาดอนุภาคไทเทเนียมทรงกลมกลวงมีขนาดลดลงเมื่อเพิ่มอัตราการไหลของสารละลายไทเทเนียมซัลเฟต ความเข้มข้นของสารลดแรงตึงผิวและระยะทางระหว่างหัวพ่นกับผิวของของเหลว โดยค่าเฉลี่ยของขนาดอนุภาคไทเทเนียมทรงกลมกลวงที่สังเคราะห์ได้มีขนาดประมาณ 100-170 nm

สถาบันวิทยบริการ จุฬาลงกรณ์มหาวิทยาลัย

ภาควิชา...วิศวกรรมเคมี.....

ลายมือชื่อนิสิต.....  ทนแก้ว.....

สาขาวิชา...วิศวกรรมเคมี.....

ลายมือชื่ออ.ที่ปริกษาวิทยานิพนธ์หลัก..... 

ปีการศึกษา.... 2551.....

5070530121: MAJOR CHEMICAL ENGINEERING

KEYWORDS: TITANIA / HOLLOW SPHERES / SPRAYING TECHNIQUE / SURFACTANT

EAKASIT NAMKAE0: SYNTHESIS AND CHARACTERIZATION OF TiO₂ HOLLOW SPHERES USING SPRAYING TECHNIQUE. ADVISOR: AKAWAT SIRISUK, Ph.D., 98 pp.

The synthesis of titania hollow spheres from titanium sulfate solution was carried out by a spraying technique. Titanium sulfate solution was sprayed into an aqueous solution of a surfactant (tween 20, polyethylene glycol and sodium dodecyl sulfate), which acted under atmospheric condition. Effects of various preparation parameters, namely, flow rate of precursor, concentration of surfactant, the distance from the nozzle to the surfactant solution, and type of surfactant on the products were investigated. X-ray diffractometry confirmed that the products were anatase TiO₂. The size and morphology of the products were studied using laser diffraction technique, scanning electron microscopy, and transmission electron microscopy. The average particle sizes of TiO₂ decreased when the flow rate of titanium sulfate solution, concentration of surfactant and the distances from the nozzle to the surfactant solution increased. The average particle size of the synthesis TiO₂ hollow spheres was in the range of 100-170 nm.

สถาบันวิทยบริการ
จุฬาลงกรณ์มหาวิทยาลัย

Department :...Chemical Engineering.....

Field of Study :...Chemical Engineering...

Academic Year :.....2008.....

Student's Signature : *Eakasit Namkaeo*

Advisor's Signature : *Art Sirisuk*

ACKNOWLEDGEMENTS

This thesis would not have been possible to complete without the support of the following individuals. Firstly, I would like to express my greatest gratitude to my advisor, Dr. Akawat Sirisuk for his invaluable guidance during the course of this work. And I am also very grateful to Professor Dr. Piyasan Praserttham, for his kind supervision over this thesis as the chairman, Associate Professor Tawatchai Charinpanitkul, and Soipatta Soisuwan, members of the thesis committee for their kind cooperation.

The financial supported from the Graduate School of Chulalongkorn University are also gratefully acknowledged.

Many thanks for kind suggestions and useful help from Mr. Kongkiat Suriye and several friends at Center of Excellence in Catalysis and Catalytic Reaction Engineering who always provide the encouragement and assistance along the way.

Finally, I also would like to dedicate this thesis to my parents, my aunt, and my sister, who have always been the source of my support and encouragement.

สถาบันวิทยบริการ
จุฬาลงกรณ์มหาวิทยาลัย

CONTENTS

| | Page |
|---|-------------|
| ABSTRACT (THAI)..... | iv |
| ABSTRACT (ENGLISH)..... | v |
| ACKNOWLEDGEMENTS..... | vi |
| CONTENTS..... | vii |
| LIST OF TABLES..... | x |
| LIST OF FIGURES..... | xi |
| CHAPTER | |
| I INTRODUCTION..... | 1 |
| II BACKGROUND INFORMATION..... | 3 |
| 2.1 Information on titanium dioxide..... | 3 |
| 2.1.1 Physical and Chemical Properties of titanium dioxide..... | 3 |
| 2.1.2 Application of titanium dioxide..... | 6 |
| 2.2 Surfactant..... | 7 |
| 2.2.1 Anionic surfactant..... | 8 |
| 2.2.2 Cationic surfactants..... | 11 |
| 2.2.3 Nonionic surfactants..... | 13 |
| 2.2.4 Amphoteric surfactant..... | 16 |
| 2.3 Viscosity..... | 16 |
| 2.4 Preparation methods for hollow particles..... | 18 |
| 2.4.1 Spray method..... | 18 |
| 2.4.2 Sol-gel method..... | 19 |
| 2.4.3 Surfactant-assisted method..... | 20 |
| 2.4.4 Bubble-template method..... | 21 |
| 2.4.5 Hydrothermal method..... | 21 |
| 2.5 Effect of surfactant concentration on particle size..... | 23 |
| III MATERIALS AND EXPERIMENTS..... | 24 |
| 3.1. Chemical..... | 24 |
| 3.2 Assembly of spray apparatus..... | 24 |

| | Page |
|--|-------------|
| 3.3 Preparation of titanium dioxide hollow spheres..... | 25 |
| 3.3.1 Influence of spraying flow rate of titanium sulfate solution..... | 26 |
| 3.3.2 Influence of concentration of surfactant solution..... | 26 |
| 3.3.3 Influence of distance from nozzle to liquid surfactant..... | 26 |
| 3.3.4 Influence of types of surfactant..... | 27 |
| 3.4 Characterization of titanium dioxide hollow spheres..... | 27 |
| 3.4.1 Viscometer..... | 28 |
| 3.4.2 Laser Diffraction Technique..... | 28 |
| 3.4.3 X-ray diffractometry (XRD)..... | 28 |
| 3.4.4 Scanning Electron Microscope (SEM)..... | 29 |
| 3.4.5 Transmission Electron Microscope (TEM)..... | 29 |
| 3.4.6 Average particle size..... | 29 |
| 3.4.7 Standard deviation..... | 29 |
| 3.4.8 Program MINITAB..... | 30 |
| IV RESULTS AND DISCUSSION..... | 31 |
| 4.1 The prepared of surfactants solution..... | 31 |
| 4.2 The viscosity of surfactants solution..... | 32 |
| 4.3 The Laser Diffraction Technique..... | 34 |
| 4.4 The surfactant solution as Tween 20..... | 38 |
| 4.4.1 Phase structures..... | 38 |
| 4.4.1.1 X-ray diffractometer (XRD)..... | 38 |
| 4.4.2 Morphology of TiO ₂ hollow spheres..... | 40 |
| 4.4.2.1 Scanning Electron Microscopy (SEM)..... | 40 |
| 4.4.2.2 Transmission Electron Microscopy (TEM)..... | 43 |
| 4.4.3 Average particles size of TiO ₂ hollow spheres..... | 45 |
| 4.4.4 Influence of spraying flow rate of titanium sulfate solution..... | 46 |
| 4.4.5 Influence of concentration of surfactant solution..... | 48 |
| 4.4.6 Influence of distance from nozzle to liquid surfactant..... | 49 |

| | Page |
|--|-------------|
| 4.5 The surfactant solution as polyethylene glycol..... | 51 |
| 4.5.1 Phase structures..... | 51 |
| 4.5.1.1 X-ray diffractometer (XRD)..... | 51 |
| 4.5.2 Morphology of TiO ₂ hollow spheres..... | 53 |
| 4.5.2.1 Scanning Electron Microscopy (SEM)..... | 53 |
| 4.5.2.2 Transmission Electron Microscopy (TEM)..... | 55 |
| 4.5.3 Average particles size of TiO ₂ hollow spheres..... | 58 |
| 4.5.4 Influence of spraying flow rate of titanium sulfate solution..... | 58 |
| 4.5.5 Influence of concentration of surfactant solution..... | 60 |
| 4.5.6 Influence of distance from nozzle to liquid surfactant... | 62 |
| 4.6 The surfactant solution as sodium dodecyl sulfate..... | 63 |
| 4.6.1 Phase structures..... | 63 |
| 4.6.1.1 X-ray diffractometer (XRD)..... | 63 |
| 4.6.2 Morphology of TiO ₂ hollow spheres..... | 65 |
| 4.6.2.1 Scanning Electron Microscopy (SEM)..... | 65 |
| 4.6.2.2 Transmission Electron Microscopy (TEM)..... | 68 |
| 4.6.3 Average particles size of TiO ₂ hollow spheres..... | 70 |
| 4.6.4 Influence of spraying flow rate of titanium sulfate solution..... | 71 |
| 4.6.5 Influence of concentration of surfactant solution..... | 73 |
| 4.6.6 Influence of distance from nozzle to liquid surfactant..... | 74 |
| 4.7 The analysis from program Minitab..... | 76 |
| 4.8 Influence of spraying flow rate titanium sulfate solution..... | 80 |
| 4.9 Influence of concentration of surfactant solution..... | 81 |
| 4.10 Influence of distance from nozzle to liquid surfactant..... | 81 |
| 4.11 Influence of types of surfactant..... | 81 |
| V CONCLUSIONS AND RECOMMENDATIONS..... | 82 |
| 5.1 Conclusions..... | 82 |
| 5.2 Recommendations for future studies..... | 83 |

| | |
|-----------------|----|
| REFERENCES..... | 84 |
| APPENDICE..... | 87 |
| VITA..... | 98 |



สถาบันวิทยบริการ
จุฬาลงกรณ์มหาวิทยาลัย

LIST OF TABLES

| Table | Page |
|--|-------------|
| 2.1 Comparison of rutile, brookite and anatase..... | 4 |
| 4.1 The critical micelle concentration of the surfactant..... | 32 |
| 4.2 Crystallite size of TiO ₂ hollow spheres using Tween 20 as a surfactant | 40 |
| 4.3 Average particles size of TiO ₂ hollow spheres using Tween 20 as a surfactant..... | 46 |
| 4.4 Crystallite size of TiO ₂ hollow spheres using polyethylene glycol as a surfactant..... | 52 |
| 4.5 Average particles size of TiO ₂ hollow spheres using polyethylene glycol as a surfactant..... | 58 |
| 4.6 Crystallite size of TiO ₂ hollow spheres using sodium dodecyl sulfate as a surfactant..... | 65 |
| 4.7 Average particles size of TiO ₂ hollow spheres using sodium dodecyl sulfate as a surfactant..... | 71 |
| 4.8 The 2 ⁴ full factorial designs of experiments..... | 76 |
| 4.9 The 2 ⁴ full factorial designs of experiments on the average particle sizes of TiO ₂ hollow spheres of two surfactants were sodium dodecyl sulfate and tween 20..... | 77 |
| 4.10 The 2 ⁴ full factorial designs of experiments on the average particle sizes of TiO ₂ hollow spheres of two surfactants were sodium dodecyl sulfate and polyethylene glycol..... | 79 |
| B.1 Particle sizes distribution of titanium dioxide..... | 91 |

LIST OF FIGURES

| Figure | Page |
|---|------|
| 2.1 Crystal structure of anatase (left-hand) and rutile (right-hand) TiO_2 | 5 |
| 2.2 The surfactant can exist as different phases depending upon the concentration of the sample..... | 8 |
| 2.3 Some common soaps: sodium oleate, sodium palmitate, sodium myristate and sodium stearate..... | 9 |
| 2.4 Sodium dodecyl sulfate, one of the most common of the alkyl sulfate style of anionic surfactant..... | 9 |
| 2.5 Two alkyl phosphates, an alkyl sulfonate, and an alkyl benzene sulfonate sulfosuccinates..... | 10 |
| 2.6 The sulfosuccinate surfactant sodium di(2-ethylhexyl) sulfosuccinate (sold under the name Aerosol-OT or AOT)..... | 10 |
| 2.7 Fatty amine salts were the first style of cationic surfactant synthesised..... | 11 |
| 2.8 An alcohol ethoxylate and an alkylphenol ethoxylate. The poly(ethylene oxide) chain forms the water soluble surfactant "head"..... | 14 |
| 2.9 Examples of alkyl polyglycosides: an alkyl glucoside and a glucose ester... | 15 |
| 2.10 "Tween 85" (sorbitan trioleate poly(ethylene oxide)) is one of the sorbitan ester surfactants..... | 15 |
| 3.1 Schematic diagram of spray technique..... | 25 |
| 4.1 Viscosity of surfactant solution at concentration 0.2 % and 2% (V/V) Tween 20..... | 33 |
| 4.2 Viscosity of surfactant solution at concentration 0.2 % and 2% (V/V) Polyethylene glycol..... | 33 |
| 4.3 Viscosity of surfactant solution at concentration 0.2 % and 2% (V/V) Sodium dodecyl sulfate by vary shear rate..... | 34 |
| 4.4 The laser diffraction technique in measurements size droplets of sprayed exist nozzle. The flow rates and the nozzle-solution distance were fixed at 3 L/h and at 10 cm respectively..... | 35 |

| Figure | Page |
|---|-------------|
| 4.5 The laser diffraction technique in measurements size droplets of sprayed exist nozzle. The flow rates and the nozzle-solution distance were fixed at 5 L/h and at 10 cm respectively..... | 36 |
| 4.6 The laser diffraction technique in measurements size droplets of sprayed exist nozzle. The flow rates and the nozzle-solution distance were fixed at 3 L/h and at 30 cm respectively..... | 37 |
| 4.7 The laser diffraction technique in measurements size droplets of sprayed exist nozzle. The flow rates and the nozzle-solution distance were fixed at 5 L/h and at 30 cm respectively..... | 38 |
| 4.8 XRD patterns of TiO ₂ hollow spheres using Tween 20 as a surfactant..... | 39 |
| 4.9 SEM image of TiO ₂ hollow spheres using Tween 20 as the surfactant with 10000 magnifications..... | 41 |
| 4.10 SEM image of TiO ₂ hollow spheres using Tween 20 as the surfactant with 10000 magnifications..... | 41 |
| 4.11 SEM image of TiO ₂ hollow spheres using Tween 20 as the surfactant with 30000 magnifications..... | 42 |
| 4.12 SEM image of TiO ₂ hollow spheres using Tween 20 as the surfactant with 30000 magnifications..... | 42 |
| 4.13 TEM image of TiO ₂ hollow spheres using Tween 20 as the surfactant at scale bar 200 nm..... | 43 |
| 4.14 TEM image of TiO ₂ hollow spheres using Tween 20 as the surfactant at scale bar 0.5 μm..... | 44 |
| 4.15 TEM image of TiO ₂ hollow spheres using Tween 20 as the surfactant at scale bar 200 nm..... | 44 |
| 4.16 TEM image of TiO ₂ hollow spheres using Tween 20 as the surfactant at scale bar 50 nm..... | 45 |

| Figure | Page |
|---|-------------|
| 4.17 The average particle sizes of TiO ₂ hollow spheres prepared by spraying titanium sulfate solution the flow rates were varied at F 3 and 5 L/h and fixed concentration C 0.2% and 2% (v/v) of nozzle-solution distance L 10 cm | 47 |
| 4.18 The average particle sizes of TiO ₂ hollow spheres prepared by spraying titanium sulfate solution the flow rates were varied at F 3 and 5 L/h and fixed concentration C 0.2% and 2% (v/v) of nozzle-solution distance L 30 cm..... | 47 |
| 4.19 The averages particle sizes of TiO ₂ hollow spheres by varied concentration C 0.2% and 2% (v/v) and fixed flow rate F 3 and 5 L/h of nozzle-solution distances L 10 cm..... | 48 |
| 4.20 The averages particle sizes of TiO ₂ hollow spheres by varied concentration C 0.2% and 2% (v/v) and fixed flow rate F 3 and 5 L/h of nozzle-solution distances L 30 cm..... | 49 |
| 4.21 The averages particle sizes of TiO ₂ hollow spheres by the nozzle-solution distances varied at L 10 and 30 cm and fixed concentration C 0.2% and 2% (v/v) and flow rate F 3 L/h..... | 50 |
| 4.22 The averages particle sizes of TiO ₂ hollow spheres by the nozzle-solution distances varied at L 10 and 30 cm and fixed concentration C 0.2% and 2% (v/v) and flow rate F 5 L/h..... | 50 |
| 4.23 XRD patterns of TiO ₂ hollow spheres using polyethylene glycol as a surfactant..... | 52 |
| 4.24 SEM image of TiO ₂ hollow spheres using polyethylene glycol as the surfactant with 10000 magnifications..... | 53 |
| 4.25 SEM image of TiO ₂ hollow spheres using polyethylene glycol as the surfactant with 10000 magnifications..... | 54 |
| 4.26 SEM image of TiO ₂ hollow spheres using polyethylene glycol as the surfactant with 30000 magnifications..... | 54 |

| Figure | Page |
|--|-------------|
| 4.27 SEM image of TiO ₂ hollow spheres using polyethylene glycol as the surfactant with 30000 magnifications..... | 55 |
| 4.28 TEM image of TiO ₂ hollow spheres using polyethylene glycol as the surfactant at scale bar 0.5 μm..... | 56 |
| 4.29 TEM image of TiO ₂ hollow spheres using polyethylene glycol as the surfactant at scale bar 50 nm..... | 56 |
| 4.30 TEM image of TiO ₂ hollow spheres using polyethylene glycol as the surfactant at scale bar 100 nm..... | 57 |
| 4.31 TEM image of TiO ₂ hollow spheres using polyethylene glycol as the surfactant at scale bar 100 nm..... | 57 |
| 4.32 The average particle sizes of TiO ₂ hollow spheres prepared by spraying titanium sulfate solution the flow rates were varied at F 3 and 5 L/h and fixed concentration C 0.2% and 2% (v/v) of nozzle-solution distance L 10 cm..... | 59 |
| 4.33 The average particle sizes of TiO ₂ hollow spheres prepared by spraying titanium sulfate solution the flow rates were varied at F 3 and 5 L/h and fixed concentration C 0.2% and 2% (v/v) of nozzle-solution distance L 30 cm..... | 60 |
| 4.34 The averages particle sizes of TiO ₂ hollow spheres by varied concentration C 0.2% and 2% (v/v) and fixed flow rate F 3 and 5 L/h of nozzle-solution distances L 10 cm..... | 61 |
| 4.35 The averages particle sizes of TiO ₂ hollow spheres by varied concentration C 0.2% and 2% (v/v) and fixed flow rate F 3 and 5 L/h of nozzle-solution distances L 30 cm..... | 61 |
| 4.36 The averages particle sizes of TiO ₂ hollow spheres by the nozzle-solution distances varied at L 10 and 30 cm and fixed concentration C 0.2% and 2% (v/v) and flow rate F 3 L/h..... | 62 |

| Figure | Page |
|--|-------------|
| 4.37 The averages particle sizes of TiO ₂ hollow spheres by the nozzle-solution distances varied at L 10 and 30 cm and fixed concentration C 0.2% and 2% (v/v) and flow rate F 5 L/h..... | 63 |
| 4.38 XRD patterns of TiO ₂ hollow spheres using sodium dodecyl sulfate as a surfactant..... | 64 |
| 4.39 SEM image of TiO ₂ hollow spheres using sodium dodecyl sulfate as the surfactant with 10000 magnifications..... | 66 |
| 4.40 SEM image of TiO ₂ hollow spheres using sodium dodecyl sulfate as the surfactant with 10000 magnifications..... | 66 |
| 4.41 SEM image of TiO ₂ hollow spheres using sodium dodecyl sulfate as the surfactant with 30000 magnifications..... | 67 |
| 4.42 SEM image of TiO ₂ hollow spheres using sodium dodecyl sulfate as the surfactant with 30000 magnifications..... | 67 |
| 4.43 TEM image of TiO ₂ hollow spheres using polyethylene glycol as the surfactant at scale bar 50 nm..... | 68 |
| 4.44 TEM image of TiO ₂ hollow spheres using polyethylene glycol as the surfactant at scale bar 100 nm..... | 69 |
| 4.45 TEM image of TiO ₂ hollow spheres using polyethylene glycol as the surfactant at scale bar 200 nm..... | 69 |
| 4.46 TEM image of TiO ₂ hollow spheres using polyethylene glycol as the surfactant at scale bar 100 nm..... | 70 |
| 4.47 The average particle sizes of TiO ₂ hollow spheres prepared by spraying titanium sulfate solution the flow rates were varied at F 3 and 5 L/h and fixed concentration C 0.2% and 2% (v/v) of nozzle-solution distance L 10 cm..... | 72 |

| Figure | Page |
|--|-------------|
| 4.48 The average particle sizes of TiO ₂ hollow spheres prepared by spraying titanium sulfate solution the flow rates were varied at F 3 and 5 L/h and fixed concentration C 0.2% and 2% (v/v) of nozzle-solution distance L 30 cm..... | 72 |
| 4.49 The averages particle sizes of TiO ₂ hollow spheres by varied concentration C 0.2% and 2% (v/v) and fixed flow rate F 3 and 5 L/h of nozzle-solution distances L 10 cm..... | 73 |
| 4.50 The averages particle sizes of TiO ₂ hollow spheres by varied concentration C 0.2% and 2% (v/v) and fixed flow rate F 3 and 5 L/h of nozzle-solution distances L 30 cm..... | 74 |
| 4.51 The averages particle sizes of TiO ₂ hollow spheres by the nozzle-solution distances varied at L 10 and 30 cm and fixed concentration C 0.2% and 2% (v/v) and flow rate F 3 L/h..... | 75 |
| 4.52 The averages particle sizes of TiO ₂ hollow spheres by the nozzle-solution distances varied at L 10 and 30 cm and fixed concentration C 0.2% and 2% (v/v) and flow rate F 5 L/h..... | 75 |
| 4.53 The effects on the average particle sizes of TiO ₂ hollow spheres of two surfactants were sodium dodecyl sulfate and tween 20..... | 78 |
| 4.54 The effects on the average particle sizes of TiO ₂ hollow spheres of two surfactants were sodium dodecyl sulfate and polyethylene glycol..... | 80 |
| A.1 The 101 diffraction peak of titania for calculation of the crystallite size..... | 89 |
| A.2 The plot indicating the value of line broadening due to the equipment. The data were obtained by using α -alumina as standard..... | 90 |

CHAPTER I

INTRODUCTION

Titanium dioxide (TiO_2) or titania has been used in many applications such as microcapsules for controlled release, catalyst supports and electric insulators. The traditional techniques for the preparation of inorganic hollow microstructures to nanostructures are spray drying, spray pyrolysis, and a sol-gel method in surfactant stabilized emulsions. Recently, the spray precipitation method for which a solid precursor solution is sprayed into another liquid phase containing a precipitation agent has been developed (Nagamine et al., 2006).

Hollow titania particle is one form of titania that has possible utilization in many applications including drug delivery because of its high surface area, good surface permeability, and greater light-harvesting capacity. Moreover, higher energy conversion efficiency and photocatalytic activity are expected using TiO_2 hollow structures as photocatalysts (Yu et al., 1998). Syoufian and coworkers (2007) showed that photocatalytic activity of commercially-available TiO_2 was lower than that of the hollow particles.

This thesis describes the design, Synthesis of titania hollow spheres by spraying technique. Hollow spheres of titania were obtained by spraying a solution of titanium precursor into a solution of surfactant and produce titania hollow spheres with uniform size.

The objectives of this research are as follow:

1. Synthesis titania hollow spheres by spraying technique.
2. To study effects of spraying conditions and surfactant on physical properties of titania hollow spheres.

The thesis is arranged as follows:

Chapter I is the introduction of this work.

Chapter II presents background information of the research.

Chapter III presents materials and methods of the research.

Chapter IV describes the experimental results and discussion of the research.

Chapter V the overall conclusions and recommendations for the future studies are given.

สถาบันวิทยบริการ
จุฬาลงกรณ์มหาวิทยาลัย

CHAPTER II

BACKGROUND INFORMATION

This chapter consists of four main sections. Section 2.1 discusses properties and applications of titanium dioxide. Types of surfactant are discussed in section 2.2. The viscosity in section 2.3. The presents the literature reviews performed prior to the beginning of experiment works in section 2.4. Effect of surfactant concentration on particle size in section 2.5.

2.1 Information on titanium dioxide.

2.1.1 Physical and Chemical Properties of titanium dioxide.

Titanium dioxide has three crystalline phases: anatase, rutile and brookite (Hoffmann et al., 1995; Linsebigler et al., 1995). Anatase phase is generally more chemically and optically active. Crystalline structures of titanium dioxide can be controlled by heat treatment (Kontos et al., 2005) and sometimes by addition of dopants (Calza et al., 1997; Mills and wang, 1997; Nam and Han, 2003). Comparison of typical physical properties of rutile, brookite and anatase is displayed in Table 2.1.

Although anatase and rutile are both tetragonal, they do not have the same crystal structures. Anatase exists in near-regular octahedral and rutile forms slender prismatic crystal. Rutile is the thermally stable form and is one of the two most important ores of titanium. The crystal structures of anatase and rutile are shown in Figure 2.1.

Brookite has been produced by heating amorphous titanium oxide, which is prepared from an alkyl titanate or sodium titanate, with sodium or potassium hydroxide in an autoclave at 200 to 600 °C for several days. The important commercial forms of

titanium oxide are anatase and rutile, and they can readily be distinguished by X-ray diffractometry.

Since both anatase and rutile are tetragonal structure, they are both anisotropic. Their physical properties, e.g. refractive index, vary according to the direction.

Table 2.1 Comparison of rutile, brookite and anatase.

| Properties | Anatase | Brookite | Rutile |
|----------------------------|--|--|--|
| Crystal structure | Tetragonal | Orthorhombic | Tetragonal |
| Optical | Uniaxial, negative | Biaxial, positive | Uniaxial, negative |
| Density, g/cm ³ | 3.84 | 4.0 | 4.26 |
| Hardness, Mohs scale | 5 ^{1/2} – 6 | 5 ^{1/2} – 6 | 7 – 7 ^{1/2} |
| Unit cell | D _{4h} ¹⁹ .4TiO ₂ | D _{2h} ¹⁵ .8TiO ₂ | D _{4h} ¹² .3TiO ₂ |
| Dimension, nm | | | |
| a | 0.3758 | 0.9166 | 0.4584 |
| b | - | 0.5436 | - |
| c | 0.9514 | 0.5135 | 2.953 |
| Refractive index | 2.490 | - | 2.903 |
| Permittivity | 31 | - | 114 |
| Melting point | changes to rutile at high temp | - | 1858°C |

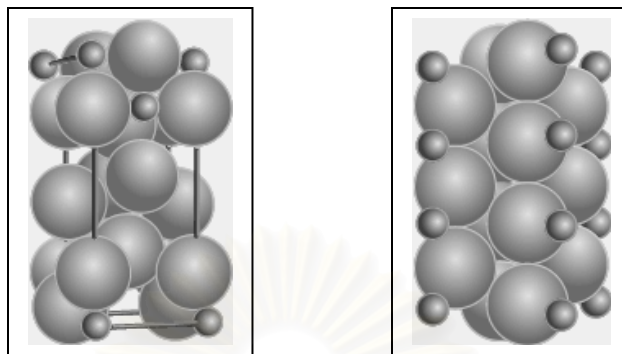


Figure 2.1 Crystal structure of anatase (left-hand) and rutile (right-hand) TiO_2

Measurement of physical properties, which the crystallographic directions are taken into account, may be made for both natural and synthetic rutile, natural anatase crystals, and natural brookite crystals. Measurement of the refractive index of titanium oxide must be made by using a crystal that is suitably orientated with respect to the crystallographic axis as a prism in a spectrometer. Crystals of suitable size of all three modifications occur naturally and have been studied. However, rutile is the only form that can be obtained in large artificial crystals from melts. The refractive index of rutile is 2.903. The dielectric constant of rutile varies with direction in the crystal and with any variation from the stoichiometric formula, TiO_2 ; an average value for rutile in powder form is 114. The dielectric constant of anatase powder is 48.

Titanium oxide is thermally stable (mp. $1855\text{ }^\circ\text{C}$) and very resistant to chemical attack. When it is heated strongly under vacuum, there is a slight loss of oxygen corresponding to a change in composition to $\text{TiO}_{1.97}$. The product is dark blue but reverts to the original white color when it is heated in air.

2.1.2 Application of titanium dioxide.

Titanium dioxide is one of the most basic materials in our daily life. Titanium dioxide has been widely used in a variety of paints, plastics, paper, inks, fibers, cosmetics, sunscreens, foodstuffs and drug delivery.

Cosmetics and food producers are “nano-sizing” some ingredients, claiming that improves their effectiveness. Sunscreens containing nanoscale titanium dioxide or zinc oxide are transparent and reflect ultraviolet (UV) light to prevent sunburns. Scratch- and glare-resistant coatings are being applied to eye glasses, windows, and car mirrors.

Drug delivery is the method or process of administering a pharmaceutical compound to achieve a therapeutic effect in humans or animals. Drug Delivery technologies are patent protected formulation technologies that modifies drug release profile, absorption, distribution and elimination for the benefit of improving product efficacy & safety and patient convenience & compliance. Most common methods of delivery include the preferred non-invasive peroral (through the mouth), topical (skin), transmucosal (nasal, buccal/sublingual, vaginal, ocular and rectal) and inhalation routes. Many medications such as peptide and protein, antibody, vaccine and gene based drugs, in general may not be delivered using these routes because they might be susceptible to enzymatic degradation or can not be absorbed into the systemic circulation efficiently due to molecular size and charge issues to be therapeutically effective.

Current efforts in the area of drug delivery include the development of targeted delivery in which the drug is only active in the target area of the body and sustained release formulations in which the drug is released over a period of time in a controlled manner from a formulation.

2.2 Surfactant

Surfactants are wetting agents that lower the surface tension of a liquid, allowing easier spreading, and lower the interfacial tension between two liquids.

Surfactants are usually organic compounds that are amphiphilic, meaning they contain both hydrophobic groups (their "tails") and hydrophilic groups (their "heads"). Therefore, they are soluble in both organic solvents and water. The term surfactant was coined by Antara Products in 1950.

Surfactants reduce the surface tension of water by adsorbing at the liquid-gas interface. They also reduce the interfacial tension between oil and water by adsorbing at the liquid-liquid interface. Many surfactants can also assemble in the bulk solution into aggregates. Examples of such aggregates are vesicles and micelles. The concentration at which surfactants begin to form micelles is known as the critical micelle concentration or CMC. At low concentrations, surfactant molecules are unassociated monomers. As the concentration of surfactant is increased, the attractive and repulsive forces between the molecules cause self-aggregation to occur resulting in the formation of monolayers or micelles (Figure 2.2). The concentration at which these micelles form is called the critical micelle concentration (cmc). The characteristics of micelles can be controlled by small changes in the chemical structure of the surfactant molecules or by varying the conditions of the disperse phase. Changes in the pH, ionic strength and temperature are all known to influence the size and shape of surfactant micelles. For some cases, the micelle size can be affected by the concentration of surfactant.

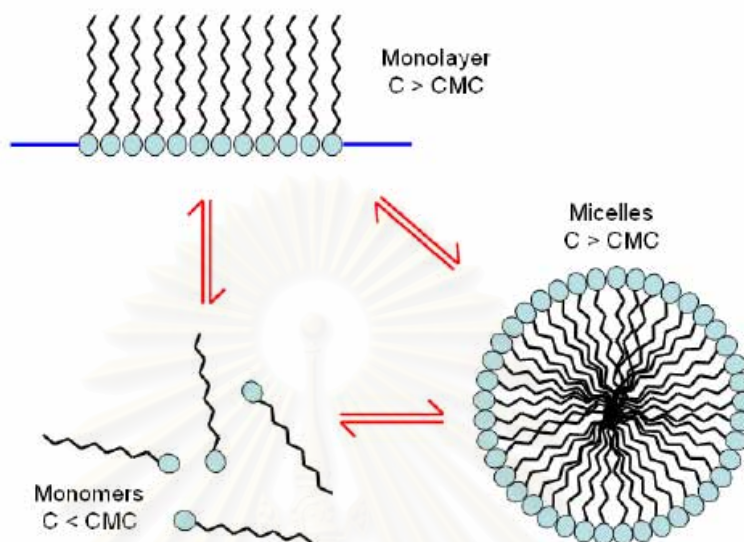


Figure 2.2 The surfactant can exist as different phases depending upon the concentration of the sample.

When micelles form in water, their tails form a core that can encapsulate an oil droplet, and their (ionic/polar) heads form an outer shell that maintains favorable contact with water. When surfactants assemble in oil, the aggregate is referred to as a reverse micelle. In a reverse micelle, the heads are in the core and the tails maintain favorable contact with oil. Surfactants are also often classified into four primary groups; anionic, cationic, non-ionic, and amphoteric.

2.2.1 Anionic surfactant

The defining feature of the anionic surfactant is, of course, that it is an anion (i.e. a negatively charged ion). All of the soaps (the fatty acid salts) are anionic surfactants (see the section on soaps for more information).

One of the first steps in the development of surfactants that were insensitive to metal lines was the development of the alkyl sulfate surfactants. Like the soaps, these are

anionic surfactants. In fact, probably the most studied surfactant over the years is one of these alkyl sulfates: sodium dodecyl sulfate (SDS). Unlike soaps, alkyl sulfates will not precipitate in low pH solutions.

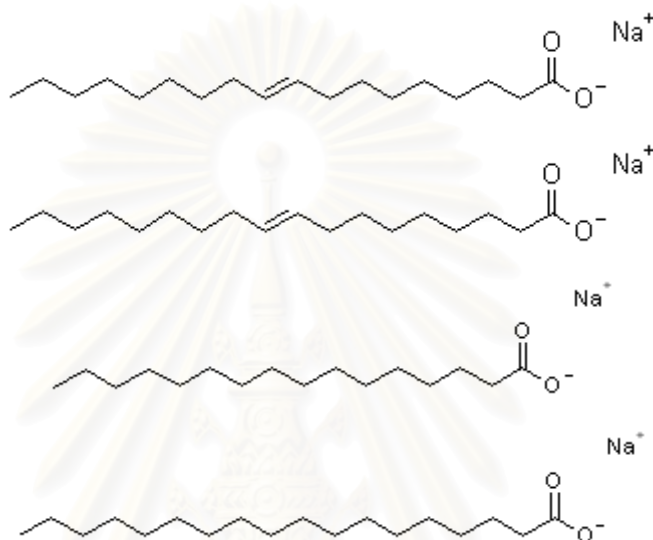


Figure 2.3 Some common soaps: sodium oleate, sodium palmitate, sodium myristate and sodium stearate.

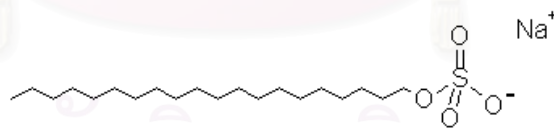


Figure 2.4 Sodium dodecyl sulfate, one of the most common of the alkyl sulfate style of anionic surfactant.

Other commonly used anionic surfactants are the alkyl benzenesulfonates, alkyl sulfonates and the alkyl phosphates.

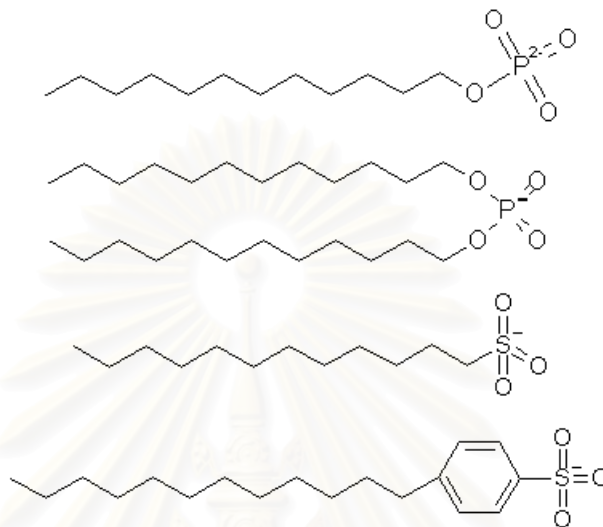


Figure 2.5 Two alkyl phosphates, an alkyl sulfonate, and an alkyl benzene sulfonate. Sulfosuccinates are similar to the alkyl sulfonates and were developed in 1939.

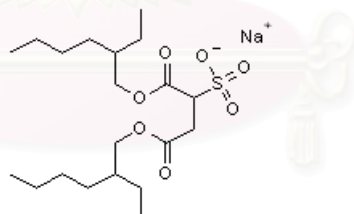


Figure 2.6 The sulfosuccinate surfactant sodium di(2-ethylhexyl) sulfosuccinate (sold under the name Aerosol-OT or AOT).

Uses of Anionic Surfactants

Anionic surfactants are used all over the place. They make up around 49% of all surfactants made. They are used in shampoos, in dishwashing detergents and in washing powders. In many industrial and commercial applications, anionic surfactants are no longer used on their own. Typically, they are used in conjunction with nonionic surfactants to provide even greater stability.

Long-term exposure to anionic surfactants has been linked to swelling of the skin in a conditioned allergic reaction. This swelling is temporary, although it tends to increase the susceptibility of the skin to permeation by other substances. Anionic surfactants are generally avoided in cosmetic products, but their use in shampoos and other products can still lead to irritation (that's why some people suggest changing shampoos every month or so).

2.2.2 Cationic surfactants

Like anionic surfactants, it is fairly easy to recognise the cationic surfactants - it has a positive charge. Fatty amine salts (or ammonium salts) were developed as the first cationic surfactants.

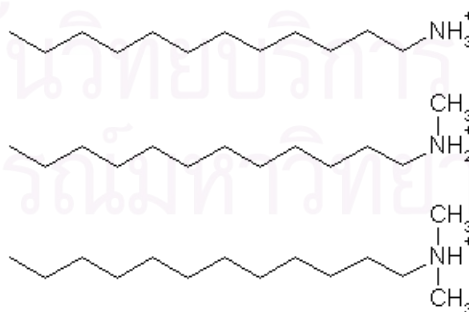
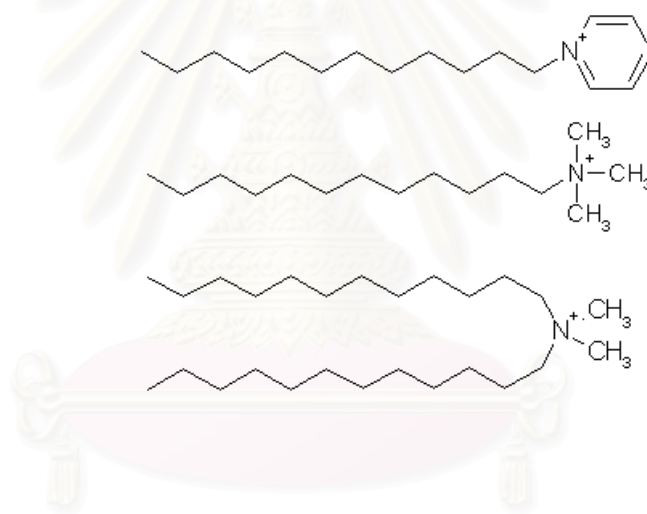


Figure 2.7 Fatty amine salts were the first style of cationic surfactant synthesised.

Unfortunately, ammonium salts can also be sensitive to pH. If we take these cationic surfactants up to high pH (10 or 11) then it is possible to deprotonate the amine, thus leaving us once again with an uncharged molecule. In the same way as the fatty acid salts tended to precipitate out once they were protonated, these fatty amine salts will precipitate out once deprotonated.

In response to this shortcoming, the alkyl pyridinium and quaternary ammonium salts were developed (quaternary means that there are four substituents on the nitrogen atom). These surfactants are incredibly stable so that they do not lose their charge in high pH conditions.



สถาบันวิทยบริการ
จุฬาลงกรณ์มหาวิทยาลัย

The development of alkyl pyridinium and quaternary ammonium salts provided excellent surfactants that could be used over a vast range of conditions.

Uses of Cationic Surfactants

Cationic surfactants are typically used in things like hair-conditioner and fabric softeners. The fatty amine salts proved quite useful in blends with nonionic surfactants, giving good stability over a range of pH levels. Cationic surfactants are generally rated as being more irritating to the skin than anionic surfactants (although this is probably a gross over-generalisation.)

You might be interested to know that having a "bad hair day" is usually due to residual surfactant on your hair. The cationic surfactants used in shampoos and hair-conditioners can stick to your hair even when you rinse it under water. This results in slightly positively charged hairs, which repel each other, giving you that "bad hair day" look.

2.2.3 Nonionic surfactants.

Nonionic surfactants differ from both cationic and anionic surfactants in that the molecules are actually uncharged. The hydrophilic group is made up of some other very water soluble moiety, (e.g. a short, water-soluble polymer chain) rather than a charged species. Traditionally, nonionic surfactants have used poly(ethylene oxide) chains as the hydrophilic group. Poly(ethylene oxide) is a water soluble polymer; the polymers used in nonionic surfactants are typically 10 to 100 units long.

The two common classes of surfactant that use poly(ethylene oxide) chains as their hydrophilic group are the alcohol ethoxylates and the alkylphenol ethoxylates.

Another class of nonionic surfactants is the alkyl polyglycosides. For at least the last 20 years these have been dubbed the "new generation nonionic surfactants". In these molecules, the hydrophilic group is sugar - in this case they are just polysaccharides, but they can be made from disaccharides, trisaccharides, maltose and various other sugars.

Although they are called polyglycosides, they generally only have one or two sugar groups in the chain.

Sorbitan ester surfactants are commercially significant surfactants. Fairly harsh conditions are required to synthesise them: 225-250 °C in the presence of an acid catalyst.

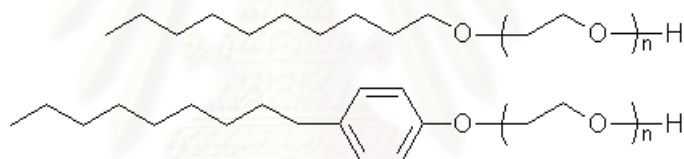


Figure 2.8 An alcohol ethoxylate and an alkylphenol ethoxylate. The poly(ethylene oxide) chain forms the water soluble surfactant "head".

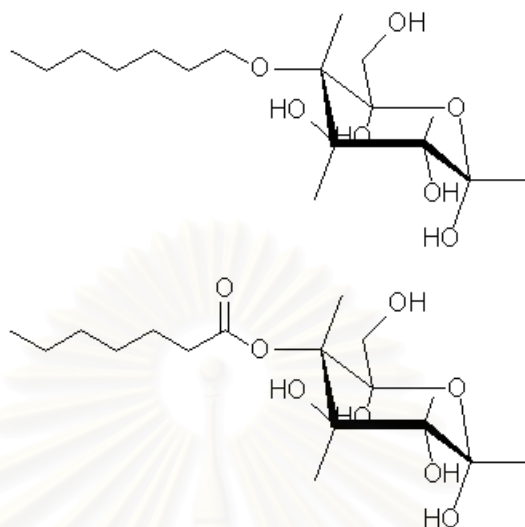


Figure 2.9 Examples of alkyl polyglycosides: an alkyl glucoside and a glucose ester.

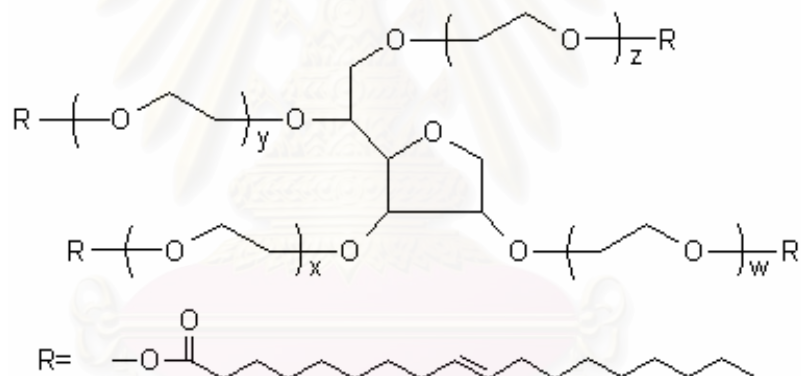


Figure 2.10 "Tween 85" (sorbitan trioleate poly(ethylene oxide)) is one of the sorbitan ester surfactants

Uses of Nonionic Surfactant

The predominant use of these surfactants is in foods and drinks, pharmaceuticals and skin-care products. It is thought that these surfactants are mild on the skin even at high loadings and long-term exposure (although they can lead to a weakening of the skin barrier by helping the transport of molecules).

2.2.4 Amphoteric surfactant.

Surface-active compounds with both acidic and alkaline properties are known as amphoteric surfactants. Amphoteric surfactants include two main groups, i.e. betaines and real amphoteric surfactants based on fatty alkyl imidazolines. The key functional groups in the chemical structures are the more or less quaternized nitrogen and the carboxylic group. Betaines are characterized by a fully quaternized nitrogen atom and do not exhibit anionic properties in alkaline solutions, which means that betaines are present only as 'zwitterions'. Another group of amphoteric surfactants is designated imidazoline derivatives because of the formation of an intermediate imidazoline structure during the synthesis of some of these surfactants. This group contains the real amphoteric surfactants that form cations in acidic solutions, anions in alkaline solutions, and 'zwitterions' in mid-pH range solutions. The mid-pH range (isoelectric range) in which the surfactant has a neutral charge is compound specific and depends on the alkalinity of the nitrogen atom and the acidity of the carboxylic group. Amphoteric surfactants are used in personal care products (e.g. hair shampoos and conditioners, liquid soaps, and cleansing lotions) and in all-purpose and industrial cleaning agents. The total volume of amphoteric surfactants consumed in commercial products today is relatively small, but the consumption of these chemicals is expected to increase in the future because of the request for milder surfactants. Besides acting as mild surfactants, the amphoteric surfactants may improve the mildness of especially anionic surfactants. By volume, the most important groups of amphoteric surfactants today consist of alkylamido betaines and alkyl betaines. The use of alkylamphoacetates in personal care products is expected to grow in coming years.

2.3 Viscosity (Symon, Keith.)

Viscosity is a measure of the resistance of a fluid to being deformed by either shear stress or extensional stress. It is commonly perceived as "thickness", or resistance to flow. Viscosity describes a fluid's internal resistance to flow and may be thought of as

a measure of fluid friction. Thus, water is "thin" having a lower viscosity, while vegetable oil is "thick" having a higher viscosity. All real fluids (except superfluids) have some resistance to stress, but a fluid which has no resistance to shear stress is known as an ideal fluid or inviscid fluid. The study of viscosity is known as rheology.

Viscosity is the ratio between the pressure exerted on the surface of a fluid, in the lateral or horizontal direction, to the change in velocity of the fluid as you move down in the fluid (this is what is referred to as a velocity gradient).

In general, in any flow, layers move at different velocities and the fluid's viscosity arises from the shear stress between the layers that ultimately opposes any applied force.

Isaac Newton postulated that, for straight, parallel and uniform flow, the shear stress, τ , between layers is proportional to the velocity gradient, $\partial u/\partial y$, in the direction perpendicular to the layers.

$$\tau = \eta \frac{\partial u}{\partial y}$$

Here, the constant η is known as the coefficient of viscosity, the viscosity, the dynamic viscosity, or the Newtonian viscosity. Many fluids, such as water and most gases, satisfy Newton's criterion and are known as Newtonian fluids. Non-Newtonian fluids exhibit a more complicated relationship between shear stress and velocity gradient than simple linearity.

The relationship between the shear stress and the velocity gradient can also be obtained by considering two plates closely spaced apart at a distance y , and separated by a homogeneous substance. Assuming that the plates are very large, with a large area A , such that edge effects may be ignored, and that the lower plate is fixed, let a force F be applied to the upper plate. If this force causes the substance between the plates to undergo shear flow (as opposed to just shearing elastically until the shear stress in the substance balances the applied force), the substance is called a fluid. The applied force is proportional to the area and velocity of the plate and inversely proportional to the distance between the plates. Combining these three relations results in the equation $F =$

$\eta(u/y)$, where η is the proportionality factor called the absolute viscosity (with units $\text{Pa}\cdot\text{s} = \text{kg}/(\text{m}\cdot\text{s})$ or $\text{slugs}/(\text{ft}\cdot\text{s})$). The absolute viscosity is also known as the dynamic viscosity, and is often shortened to simply viscosity. The equation can be expressed in terms of shear stress; $\tau = F/A = \eta(u/y)$. The rate of shear deformation is u / y and can be also written as a shear velocity, du/dy . Hence, through this method, the relation between the shear stress and the velocity gradient can be obtained.

2.4 Preparation methods for hollow particles.

2.4.1 Spray method.

Nagamine and coworkers (2007) prepared study hollow spherical TiO_2 microparticles, which were several tens of micrometers in diameter, by spraying water into an organic phase containing titanium tetraisopropoxide (TTIP) as a titanium source. The rapid hydrolysis of TTIP at the water–oil interface resulted in the formation of a TiO_2 shell covering the water droplet. Hexane and cyclohexane were better solvents than isopropanol for fabricating hollow spherical microparticles, suggesting the importance of immiscibility of the solvent with water in this synthesis method. The average particle size increased as the distance from the nozzle to the surface of the TTIP solution was increased. The shell thickness was reduced by the addition of ethanol to the sprayed water droplet. These results demonstrated the controllability of the structure of TiO_2 hollow microparticles, including the diameter and the shell thickness.

Konishi and coworkers (2007) prepared hollow spherical TiO_2 microparticles, which were several tens of micrometers in diameter, can be prepared by spraying water into an organic phase containing titanium tetraisopropoxide (TTIP) as a titanium source. The concentration of TTIP did not affect the shell thickness. On the contrary, the shell thickness was increased with the concentration of the additives such as acetic acid and acetylacetone, which protected TTIP from hydrolysis and condensation. The formation of

hollow particles was described by a simple model involving the hydrolysis of TTIP at the water– oil interface, the inward diffusion of hydrolyzed titanium hydroxide through the passage in the shell, and its incorporation into the TiO₂ shell by condensation. The reduction of porosity of shell inhibited the diffusion, resulting in the formation of hollow structure.

2.4.2 Sol-gel method.

Li and coworkers (2005) prepared hollow TiO₂ spheres by a convenient sol–gel method at room temperature. The products were characterized by XRD, FESEM, TEM, and FT-IR. These spheres were hollow inside with outer diameters of 200–500 nm. The average mesoporous diameter was about 9.8 nm. And the BET surface area and specific pore volume were about 161.9 m²/g and 0.441 cm³/g, respectively.

Zheng and coworkers (2006) prepared amorphous SiO₂, anatase TiO₂, and cassiterite SnO₂ hollow spheres using hydrophilic colloidal carbon spheres as template in conjunction with the sol–gel method. The hollow spherical structures were confirmed by TEM and SEM. The void sizes of these hollow spheres were about 60% smaller than the diameters of the template. The BET surface areas of hollow spheres were about 183.8, 32.5, and 74.3 m²/g, respectively.

Nakashima and Kimizuka (2003) synthesized hollow titania microspheres in ionic liquids by a single-step sol-gel synthesis, using Ti(OBu)₄ as precursor. The interfacial sol-gel reaction in ionic liquids provided an efficient one step route to the inorganic microspheres. The size of hollow spheres could be controlled by physical conditions such as stirring rate and temperature.

Chou and coworkers (2003) synthesized TiO₂ hollow particles by using spray precipitation in a liquid-liquid system. Titanium chloride (TiCl₄) was used as precursor

and interacted with precipitating agent, triethylamine (TEA). Most of the particles had a hole as a result of the sprayed droplets of titanium chloride solution colliding with TEA liquid at high momentum.

Kimura and coworkers (2005) synthesized titania microballoons by a sol-gel method using titanium tetraisopropoxide in reverse dispersion. Hexane was used as a continuous phase, in which Sorbian monooleate was dissolved as a dispersion stabilizer and buffer solution as a dispersed phase. The products were confirmed as titania microballoons of 76 μm in average diameter and 4 μm in wall thickness without any crack or dimple.

Zheng Zhu and coworkers (2007) fabricated the non-close packed (ncp) face-centered cubic (fcc) photonic crystals of titanium dioxide (TiO_2) hollow spheres connected by TiO_2 cylindrical tubes have been fabricated using silica template. With the help of self-assembly, thermal sintering, selective etching techniques and sol-gel process, the photonic bandgap calculations indicated that the ncp structure of TiO_2 hollow spheres was easier to open the pseudogaps than close packed system at the lowest energy.

2.4.3 Surfactant-assisted method.

Zhen Ren and coworkers (2003) studied hollow microspheres of mesoporous titania with a thin shell of anatase structure have been prepared by a simple procedure of surfactant poly(ethylene oxide) assisted nanoparticle assembly in nonaqueous system. A high surface area of 378 m^2/g and pore volume of 0.34 cm^3/g was obtained in the as-prepared sample with pore size of 2.6nm. A large number of surface hydroxyl groups and a reduced band gap were found, which should be significant for multi-functionalisation of the surface and photocatalysis applications. A formation mechanism of hollow microspheres was proposed.

Kim and coworkers (2005) prepared mono-dispersed mixed metal oxide micro hollow spheres by using mixed metal sulfate precursor solution and an isopropyl alcohol (IPA) solvent in a micro precipitator configured with a micro capillary tip and a millimeter scale glass tube. The prepared micro particles revealed the morphology of hollow spheres with a narrow size distribution. Size and shell thickness of particle could be controlled by capillary tip diameter or line velocity and concentration of the precursor solution, respectively.

2.4.4 Bubble-template method.

Sen Zhang and coworkers (2008) studied micrometer-scale anatase-phase TiO_2 congeries assembled with hollow spheres have been synthesized by a bubble-template method combined with a facile chemical process. The as-prepared products were characterized by means of X-ray diffraction, field emission scanning electron microscopy, and transmission electron microscopy. Some of the congeries exhibited unique three-dimensional hierarchical architectures. The bubble-template strategy used in the synthetic process may represent a general approach to fabricate hollow micro- and nanostructures and therefore contribute to the formation mechanisms of hollow micro- and nanostructures.

2.4.5 Hydrothermal method.

Jianguo Yu and coworkers (2007) studied Bimodal mesoporous anatase phase TiO_2 hollow microspheres are one pot fabricated by hydrothermal treatment of acidic $\text{Ti}(\text{SO}_4)_2$ solution with NH_4F . Fluoride not only induces the outward hollowing of the spherical TiO_2 aggregates, but also promotes the crystallization of primary anatase TiO_2 nanocrystals, resulting in enlarged crystallite sizes and decreased specific surface areas. The hierarchical mesopores exhibit peak intra-aggregated mesopore sizes of 3–10 nm and peak interaggregated mesopore sizes of 30–50 nm, depending on the specific molar ratio of fluoride to titanium (R). The pore volume increases in parallel with the average pore

size with increasing R until the collapse of interaggregated pores at $R = 2$. The photocatalytic efficiency in decomposition of gaseous acetone by as-obtained hollow TiO_2 microspheres generally exceeds that by Degussa P25 when R is < 2 . The influence of fluoride on photoactivity are discussed in terms of phase structures and pore structures.

Yanhui Ao and coworkers (2008) studied anatase titania hollow spheres were prepared using hydrothermally prepared carbon spheres as template. The prepared hollow spheres were characterized by XRD, BET, TEM, XPS and diffuse reflectance spectrum (DRS). The photocatalytic activity of the as-prepared titania hollow spheres was determined by degradation of MB in aqueous solution, and was compared to commercial P25 titania. It was revealed that the photocatalytic activity of the titania hollow spheres enhanced a lot. The apparent rate constant of the titania hollow spheres is almost 6 times as that of P25 titania.

Jianguo Yu and coworkers (2008) studied crystalline bi-phase TiO_2 hollow microspheres with mesoporous shells are one-pot fabricated by hydrothermal treatment of acidic $(\text{NH}_4)_2\text{TiF}_6$ aqueous solution in the presence of glucose at 180°C for 24 h, and then calcined at different temperatures for 4 h. The as-prepared samples are characterized by XRD, SEM, TEM and nitrogen adsorption–desorption isotherms. The photocatalytic activity of the as-prepared samples is evaluated by photocatalytic decolorization of methyl orange aqueous solution at ambient temperature. The results indicate that the prepared TiO_2 samples possess a bimodal pore size distribution in the mesoporous region. At 500°C , TiO_2 hollow microspheres exhibit the highest photocatalytic activity probably due to an optimal mass ratio of rutile to anatase.

2.5 Effect of surfactant concentration on particle size.

T. Prozorov and coworkers (1998) studied average size of the coated ferromagnetic Fe_2O_3 nanoparticles is controlled by the surfactant concentration in the coating solution. Magnetization as a function of this ratio first increases and then decreases exhibiting a peak. Surface area of the coated material shows inverse behavior, i.e. first decreases and then increases. Both curves have extrema at the same ratio of surfactant/substrate. Explain these features in terms of competition between surface and volume contribution to the total energy, where surface contribution is determined by the bonding energy between the surfactant SH-group and Fe_2O_3 . Support our conclusions by employing transmission electron microscopy and elemental analysis.

Elizabeth A and coworkers (2005) studied liquid phase deposition (LPD) of silica from soluble silicates has been performed in the presence of dodecyltrimethylammonium bromide (DTAB), sodium dodecyl sulfate (SDS) and sodium dodecylbenzyl sulfate (SDBS). The morphology of the silica varies between semi-ordered uniform spheres to low porosity agglomerates, with the choice and concentration of the surfactants. The agglomerate structures depend on the charge of the surfactant (and hence the retention of micelles under acidic LPD conditions and/or the ionic character of the surfactant solution), the critical micelle concentration (as compared to the concentration of the silica precursor), and the ionic strength of the solution. The application of surfactant micelles as templates for LPD silica is counter to a previous proposal that suggested the ionic strength of the silicate solution would cause the collapse of the ionic vesicles. The size of spherical silica particles is controlled by the relative concentration of the surfactant and the LPD precursor.

CHAPTER III

MATERIALS AND METHODS

This chapter is organized as follows: chemical, assembly of spray apparatus, preparation of titanium dioxide hollow particles, method to study influence of spraying flow rate titanium sulfate solution of titanium precursor, concentration of surfactant solution, distance from nozzle to liquid surfactant and types of surfactant respectively, and characterization techniques employed in this research. Synthesis of TiO₂ hollow spheres by spraying technique is explained in this chapter.

3.1. Chemical.

1. Titanium(III) sulfate (Ti₂(SO₄)₃), 99.99%, available from Sigma-Aldrich.
2. Tween 20, available from Sigma-Aldrich.
3. Polyethylene glycol, 99.5%, available from Fluka.
4. Sodium dodecyl sulfate, 99.0%, available from Sigma-Aldrich.
5. Distilled water

3.2 Assembly of spray apparatus.

Spray apparatus was made by connect titanium precursor container to liquid pump which can control a certain flow rate of titanium precursor solution and joint with nozzle to spray titanium precursor droplets. Nozzle and surfactant holder are in an acrylic enclosure to prevent effect of surrounding. The schematic diagram of spray apparatus is show below.

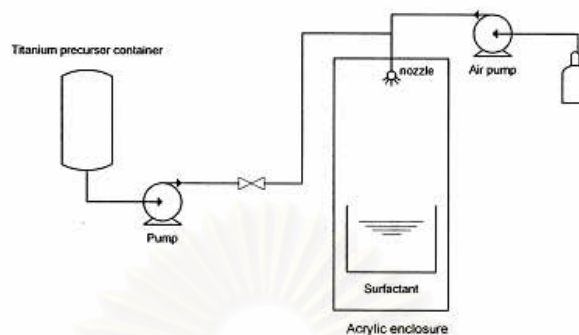


Fig 3.1 Schematic diagram of spray technique.

The MAGDOS LC4 with max flow rate equal to 4 L/h and max pressure equal to 8.0 bar as a liquid pump and Mini pancake (OL1204) as an air pump. The enclosure was made from acrylic with 33x25 cm in top and bottom and 45 cm in height and nozzle used in this research was commercial nozzle with 0.3 mm in diameter.

3.3 Preparation of titanium dioxide hollow particles.

The TiO_2 hollow particles were prepared by the following procedure. 0.05% (v/v) of titanium sulfate solution that dissolved in 100 ml of distilled water was sprayed into the surfactant solution under atmospheric condition which surfactants were nonionic surfactant (tween 20 and polyethylene glycol) and anionic surfactant (sodium dodecyl sulfate) at a concentration ranging from 0.2 to 2 % V/V that dissolved in 100 ml of distilled water. The distances from the tip of the nozzle to the solution surface and flow rate were varied in the range of 10 to 30 cm and at 3-5 L/h respectively. The particles were removed from the solution using a filter then dried at 110 °C for one day and calcined at 500 °C with a waiting rate of 10 °C/min for an hour to remove surfactant.

3.3.1 Influence of spraying flow rate of titanium sulfate solution.

To investigate the influence of flow rate on the averages particle size of TiO₂ hollow spheres. The 0.05% (v/v) of titanium sulfate solution that dissolved in distilled water was sprayed into the surfactant solution under atmospheric condition which surfactants were nonionic surfactant (tween 20 and polyethylene glycol) and anionic surfactant (sodium dodecyl sulfate). First the concentrations of surfactant solution and nozzle-solution distance were fixed at 0.2% and 2% (v/v) and at 10 and 30 cm respectively. The flow rate was varied at 3 to 5 L/h. After sprayed, particles were removed from the solution using a filter then dried at 110 °C for one day and calcined at 500 °C with a waiting rate of 10 °C/min for an hour to remove surfactant.

3.3.2 Influence of concentration of surfactant solution.

To investigate the influence of concentration of surfactant solution on the averages particle size of TiO₂ hollow spheres. The 0.05% (v/v) of titanium sulfate solution that dissolved in distilled water was sprayed into the surfactant solution under atmospheric condition which surfactants were nonionic surfactant (tween 20 and polyethylene glycol) and anionic surfactant (sodium dodecyl sulfate). First the flow rate and the nozzle-solution distance were fixed at 3 to 5 L/h and 10 to 30 cm respectively. The concentration of surfactant solution was varied 0.2% and 2% (v/v). After spraying, particles were removed from the solution using a filter then dried at 110 °C for one day and calcined at 500 °C with a waiting rate of 10 °C/min for an hour to remove surfactant.

3.3.3 Influence of distance from nozzle to liquid surfactant.

To investigate the influence of distance from nozzle to liquid surfactant on the averages particle size of TiO₂ hollow spheres. The 0.05% (v/v) of titanium sulfate solution that dissolved in distilled water was sprayed into the surfactant solution under

atmospheric condition which surfactants were nonionic surfactant (tween 20 and polyethylene glycol) and anionic surfactant (sodium dodecyl sulfate). First the concentrations of surfactant solution and flow rate were fixed at 0.2% and 2% (v/v) and 3 to 5 L/h respectively. The nozzle-solution distance was varied at 10 and 30 cm. After spraying, particles were removed from the solution using a filter then dried at 110 °C for one day and calcined at 500 °C with a waiting rate of 10 °C/min for an hour to remove surfactant.

3.3.4 Influence of types of surfactant.

To investigate the influence of surfactant on averages particle size of TiO₂ hollow spheres. The 0.05% (v/v) of titanium sulfate solution that dissolved in distilled water was sprayed into the surfactant solution under atmospheric condition which surfactants were nonionic surfactant (tween 20 and polyethylene glycol) and anionic surfactant (sodium dodecyl sulfate) at a concentration ranging from 0.2 to 2 % V/V. The distance from the tip of the nozzle to the solution surface ranged from 10 to 30 cm under atmospheric condition at flow rate ranging 3-5 L/h. The particles were removed from the solution using a filter then dried at 110 °C for one day and calcined at 500 °C with a waiting rate of 10 °C/min for an hour to remove surfactant.

3.4 Characterization of titanium dioxide hollow spheres.

In order to determine physical and chemical properties of TiO₂ hollow spheres, various characterization techniques were employed. Such techniques are discussed in this section.

3.4.1 Viscometer.

Viscosities of surfactant are measured by using viscometer model Physica Rheolab MC1. The sample is a solution of surfactant with vary percent of surfactant

3.4.2 Laser Diffraction Technique.

The light source of the Malvern Spraytec is a 1-mW HeNe laser operating at wavelength of 670 nm. The Spraytec is designed for spray with obscuration from 2% to 95%. The maximum data acquisition rate of 2500 Hz for high speed spray is available in FLASH mode. Optical design minimises vignetting problem where choice of optical systems (100mm, 200mm, and 450 mm) allows the user to get the best balance between minimum measurable droplet size and working distance. Imaging calculation increases lens working distance: 15cm for 100mm lens (1.9 - 231.27 microns), 30cm for 200mm lens (3.8 – 462.54 microns), and 67.5cm for 450mm lens (8.56 - 1040.72 microns). Multiple scattering correction is an option available in the Spraytec.

3.4.3 X-ray diffractometry (XRD)

The crystallinity and X-ray diffraction (XRD) patterns of the catalysts were performed by SIEMENS D5000 X-ray diffractometer connected with a personal computer using Diffract AT version 3.3 for a full control of the XRD analyzer. The experiments were carried out by using $\text{CuK}\alpha$ radiation with Ni filter and the operating conditions of the measurement were shown below.

| | | |
|------------------------------|---|-----------|
| 2θ range of detection | : | 20 – 80 ° |
| Resolution | : | 0.04 ° |
| Number of Scan | : | 25 |

The crystalline size was estimated from line broadening according to the Scherrer equation (see Appendix A) and α -Al₂O₃ was used as standard.

3.4.4 Scanning Electron Microscope (SEM).

The morphology and crystalline size of titania hollow spheres. The characterization was conducted using a scanning electron microscope (SEM), JSM 6400, JEOL, Tokyo, Japan.

3.4.5 Transmission Electron Microscope (TEM).

The morphology and crystalline size of titania hollow spheres was observed by JEOL 2010 Transmission Electron Microscope (TEM) operated at 100 kV.

3.4.6 Average particle size (John Bibby)

The average particle size was calculated from the equation:

$$\bar{d} = \frac{\sum_{i=1}^n d_i}{n}$$

where d_i = the diameter of each particles (nm)
 n = the number of appeared in the TEM images

3.4.7 Standard deviation.

Dodge, Y. (2003) and Pearson, K. (1894). The standard deviation is a simple measure of the variability or dispersion of a population, a data set, or a probability distribution. A low standard deviation indicates that the data points tend to be very close

to the same value (the mean), while high standard deviation indicates that the data are “spread out” over a large range of values.

The standard deviation of particle size was calculated from the equation:

$$s.d. = \sqrt{\frac{1}{n-1} \sum_{i=1}^n (d_i - \bar{d})^2}$$

Where d_i = the diameter of each particles (nm)
 \bar{d} = the average particle sizes (nm)
 n = the number of appeared in the TEM images

3.4.8 Program MINITAB.

Minitab offers four types of designed experiments: factorial, response surface, mixture, and Taguchi (robust). The steps you follow in Minitab to create, analyze, and graph an experimental design are similar for all design types. After you conduct the experiment and enter the results, Minitab provides several analytical and graphing tools to help you understand the results. The decisions to conduct 2^4 full factorial experiments to examine the relationship between two factors were surfactants type. The results of this experiment will help you make decisions.

CHAPTER IV

RESULT AND DISCUSSION

This chapter presents the results and discussion on effect of spraying conditions and surfactant on physical properties of TiO₂ hollow spheres. In case titanium sulfates as solution of titanium precursor so that spraying titanium sulfates solution into surfactant solution at flow rate ranging 3-5 L/h. By surfactant used in these research components were nonionic surfactant tween 20, polyethylene glycol and anionic surfactant sodium dodecyl sulfate at a concentration ranging from 0.2 to 2 % V/V. So order that spraying titanium sulfate solution into surfactant solution at distance from the nozzle to the solution surfactant ranging 10-30 cm.

4.1 The prepared of surfactants solution.

The information of surfactant forms micelles at a particular minimum concentration at critical micelle concentration (cmc) of tween 20, polyethylene glycol, and sodium dodecyl sulfate were 0.059, 0.010, and 7 mM respectively and actual concentration of surfactant solution prepared of TiO₂ hollow spheres of tween 20, polyethylene glycol, and sodium dodecyl sulfate were in the range of 1.6-16, 2-20, and 7-70 mM respectively. When increasing concentration of surfactant solution that might gave the average particle size of TiO₂ hollow spheres decreased. Types of surfactant used in this research are listed in Table 4.1.

Table 4.1 The critical micelle concentration of the surfactant.

| Surfactant | Critical Micelle Concentration (mM) | Actual concentration of surfactant (mM) |
|------------------------|-------------------------------------|---|
| Tween 20 | 0.059 | 1.6-16 |
| Polyethylene glycol | 0.010 | 2-20 |
| Sodium dodecyl sulfate | 7 | 7-70 |

4.2 The viscosity of surfactants solution.

The relationship of viscosity of surfactant solution and shear rate of tween 20, polyethylene glycol and sodium dodecyl sulfate at concentration of 0.2% and 2% (V/V) were shown in figure 4.1, 4.2, and 4.3 respectively. Every surfactant solution had shown non-continuously increasing of viscosity with shear rate which are property of non-newtonian fluids. The fluids without a constant viscosity are called Non-Newtonian fluids, their viscosity cannot be described by a single number, non-newtonian fluids exhibit a variety of different correlations between viscosities and shear rate, if viscosity was constant over a wide range of shear rates, the fluids were so-called newtonian fluids. Moreover, the result had shown that surfactant solutions at concentration of 2% (V/V) gave more viscosity than 0.2% (V/V) and sodium dodecyl sulfate gave highest viscosity of all three surfactant solutions that might gave smallest average particle sizes of TiO₂ hollow spheres also.

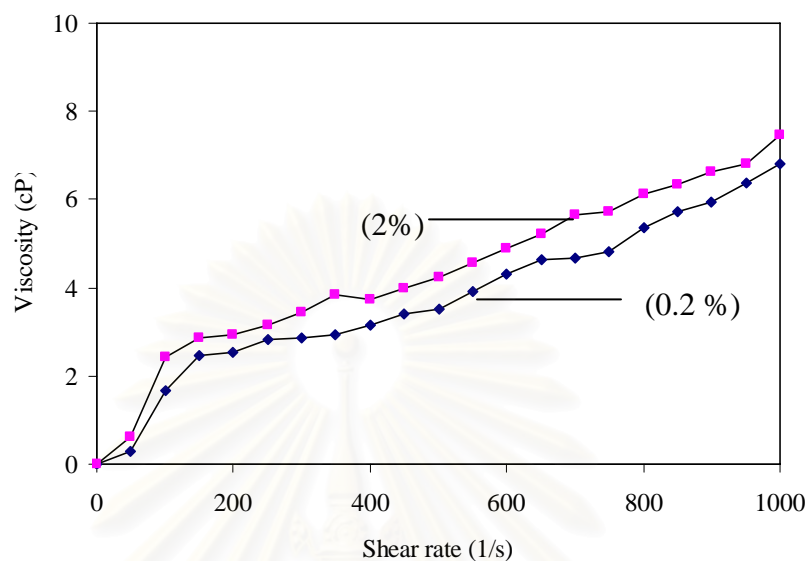


Figure 4.1 Viscosity of surfactant solution at concentration 0.2 % and 2% (V/V) Tween 20

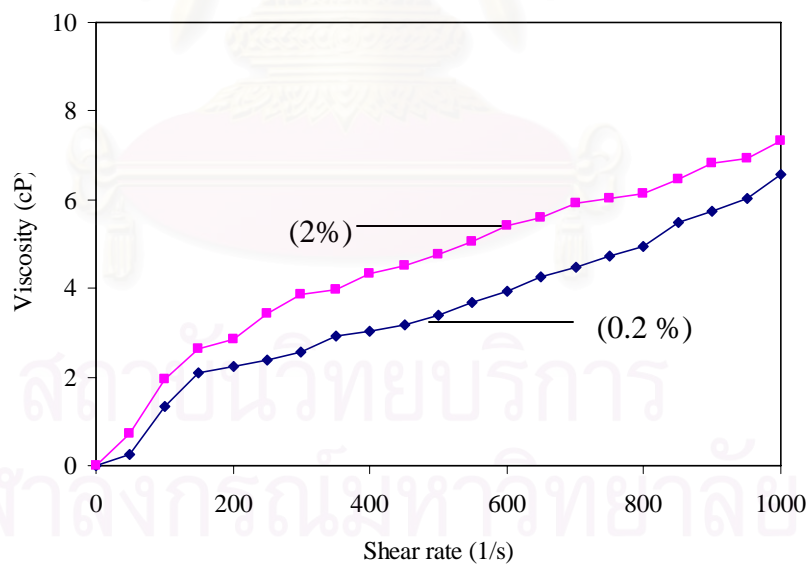


Figure 4.2 Viscosity of surfactant solution at concentration 0.2 % and 2% (V/V) Polyethylene glycol

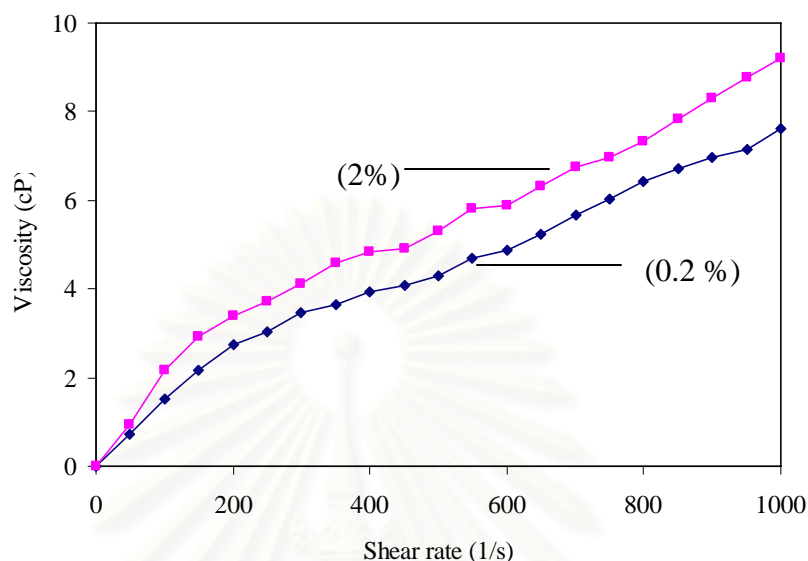


Figure 4.3 Viscosity of surfactant solution at concentration 0.2 % and 2% (V/V) Sodium dodecyl sulfate by vary shear rate.

4.3 The Laser Diffraction Technique.

The laser diffraction was chosen as a size droplets of sprayed exist nozzle measurement technique. Sizes of droplets were fixed by the flow rates and the nozzle-solution distance of 3 L/h and 10 cm respectively. The results found that the size droplets of sprayed exist nozzle were divided in 3 ranges from $Dv(10) = 11.91 \mu\text{m}$ which was the size droplets of sprayed exist nozzle have size from 1 to $11.91 \mu\text{m}$ 10 % in 100 % volume, $Dv(50) = 59.11 \mu\text{m}$ that showed the size droplets of sprayed exist nozzle have size from 1 to $59.11 \mu\text{m}$ 50 % in 100 % volume, and $Dv(90) = 213.56 \mu\text{m}$ that showed the size droplets of sprayed exist nozzle have size from 1 to $213.56 \mu\text{m}$ 90 % in 100 % volume that shown in figure 4.4.

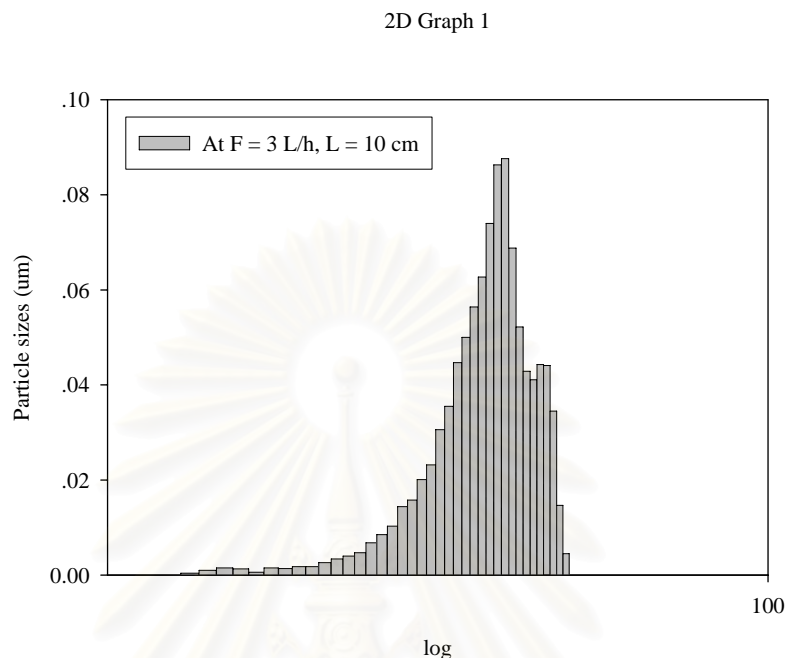


Figure 4.4 The laser diffraction technique in measurements size droplets of sprayed exist nozzle. The flow rates and the nozzle-solution distance were fixed at 3 L/h and at 10 cm respectively.

The laser diffraction was chosen as a size droplets of sprayed exist nozzle measurement technique. Sizes of droplets were fixed by the flow rates and the nozzle-solution distance of 5 L/h and 10 cm respectively. The results found that the size droplets of sprayed exist nozzle were divided in 3 ranges from $D_v(10) = 12.67 \mu\text{m}$ which was the size droplets of sprayed exist nozzle have size from 1 to $12.67 \mu\text{m}$ 10 % in 100 % volume, $D_v(50) = 64.61 \mu\text{m}$ that showed the size droplets of sprayed exist nozzle have size from 1 to $64.61 \mu\text{m}$ 50 % in 100 % volume, and $D_v(90) = 237.90 \mu\text{m}$ that showed the size droplets of sprayed exist nozzle have size from 1 to $237.90 \mu\text{m}$ 90 % in 100 % volume that shown in figure 4.5.

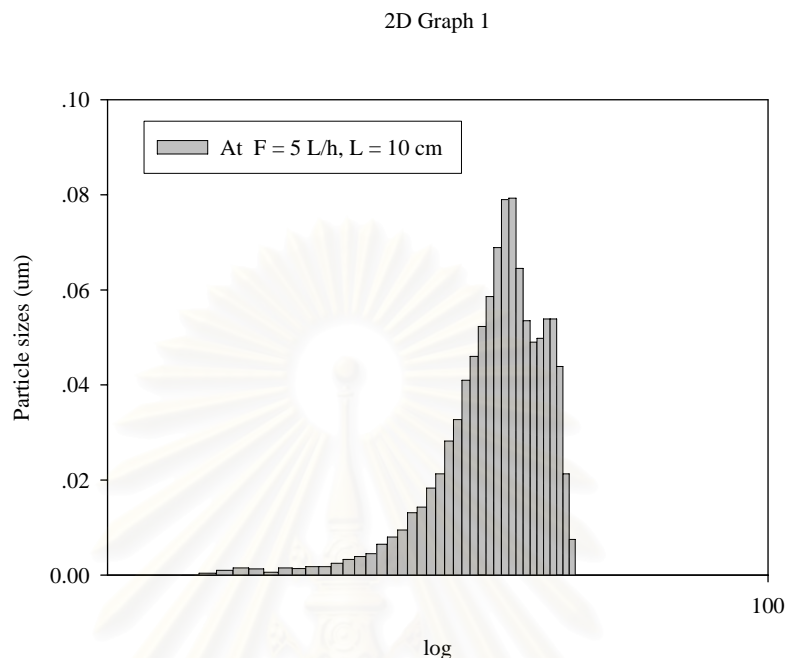


Figure 4.5 The laser diffraction technique in measurements size droplets of sprayed exist nozzle. The flow rates and the nozzle-solution distance were fixed at 5 L/h and at 10 cm respectively.

The laser diffraction was chosen as a size droplets of sprayed exist nozzle measurement technique. Sizes of droplets were fixed by the flow rates and the nozzle-solution distance of 3 L/h and 30 cm respectively. The results found that the size droplets of sprayed exist nozzle were divided in 3 ranges from $Dv(10) = 15.34 \mu\text{m}$ which was the size droplets of sprayed exist nozzle have size from 1 to $15.34 \mu\text{m}$ 10 % in 100 % volume, $Dv(50) = 60.33 \mu\text{m}$ that showed the size droplets of sprayed exist nozzle have size from 1 to $60.33 \mu\text{m}$ 50 % in 100 % volume, and $Dv(90) = 154.29 \mu\text{m}$ that showed the size droplets of sprayed exist nozzle have size from 1 to $154.29 \mu\text{m}$ 90 % in 100 % volume that shown in figure 4.6.

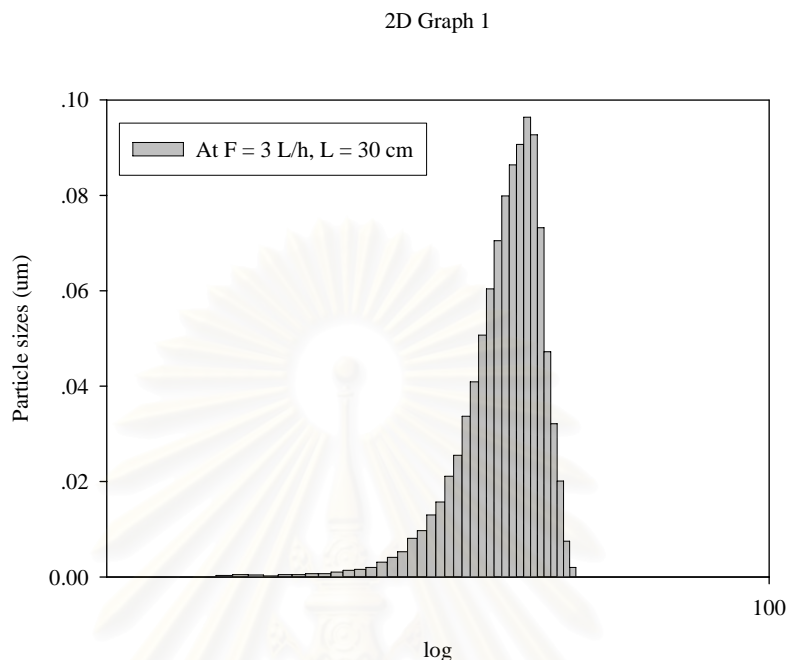


Figure 4.6 The laser diffraction technique in measurements size droplets of sprayed exist nozzle. The flow rates and the nozzle-solution distance were fixed at 3 L/h and at 30 cm respectively.

The laser diffraction was chosen as a size droplets of sprayed exist nozzle measurement technique. Sizes of droplets were fixed by the flow rates and the nozzle-solution distance of 5 L/h and 30 cm respectively. The results found that the size droplets of sprayed exist nozzle were divided in 3 ranges from $D_v(10) = 19.27 \mu\text{m}$ which was the size droplets of sprayed exist nozzle have size from 1 to $19.27 \mu\text{m}$ 10 % in 100 % volume, $D_v(50) = 76.21 \mu\text{m}$ that showed the size droplets of sprayed exist nozzle have size from 1 to $76.21 \mu\text{m}$ 50 % in 100 % volume, and $D_v(90) = 184.98 \mu\text{m}$ that showed the size droplets of sprayed exist nozzle have size from 1 to $184.98 \mu\text{m}$ 90 % in 100 % volume that shown in figure 4.7.

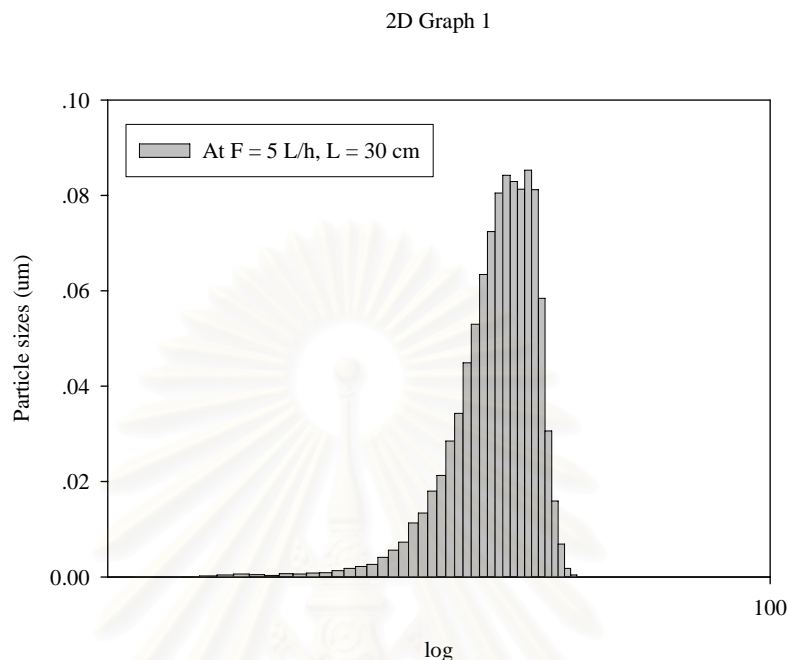


Figure 4.7 The laser diffraction technique in measurements size droplets of sprayed exist nozzle. The flow rates and the nozzle-solution distance were fixed at 5 L/h and at 30 cm respectively.

4.4 The surfactant solution as Tween 20.

4.4.1 Phase structures

4.4.1.1 X-ray diffractometer (XRD)

The crystalline phases of all samples were determined using X-ray diffractometer (XRD). TiO₂ hollow spheres samples, when using tween 20 as a surfactant were prepared by spraying technique. Then the all samples were calcined at 500°C for one hour under atmospheres.

From the XRD patterns of TiO₂ hollow spheres when using tween 20 as a surfactant in the Figure 4.8. The dominant peaks of anatase were observed at 2θ of about

25.2°, 37.9°, 47.8°, and 53.8°, which corresponded to the index of (101), (004), (200), and (105) plane, respectively. The peaks corresponding to other planes of anatase phase. No peak of other phase such as rutile and brookite were observed, which indicates that the products are pure.

The crystalline size calculated by the Scherrer formula from anatase (101) peak is about 5-7 nm. Crystallite size was not depend with flow rate of titanium precursor, percent concentration of surfactant solution and distance from nozzle to liquid surfactant solution. The results are listed in Table 4.2.

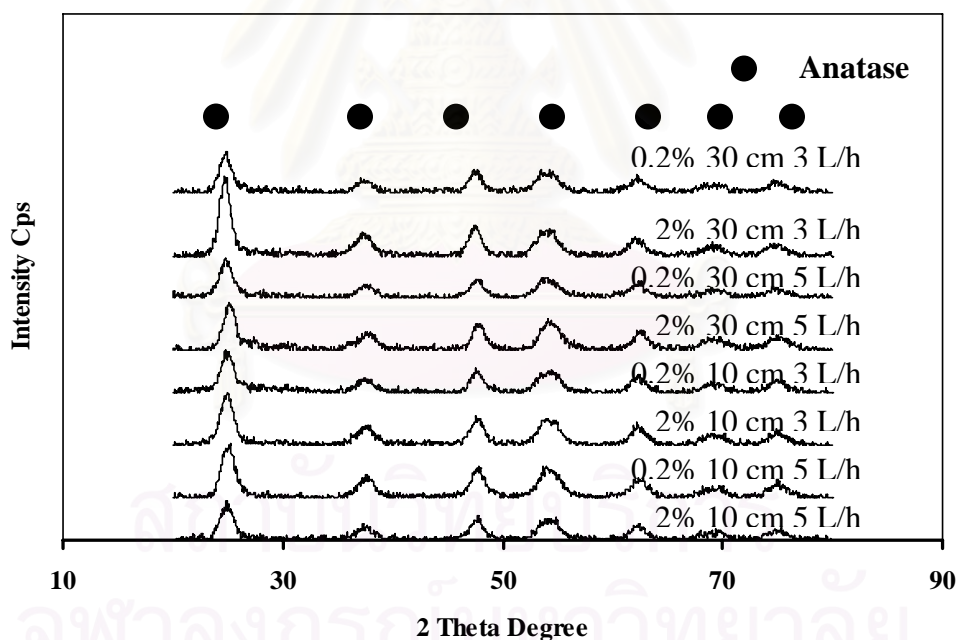


Figure 4.8 XRD patterns of TiO₂ hollow spheres using Tween 20 as a surfactant.

Table 4.2 Crystallite size of TiO₂ hollow spheres using Tween 20 as a surfactant, and determined from XRD pattern.

| Distance (cm) | Flow rate (L/h) | Conc (v/v) | Crystallite size (nm) |
|---------------|-----------------|------------|-----------------------|
| 10 | 3 | 0.2% | 6.2 |
| | | 2% | 5.5 |
| | 5 | 0.2% | 5.8 |
| | | 2% | 5.4 |
| 30 | 3 | 0.2% | 6.6 |
| | | 2% | 7.0 |
| | 5 | 0.2% | 5.9 |
| | | 2% | 5.9 |

4.4.2 Morphology of TiO₂ hollow spheres.

4.4.2.1 Scanning Electron Microscopy (SEM).

The morphologies of TiO₂ hollow spheres were observed with a scanning electron microscopy (SEM). Then the all samples were calcined at 500°C for one hour. Figure 4.9, 4.10, 4.11 and 4.12 shows an SEM image of the particles produced using Tween 20 as the surfactant. It can be seen that almost all samples are nanometer spheres with diameters of 100-150 nm. The morphologies of particles were uniformed and round shaped. The inset in Figure 4.11 and 4.12 shows a broken sphere.

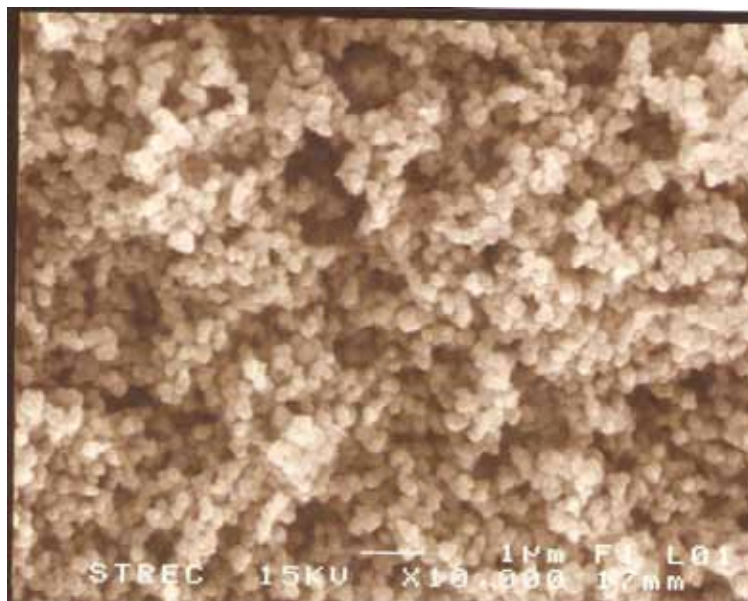


Figure 4.9 SEM image of TiO₂ hollow spheres using Tween 20 as the surfactant with 10000 magnifications.

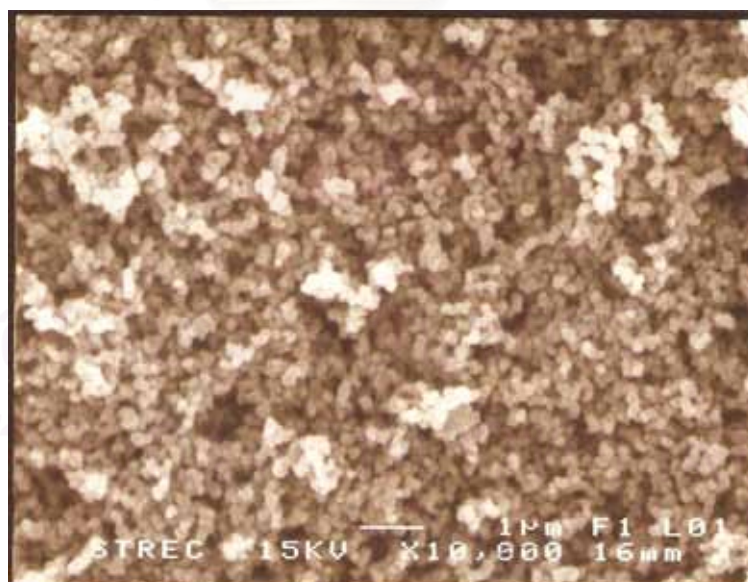


Figure 4.10 SEM image of TiO₂ hollow spheres using Tween 20 as the surfactant with 10000 magnifications.

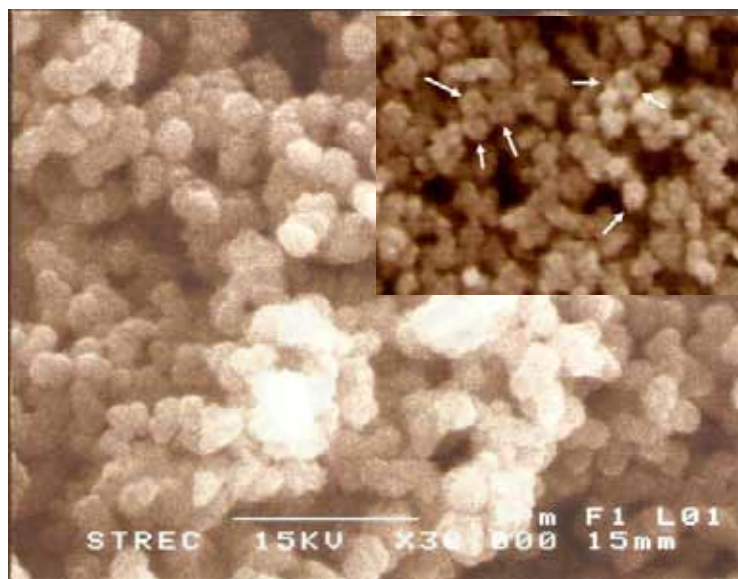


Figure 4.11 SEM image of TiO₂ hollow spheres using Tween 20 as the surfactant with 30000 magnifications.

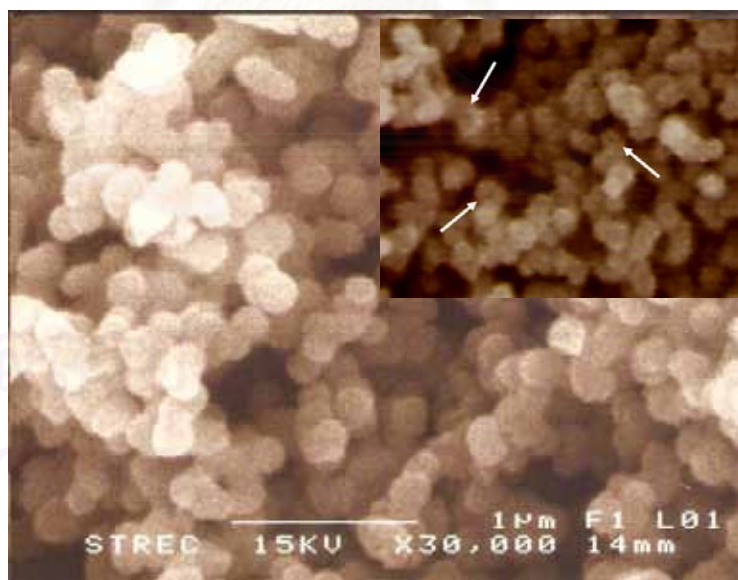


Figure 4.12 SEM image of TiO₂ hollow spheres using Tween 20 as the surfactant with 30000 magnifications.

4.4.2.2 Transmission Electron Microscopy (TEM).

The transmission Electron Microscopy (TEM) observations further display the morphology of TiO₂ hollow spheres. Then the all samples were calcined at 500°C for one hour. Figure 4.13, 4.14, 4.15, and 4.16 show a TEM image of the particles produced using Tween 20 as the surfactant. Apparently, each spheres after calcination is composed of a large amount of very small particles. It can be seen that almost all samples are nanometer spheres with diameters of 100-150 nm.

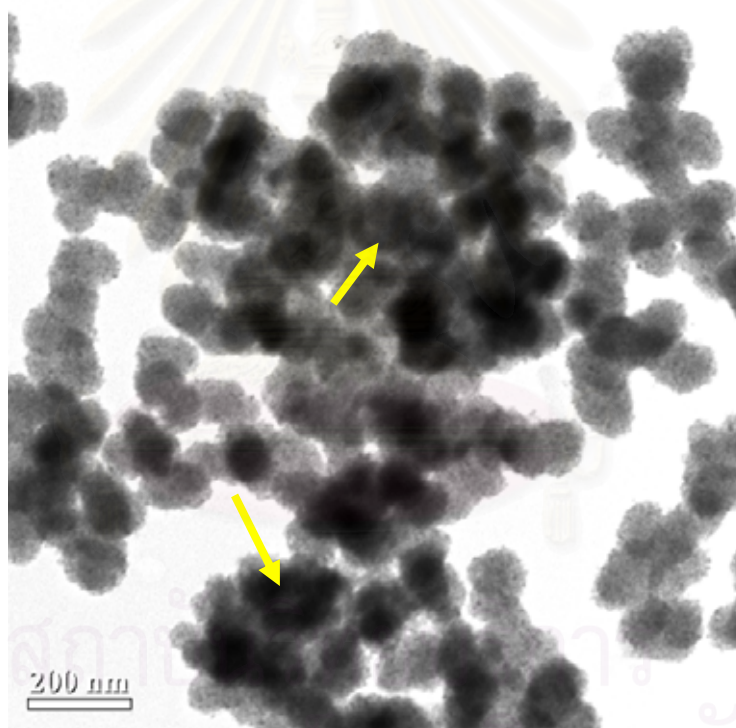


Figure 4.13 TEM image of TiO₂ hollow spheres using Tween 20 as the surfactant at scale bar 200 nm.

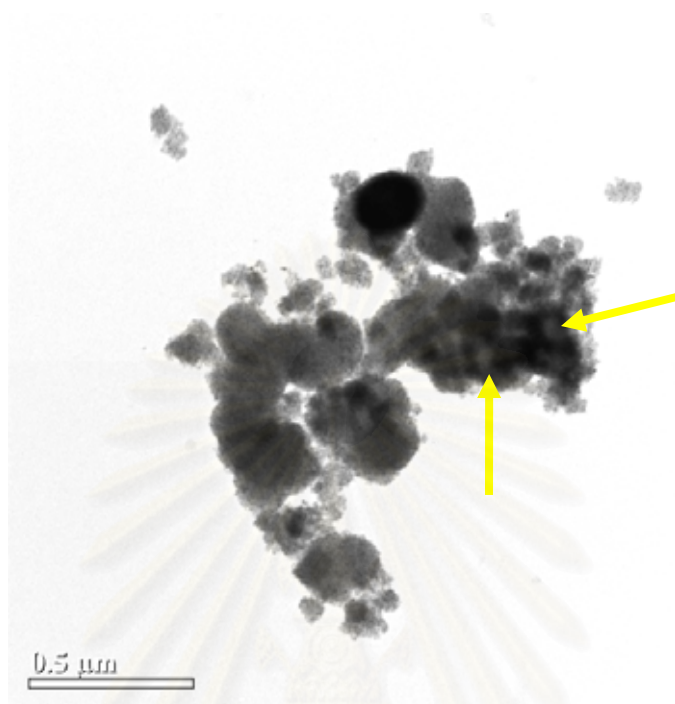


Figure 4.14 TEM image of TiO₂ hollow spheres using Tween 20 as the surfactant at scale bar 0.5 μm.

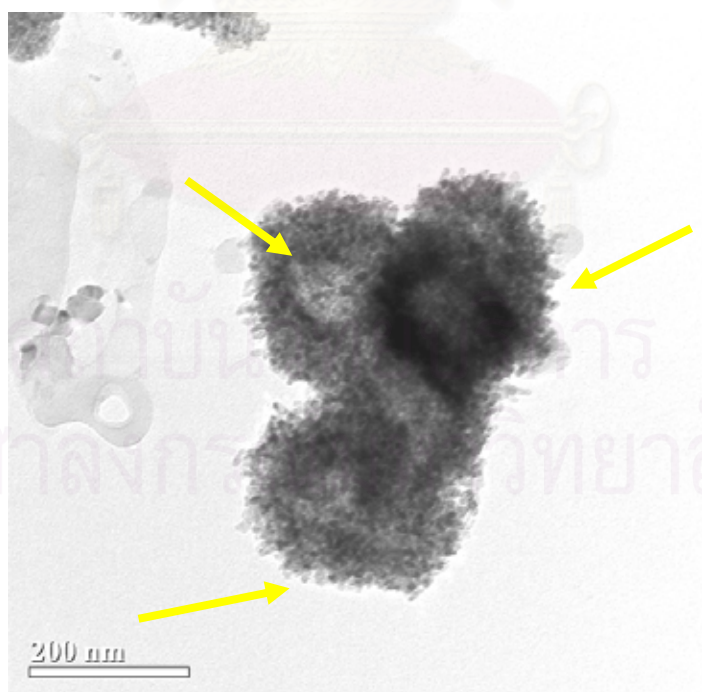


Figure 4.15 TEM image of TiO₂ hollow spheres using Tween 20 as the surfactant at scale bar 200 nm.

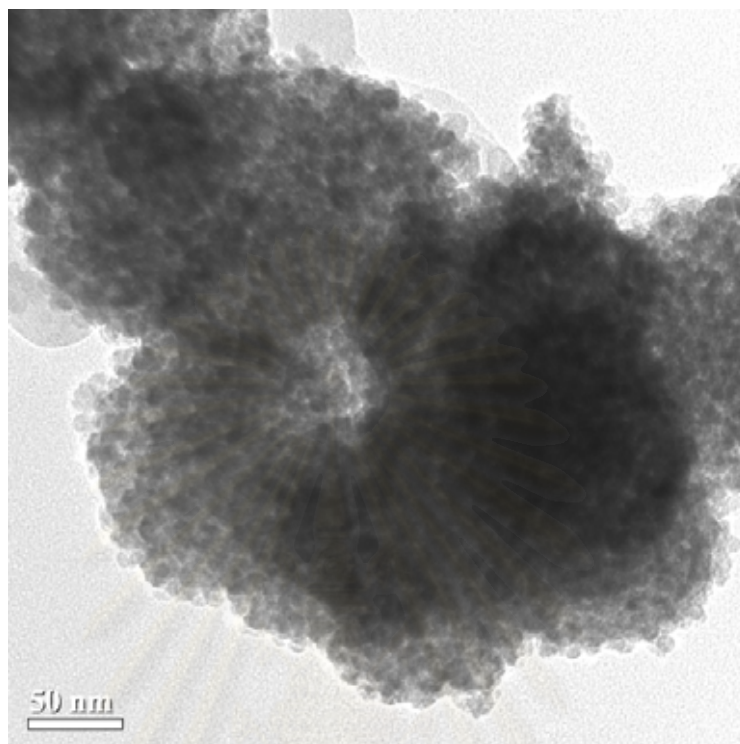


Figure 4.16 TEM image of TiO₂ hollow spheres using Tween 20 as the surfactant at scale bar 50 nm.

4.4.3 Average particles size of TiO₂ hollow spheres.

The general information of TiO₂ hollow spheres were determined from SEM and TEM image. By to consist of nozzle-solution distances, spraying flow rate of titanium sulfate solution, concentration of surfactant solution, average particles size, standard deviations (SD) and Z-score respectively. The results are listed in Table 4.3.

Table 4.3 Average particles size of TiO₂ hollow spheres using Tween 20 as a surfactant.

| Distance (cm) | Flow rate (L/h) | Conc (v/v) | Average Particle size (nm) | SD |
|---------------|-----------------|------------|----------------------------|-------|
| 10 | 3 | 0.2% | 151 | 14.33 |
| | | 2% | 120 | 12.08 |
| | 5 | 0.2% | 138 | 13.45 |
| | | 2% | 111 | 17.94 |
| 30 | 3 | 0.2% | 133 | 12.19 |
| | | 2% | 112 | 10.37 |
| | 5 | 0.2% | 118 | 13.36 |
| | | 2% | 99 | 11.34 |

4.4.4 Influence of spraying flow rate of titanium sulfate solution.

The influence of spraying flow rate of titanium sulfate solution on the average particle sizes were showed in Figure 4.17, the concentrations of surfactant solution and the nozzle-solution distance were fixed at 0.2% and 2% (v/v) and at 10 cm respectively. The flow rates were varied at 3 and 5 L/h. The results found that the average particle sizes of resultant were decrease from 151 to 138 nm and 120 to 111 nm respectively. However, in Figure 4.18 when changed the nozzle-solution distance was at 30 cm and the concentrations of surfactant solution was fixed at 0.2% and 2% (v/v). The flow rates were varied at 3 and 5 L/h. The result found that the average particles size decrease from 133 to 118 nm and 112 to 99 nm respectively, with observed in the same way with the results in Figure 4.17. With influence of spraying flow rate of titanium sulfate solution on the average particle sizes, the result found that the average particles size decrease 8-13 %.

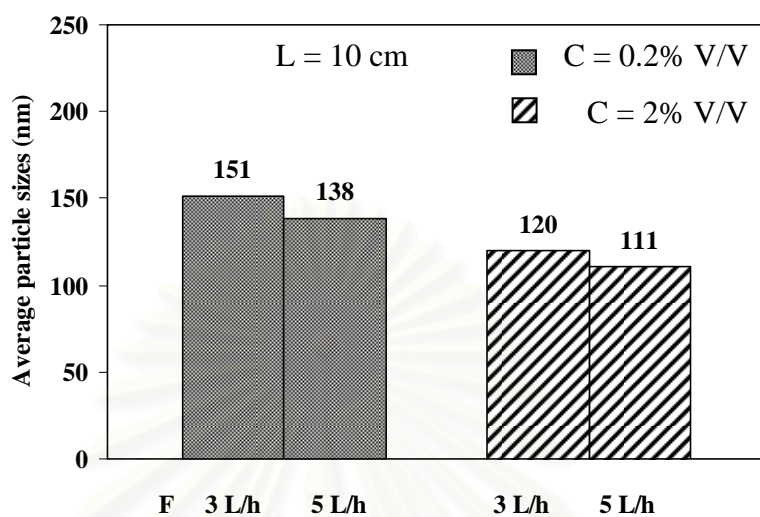


Figure 4.17 The average particle sizes of TiO₂ hollow spheres prepared by spraying titanium sulfate solution the flow rates were varied at F 3 and 5 L/h and fixed concentration C 0.2% and 2% (v/v) of nozzle-solution distance L 10 cm

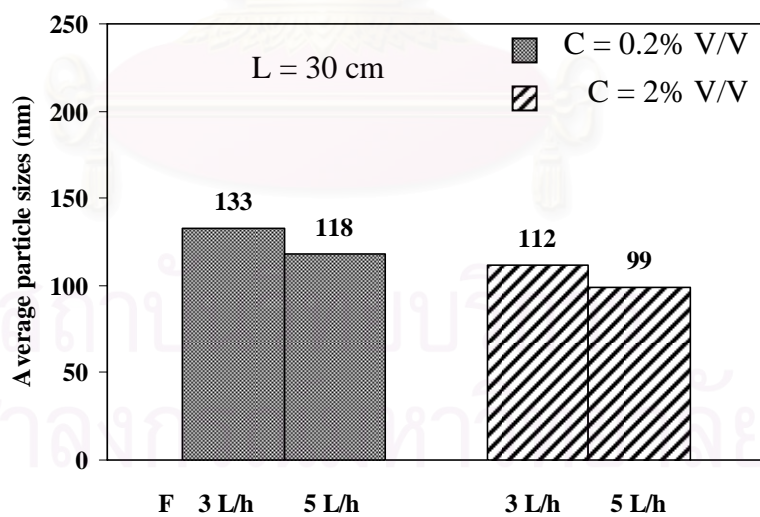


Figure 4.18 The average particle sizes of TiO₂ hollow spheres prepared by spraying titanium sulfate solution the flow rates were varied at F 3 and 5 L/h and fixed concentration C 0.2% and 2% (v/v) of nozzle-solution distance L 30 cm.

4.4.5 Influence of concentration of surfactant solution.

The influence of concentration of surfactant solution on the average particle sizes were showed in Figure 4.19, the flow rate and the nozzle-solution distance were fixed at 3 and 5 L/h and 10 cm respectively. The concentration of surfactant solution was varied 0.2% and 2% (v/v). The result found that the average particles size of resultant were decrease from 151 to 120 nm and 138 to 111 nm respectively. However, in Figure 4.20 when change the nozzle-solution distance was at 30 cm and the flow rates were fixed at 3 and 5 L/h. The concentrations of surfactant solution were varied 0.2% and 2% (v/v). The result found that the average particles size decrease from 133 to 112 nm and 118 to 99 nm respectively, with observed in the same way with the results in Figure 4.19. With the influence of concentration of surfactant solution on the average particle sizes, the result found that the average particles size decrease 15-20 %.

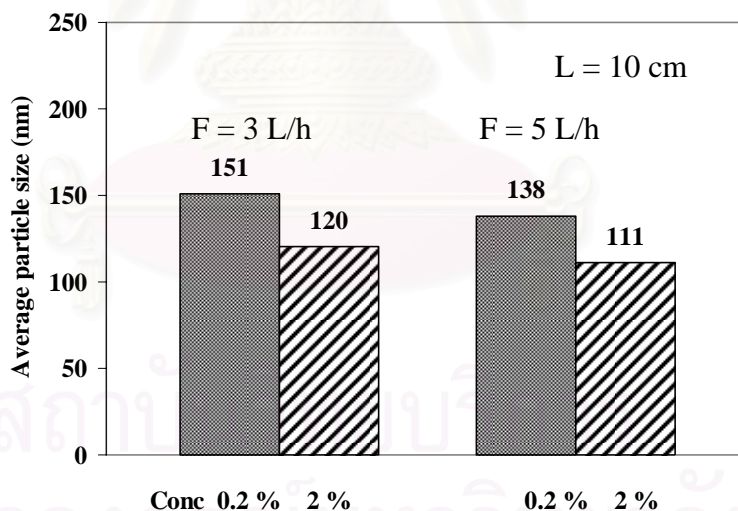


Figure 4.19 The averages particle sizes of TiO₂ hollow spheres by varied concentration C 0.2% and 2% (v/v) and fixed flow rate F 3 and 5 L/h of nozzle-solution distances L 10 cm

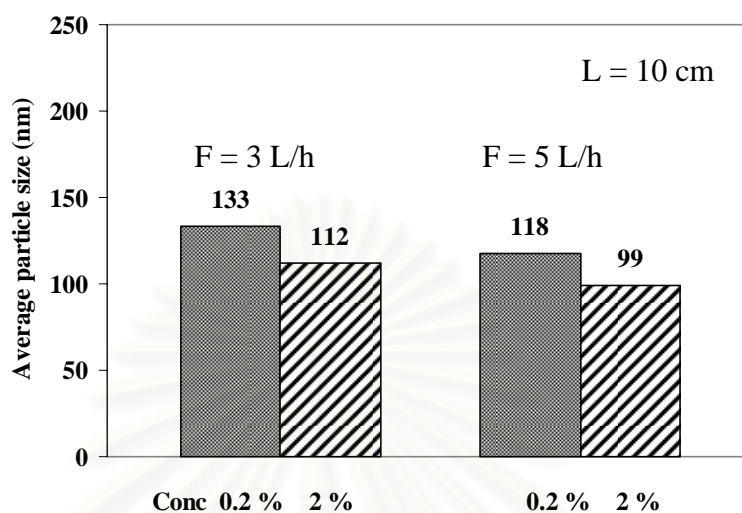


Figure 4.20 The averages particle sizes of TiO_2 hollow spheres by varied concentration C 0.2% and 2% (v/v) and fixed flow rate F 3 and 5 L/h of nozzle-solution distances L 30 cm.

4.4.6 Influence of distance from nozzle to liquid surfactant.

The influence of distance from nozzle to liquid surfactant on the average particle sizes were showed in Figure 4.21, the spraying flow rate of titanium sulfate solution and concentration of surfactant solution were fixed at 3 L/h and at 0.2% and 2% (v/v) respectively. The nozzle-solution distance was varied at 10 and 30 cm. The result found that the average particles sizes of resultant were decrease from 151 to 133 nm and 120 to 112 nm respectively. However, in Figure 4.22 when change the flow rate was at 5 L/h and concentrations of surfactant solution was fixed at 0.2% and 2% (v/v). The nozzle-solution distance was varied at 10 and 30 cm. The result found that the average particles size decrease 138 to 118 nm and 111 to 99 nm respectively, with observed in the same way with the results in Figure 4.21. With the influence of distance from nozzle to liquid surfactant on the average particle sizes, the result found that the average particles size decrease 6-12 %.

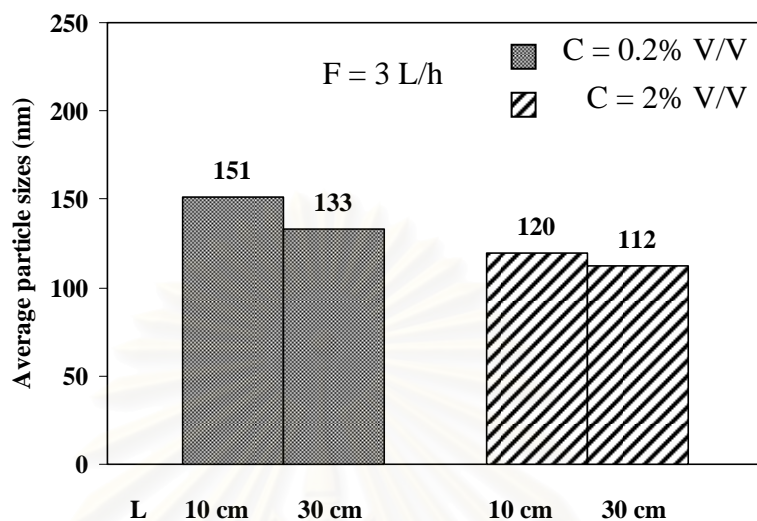


Figure 4.21 The averages particle sizes of TiO₂ hollow spheres by the nozzle-solution distances varied at L 10 and 30 cm and fixed concentration C 0.2% and 2% (v/v) and flow rate F 3 L/h

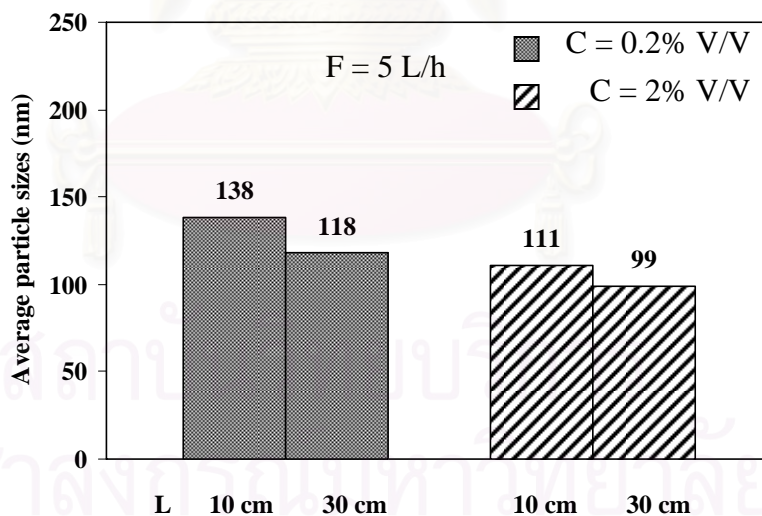


Figure 4.22 The averages particle sizes of TiO₂ hollow spheres by the nozzle-solution distances varied at L 10 and 30 cm and fixed concentration C 0.2% and 2% (v/v) and flow rate F 5 L/h.

4.5 The surfactant solution as polyethylene glycol.

4.5.1 Phase structures.

4.5.1.1 X-ray diffractometer (XRD).

The crystalline phases of all samples were determined using X-ray diffractometry (XRD). TiO₂ hollow spheres samples, when using polyethylene glycol as a surfactant were prepared by spraying technique. Then the all samples were calcined at 500°C for one hour under atmospheres.

From the XRD patterns of TiO₂ hollow spheres when using polyethylene glycol as a surfactant in the Figure 4.23. The XRD patterns can be indexed peaks of phase anatase were observed at 2θ of about 25.2°, 37.9°, 47.8°, and 53.8°, which corresponded to the index of (101), (004), (200), and (105) plane, respectively. The weak peak at 2θ of 26.6° was assigned to rutile phase of TiO₂. XRD peaks that belong to brookite were not detected at this temperature.

The crystalline size calculated by the Scherrer formula from anatase (101) peak is about 5.5-7 nm. Crystallite size was not depend with flow rate of titanium precursor, percent concentration of surfactant solution and distance from nozzle to liquid surfactant solution. The results are listed in Table 4.4.

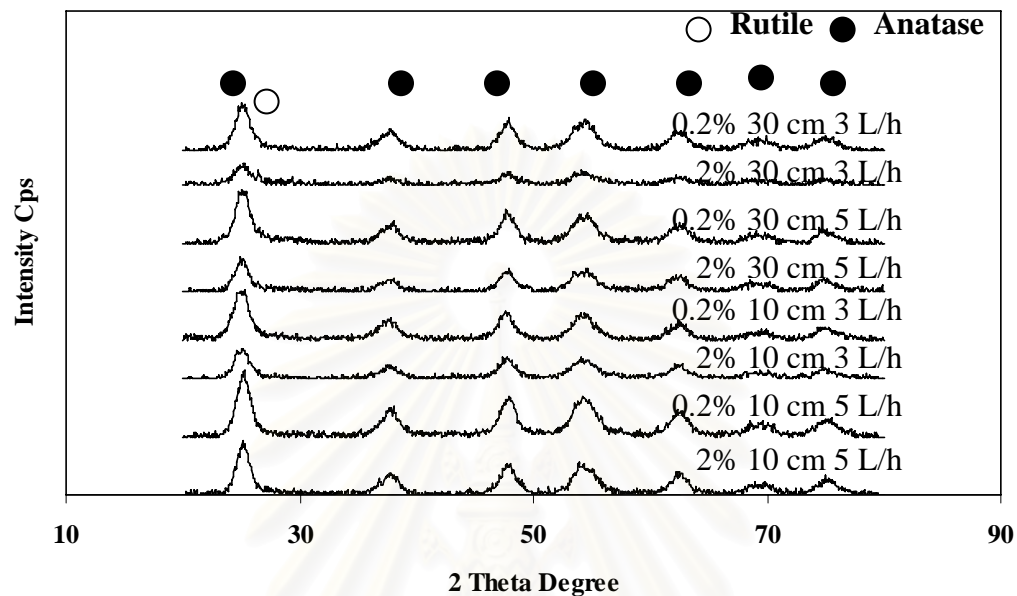


Figure 4.23 XRD patterns of TiO₂ hollow spheres using polyethylene glycol as a surfactant.

Table 4.4 Crystallite size of TiO₂ hollow spheres using polyethylene glycol as a surfactant, and determined from XRD pattern.

| Distance (cm) | Flow rate (L/h) | Conc (v/v) | Crystallite size (nm) |
|---------------|-----------------|------------|-----------------------|
| 10 | 3 | 0.2% | 5.4 |
| | | 2% | 5.6 |
| | 5 | 0.2% | 5.8 |
| | | 2% | 5.5 |
| 30 | 3 | 0.2% | 6.3 |
| | | 2% | 6.9 |
| | 5 | 0.2% | 6.3 |
| | | 2% | 5.5 |

4.5.2 Morphology of TiO₂ hollow spheres.

4.5.2.1 Scanning Electron Microscopy (SEM)

The morphology of the TiO₂ hollow spheres was studied by scanning electron microscopy (SEM). Then the all samples were calcined at 500°C for one hour. The hollow spheres of TiO₂ using polyethylene glycol as the surfactant can also be observed in Figure 4.24, 4.25, 4.26, and 4.27 shows that the TiO₂ hollow spheres have a spherical structure with the average particles size of about 115–177 nm. The morphologies of particles were uniform and round shape. The inset in Figure 4.26, and 4.27 shows a broken sphere.

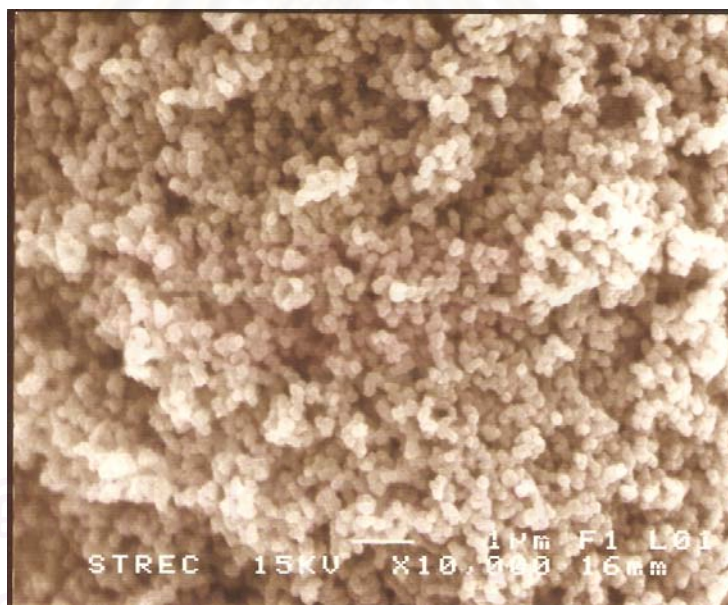


Figure 4.24 SEM image of TiO₂ hollow spheres using polyethylene glycol as the surfactant with 10000 magnifications.

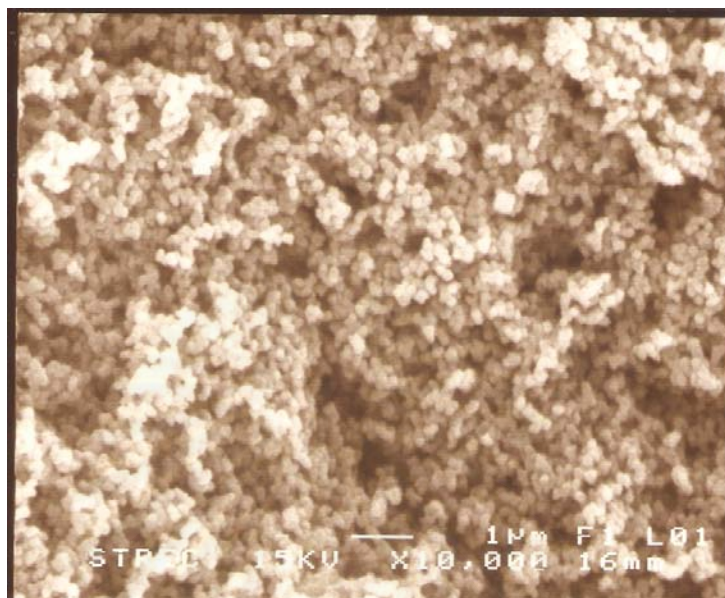


Figure 4.25 SEM image of TiO₂ hollow spheres using polyethylene glycol as the surfactant with 10000 magnifications.

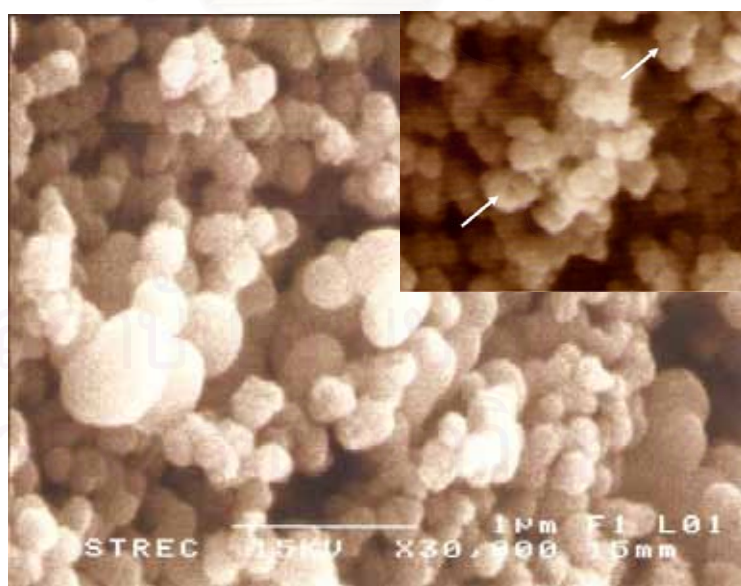


Figure 4.26 SEM image of TiO₂ hollow spheres using polyethylene glycol as the surfactant with 30000 magnifications.

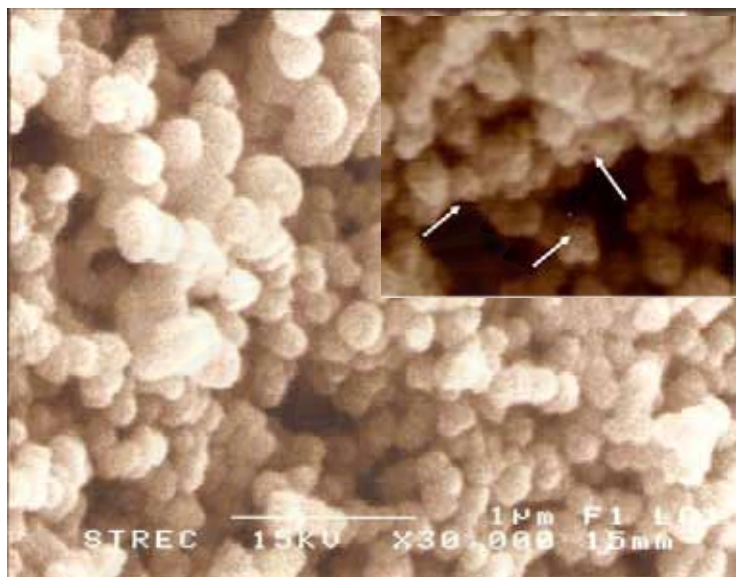


Figure 4.27 SEM image of TiO₂ hollow spheres using polyethylene glycol as the surfactant with 30000 magnifications.

4.5.2.2 Transmission Electron Microscopy (TEM).

The transmission electron microscopy (TEM) observations further display the morphology of TiO₂ hollow spheres. Then the all samples were calcined at 500°C for one hour. Figure 4.28, 4.29, 4.30, and 4.31 shows a TEM image of the particles produced using polyethylene glycol as the surfactant. Apparently, each spheres after calcination is composed of a large amount of very small particles. It can be seen that almost all samples are nanometer spheres with diameters of 115-177 nm.

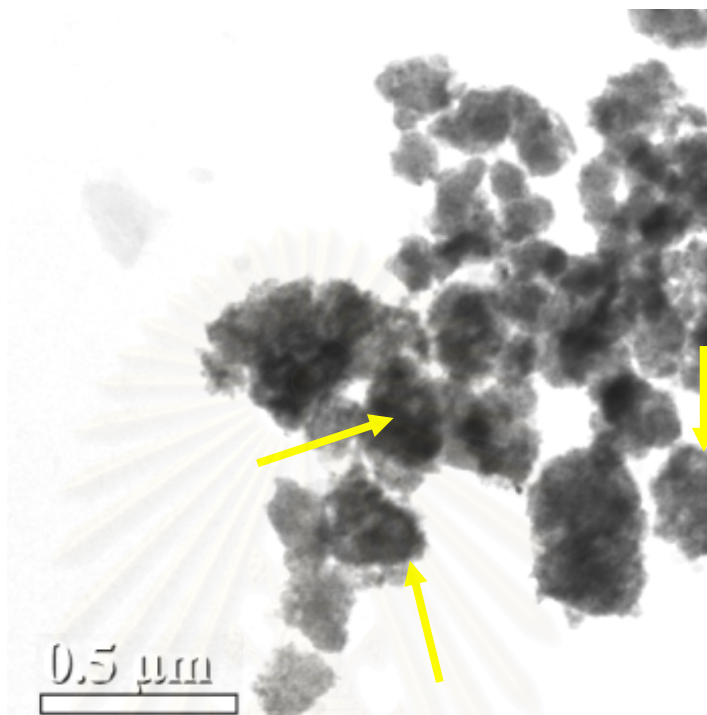


Figure 4.28 TEM image of TiO₂ hollow spheres using polyethylene glycol as the surfactant at scale bar 0.5 μm.

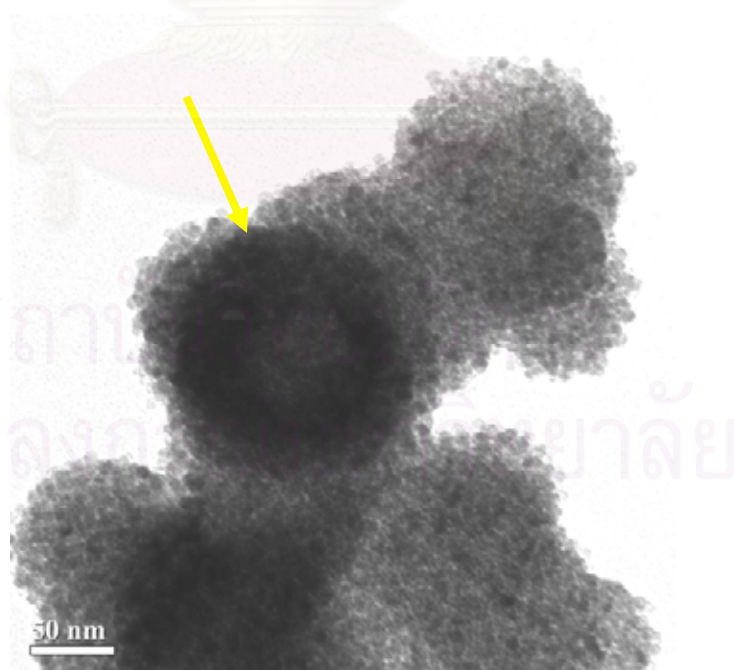


Figure 4.29 TEM image of TiO₂ hollow spheres using polyethylene glycol as the surfactant at scale bar 50nm.

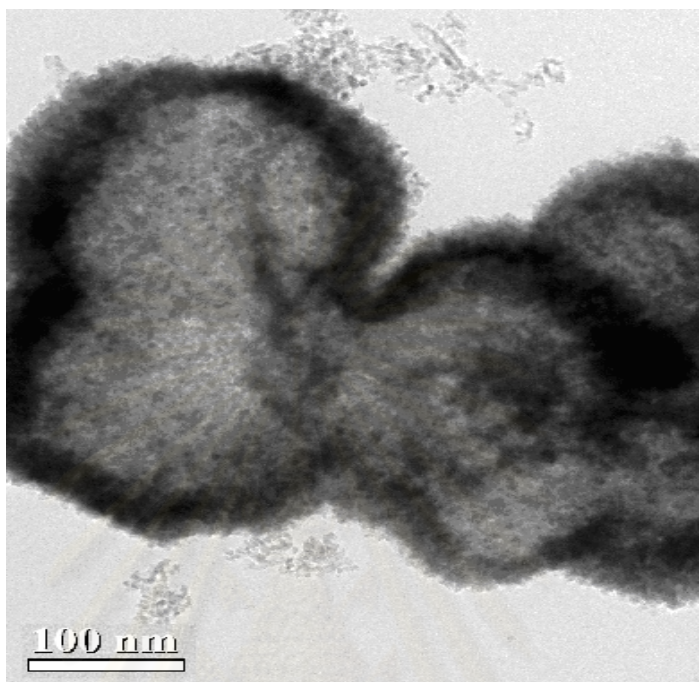


Figure 4.30 TEM image of TiO_2 hollow spheres using polyethylene glycol as the surfactant at scale bar 100nm.

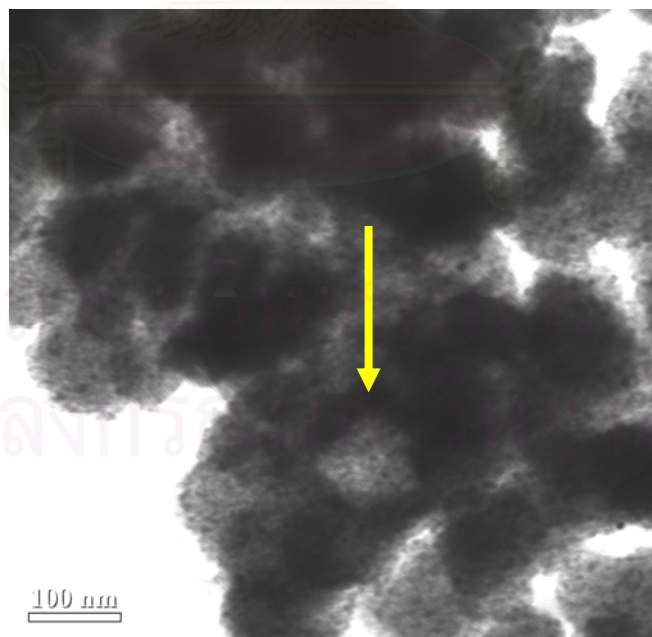


Figure 4.31 TEM image of TiO_2 hollow spheres using polyethylene glycol as the surfactant at scale bar 100nm.

4.5.3 Average particles size of TiO₂ hollow spheres.

The general information of TiO₂ hollow spheres were determined from SEM and TEM image. By to consist of nozzle-solution distances, spraying flow rate of titanium sulfate solution, concentration of surfactant solution, average particles size, standard deviations (SD) and Z-score respectively. The results are listed in Table 4.5.

Table 4.5 Average particles size of TiO₂ hollow spheres using polyethylene glycol as a surfactant.

| Distance (cm) | Flow rate (L/h) | Conc (v/v) | Average Particle size (nm) | SD |
|---------------|-----------------|------------|----------------------------|-------|
| 10 | 3 | 0.2% | 177 | 36.97 |
| | | 2% | 168 | 18.37 |
| | 5 | 0.2% | 156 | 21.16 |
| | | 2% | 147 | 18.33 |
| 30 | 3 | 0.2% | 139 | 21.37 |
| | | 2% | 132 | 16.93 |
| | 5 | 0.2% | 126 | 20.06 |
| | | 2% | 115 | 15.55 |

4.5.4 Influence of spraying flow rate titanium sulfate solution.

The influence of spraying flow rate of titanium sulfate solution on the average particle sizes were showed in Figure 4.32, the concentrations of surfactant solution and the nozzle-solution distance were fixed at 0.2% and 2% (v/v) and at 10 cm respectively. The flow rates were varied at 3 and 5 L/h. The results found that the average particle sizes of resultant were decrease from 177 to 156 nm and 168 to 147 nm respectively. However, in Figure 4.33 when changed the nozzle-solution distance was at 30 cm and the concentrations of surfactant solution were fixed at 0.2% and 2% (v/v). The flow rates were varied at 3 and 5 L/h. The result found that the average particle sizes decrease from 139 to 126 nm and 132 to 115 nm respectively, with observed in the same way with the

results in Figure 4.32. With the influence of spraying flow rate of titanium sulfate solution on the average particle sizes, the result found that the average particles size decrease 9-12 %.

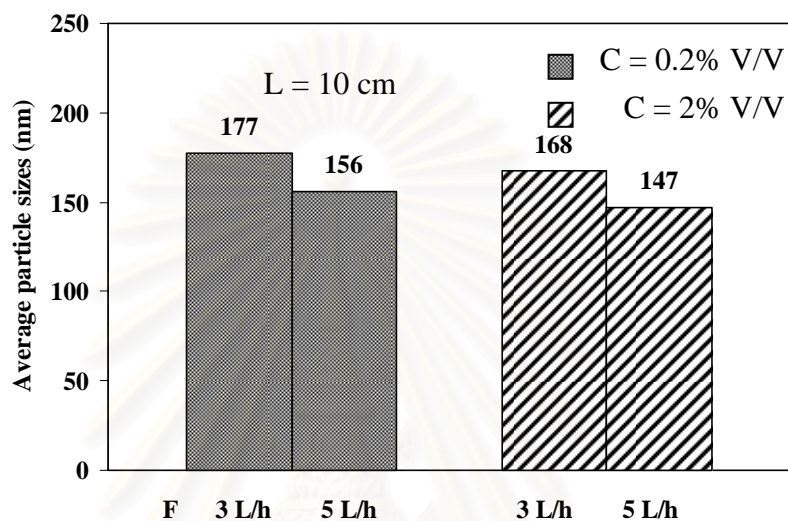


Figure 4.32 The average particle sizes of TiO_2 hollow spheres prepared by spraying titanium sulfate solution the flow rates were varied at F 3 and 5 L/h and fixed concentration C 0.2% and 2% (v/v) of nozzle-solution distance L 10 cm

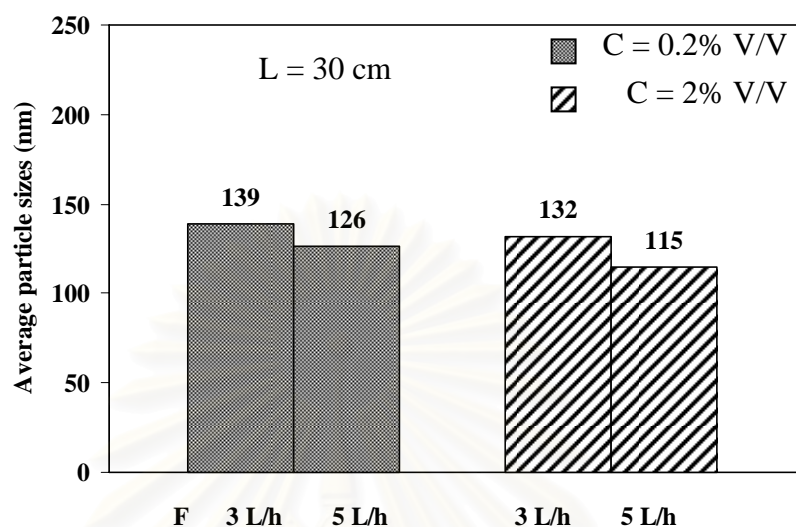


Figure 4.33 The average particle sizes of TiO₂ hollow spheres prepared by spraying titanium sulfate solution the flow rates were varied at F 3 and 5 L/h and fixed concentration C 0.2% and 2% (v/v) of nozzle-solution distance L 30 cm.

4.5.5 Influence of concentration of surfactant solution.

The influence of concentration of surfactant solution on the average particle sizes were showed in Figure 4.34, the flow rate and the nozzle-solution distance were fixed at 3 and 5 L/h and 10 cm respectively. The concentration of surfactant solution was varied 0.2% and 2% (v/v). The result found that the average particles size of resultant were decrease from 177 to 168 nm and 156 to 147 nm respectively. However, in Figure 4.35 when change the nozzle-solution distance was at 30 cm and the flow rates were fixed at 3 and 5 L/h. The concentrations of surfactant solution were varied 0.2% and 2% (v/v). The result found that the average particles size decrease from 139 to 132 nm and 126 to 115 nm respectively, with observed in the same way with the results in Figure 4.34. With the influence of concentration of surfactant solution on the average particle sizes, the result found that the average particles size decrease 5-8 %.

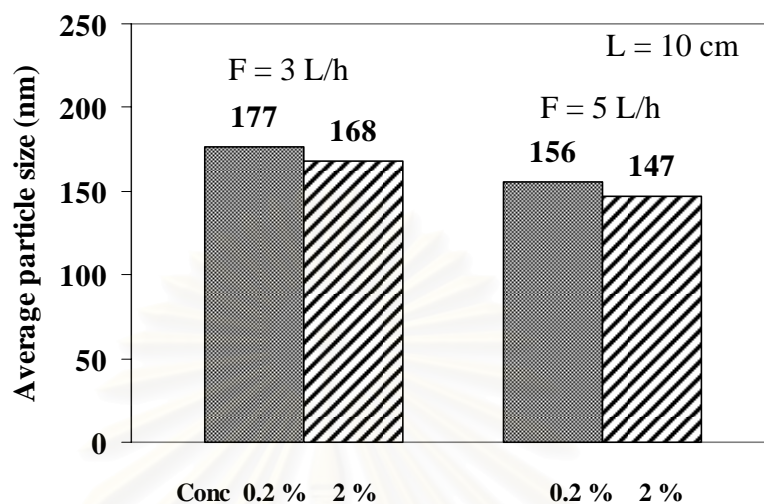


Figure 4.34 The averages particle sizes of TiO_2 hollow spheres by varied concentration C 0.2% and 2% (v/v) and fixed flow rate F 3 and 5 L/h of nozzle-solution distances L 10 cm

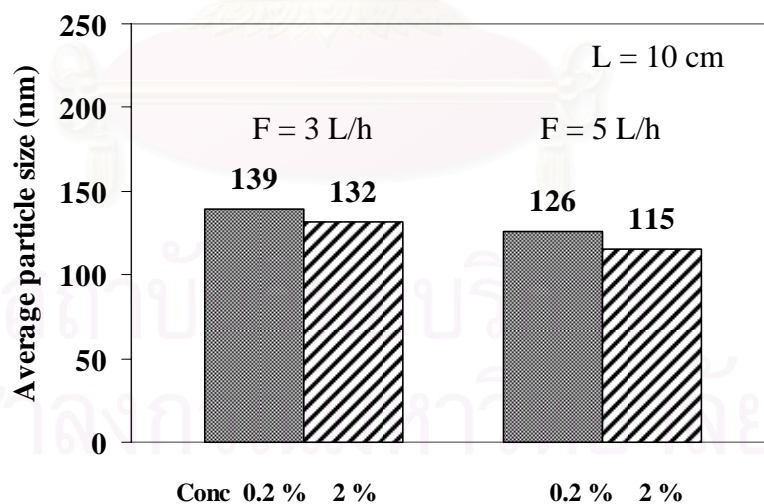


Figure 4.35 The averages particle sizes of TiO_2 hollow spheres by varied concentration C 0.2% and 2% (v/v) and fixed flow rate F 3 and 5 L/h of nozzle-solution distances L 30 cm.

4.5.6 Influence of distance from nozzle to liquid surfactant.

The influence of distance from nozzle to liquid surfactant on the average particle sizes were showed in Figure 4.36, the spraying flow rate of titanium sulfate solution and concentration of surfactant solution were fixed at 3 L/h and at 0.2% and 2% (v/v) respectively. The nozzle-solution distance was varied at 10 and 30 cm. The result found that the average particles sizes of resultant were decrease from 177 to 139 nm and 168 to 132 nm respectively. However, in Figure 4.37 when change the flow rate was at 5 L/h and concentrations of surfactant solution was fixed at 0.2% and 2% (v/v). The nozzle-solution distance was varied at 10 and 30 cm. The result found that the average particles size decrease 156 to 126 nm and 147 to 115 nm respectively, with observed in the same way with the results in Figure 4.36. With the influence of distance from nozzle to liquid surfactant on the average particle sizes, the result found that the average particles size decrease 19-21 %.

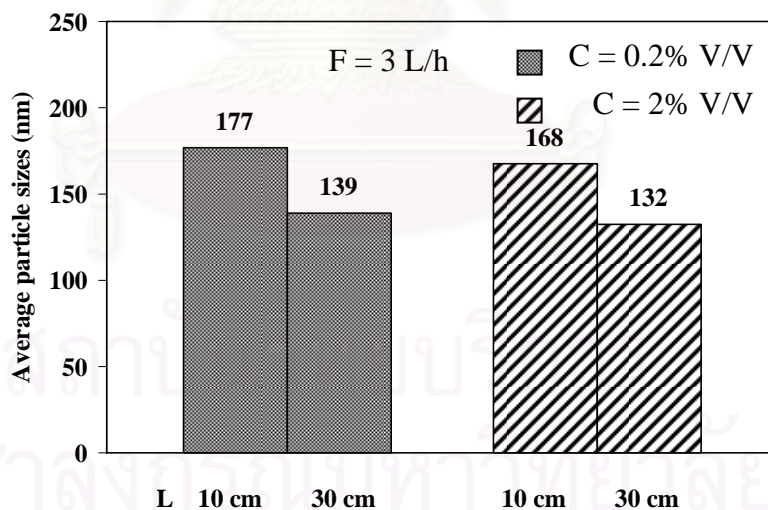


Figure 4.36 The averages particle sizes of TiO₂ hollow spheres by the nozzle-solution distances varied at L 10 and 30 cm and fixed concentration C 0.2% and 2% (v/v) and flow rate F 3 L/h

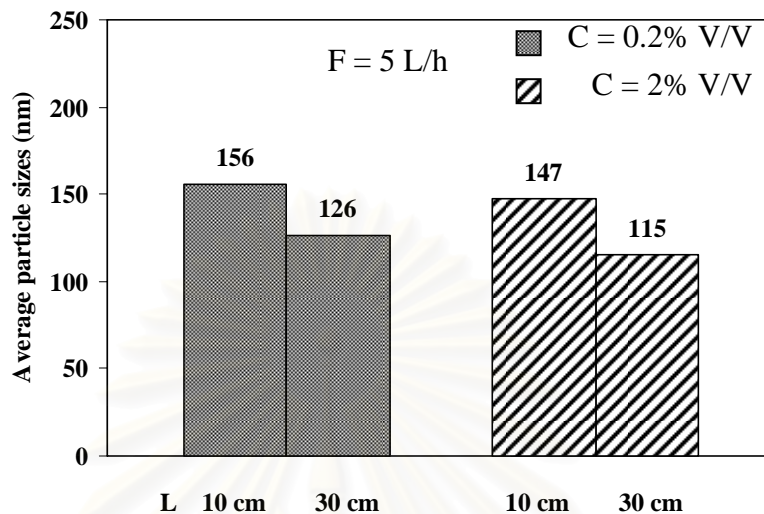


Figure 4.37 The averages particle sizes of TiO_2 hollow spheres by the nozzle-solution distances varied at L 10 and 30 cm and fixed concentration C 0.2% and 2% (v/v) and flow rate F 5 L/h.

4.6 The surfactant solution as sodium dodecyl sulfate.

4.6.1 Phase structures.

4.6.1.1 X-ray diffractometer (XRD).

The crystalline phases of all samples were determined using X-ray diffractometry (XRD). TiO_2 hollow spheres samples, when using sodium dodecyl sulfate as a surfactant were prepared by spraying technique. Then the all samples were calcined at 500°C for one hour under atmospheres.

From the XRD patterns of TiO_2 hollow spheres when using sodium dodecyl sulfate as a surfactant in the Figure 4.38. The dominant peaks of anatase were observed at

2θ of about 25.2° , 37.9° , 47.8° , and 53.8° , which corresponded to the index of (101), (004), (200), and (105) plane, respectively. The peaks corresponding to other planes of anatase phase. No peak of other phase such as rutile and brookite were observed, which indicates that the products are pure.

The crystalline size calculated by the Scherrer formula from anatase (101) peak is about 5.8-7.5 nm. Crystallite size was not depend with flow rate of titanium precursor, percent concentration of surfactant solution and distance from nozzle to liquid surfactant solution. The results are listed in Table 4.6.

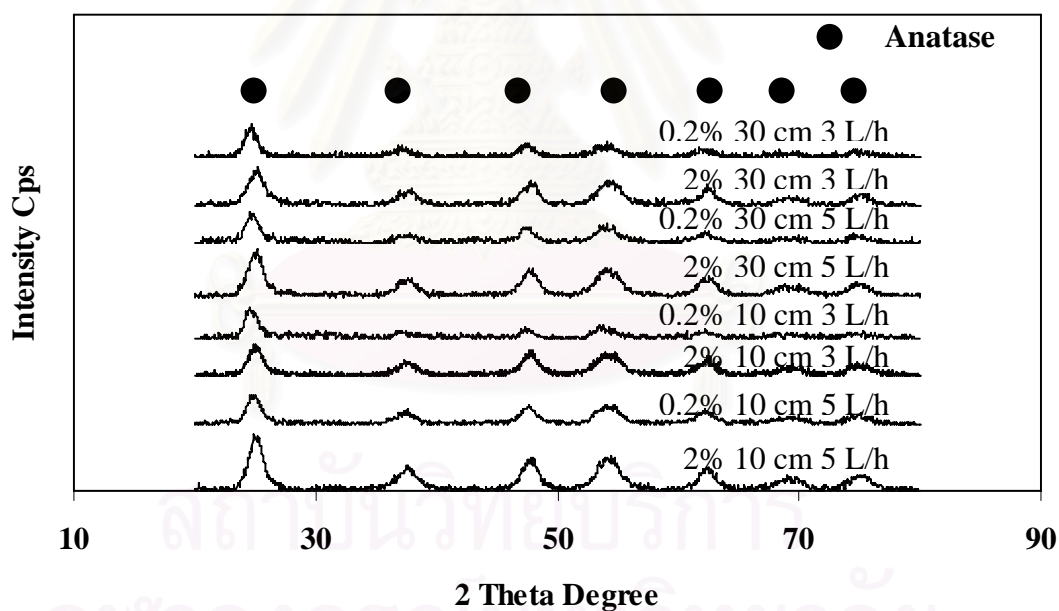


Figure 4.38 XRD patterns of TiO₂ hollow spheres using sodium dodecyl sulfate as a surfactant.

Table 4.6 Crystallite sizes of TiO₂ hollow spheres using sodium dodecyl sulfate as a surfactant, and determined from XRD pattern.

| Distance (cm) | Flow rate (L/h) | Conc (v/v) | Crystallite size (nm) |
|---------------|-----------------|------------|-----------------------|
| 10 | 3 | 0.2% | 7.5 |
| | | 2% | 6.4 |
| | 5 | 0.2% | 6.3 |
| | | 2% | 5.8 |
| 30 | 3 | 0.2% | 7.0 |
| | | 2% | 6.8 |
| | 5 | 0.2% | 6.6 |
| | | 2% | 5.8 |

4.6.2 Morphology of TiO₂ hollow spheres.

4.6.2.1 Scanning Electron Microscopy (SEM).

The morphologies of TiO₂ hollow spheres were observed with a scanning electron microscopy (SEM). Then the all samples were calcined at 500°C for one hour. Fig. 4.39, 4.40, 4.41, and 4.42 shows a SEM image of the particles produced using sodium dodecyl sulfate as the surfactant. It can be seen that almost all samples are nanometer spheres with diameters of 96-131 nm. The morphologies of particles were uniform, broken and round shape. The inset in Figure 4.41, and 4.42 shows a broken sphere.

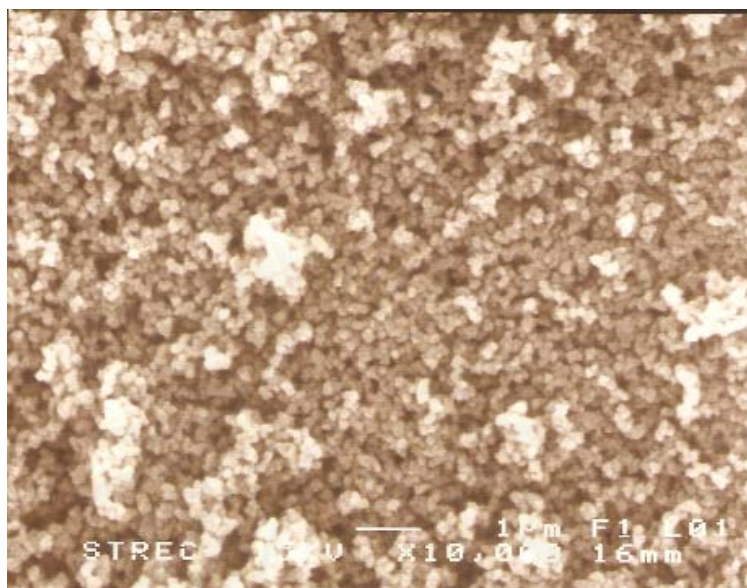


Figure 4.39 SEM image of TiO_2 hollow spheres using sodium dodecyl sulfate as the surfactant with 10000 magnifications.

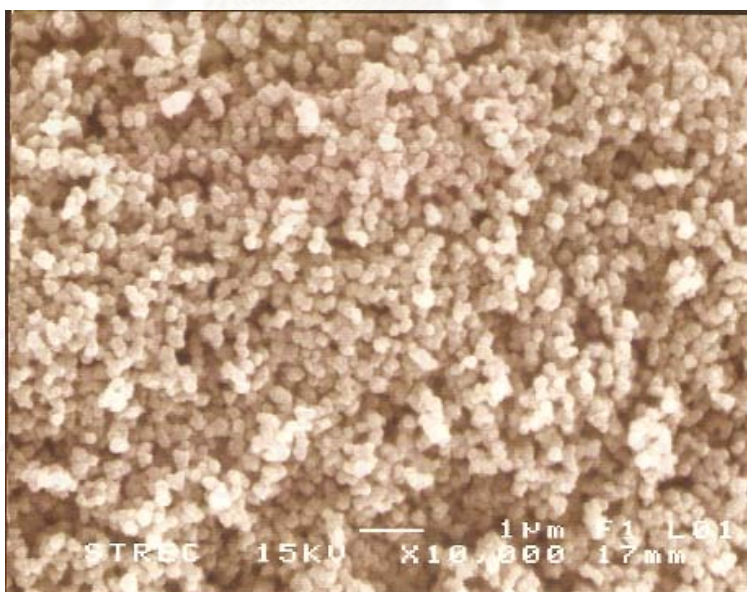


Figure 4.40 SEM image of TiO_2 hollow spheres using sodium dodecyl sulfate as the surfactant with 10000 magnifications.

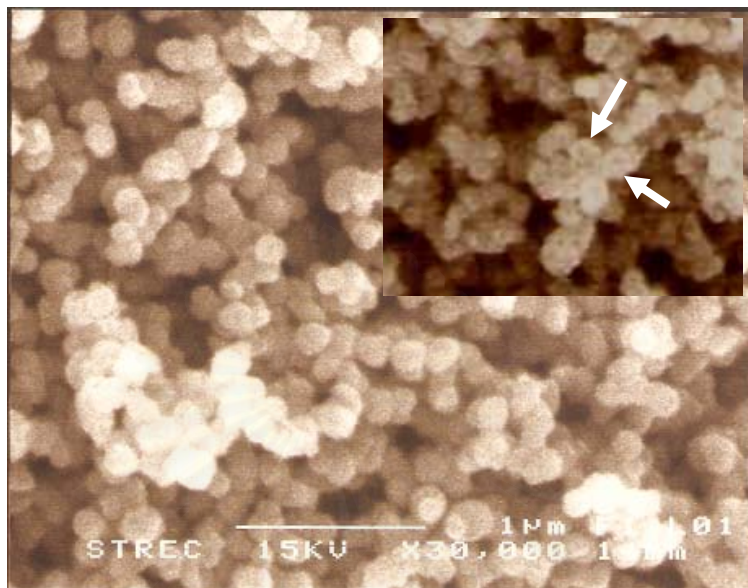


Figure 4.41 SEM image of TiO₂ hollow spheres using sodium dodecyl sulfate as the surfactant with 30000 magnifications.

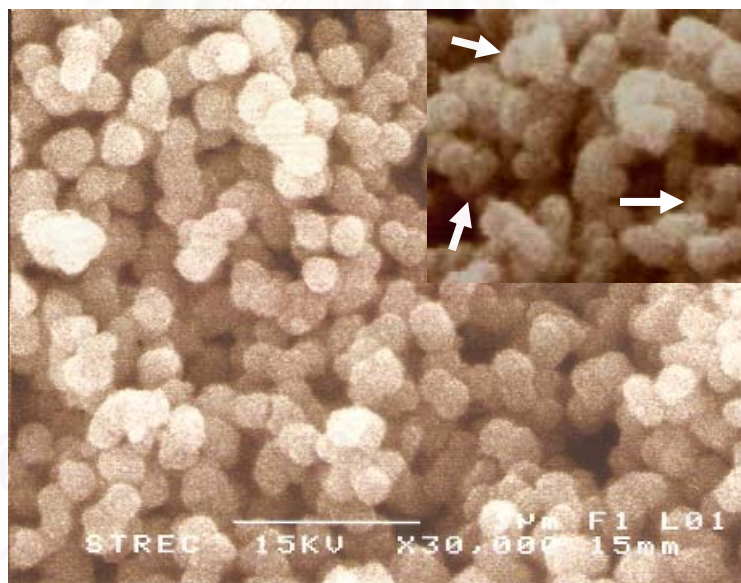


Figure 4.42 SEM image of TiO₂ hollow spheres using sodium dodecyl sulfate as the surfactant with 30000 magnifications.

4.6.2.2 Transmission Electron Microscopy (TEM).

The transmission electron microscopy (TEM) observations further display the morphology of TiO₂ hollow spheres. Then the all samples were calcined at 500°C for one hour. Fig. 4.43, 4.44, 4.45, and 4.46 show a TEM image of the particles produced using sodium dodecyl sulfate as the surfactant. Apparently, each spheres after calcination is composed of a large amount of very small particles. It can be seen that almost all samples are nanometer spheres with diameters of 96-131 nm.

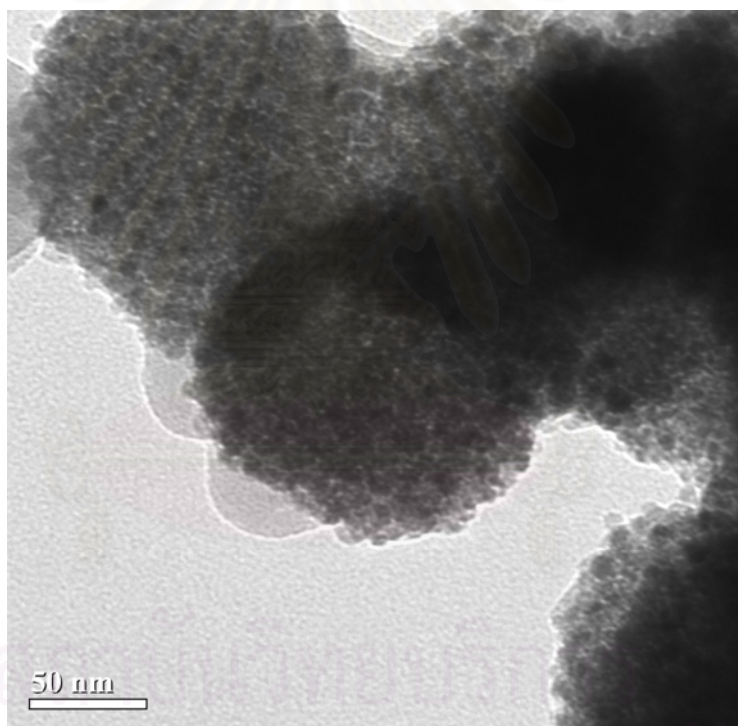


Figure 4.43 TEM image of TiO₂ hollow spheres using polyethylene glycol as the surfactant at scale bar 50 nm.

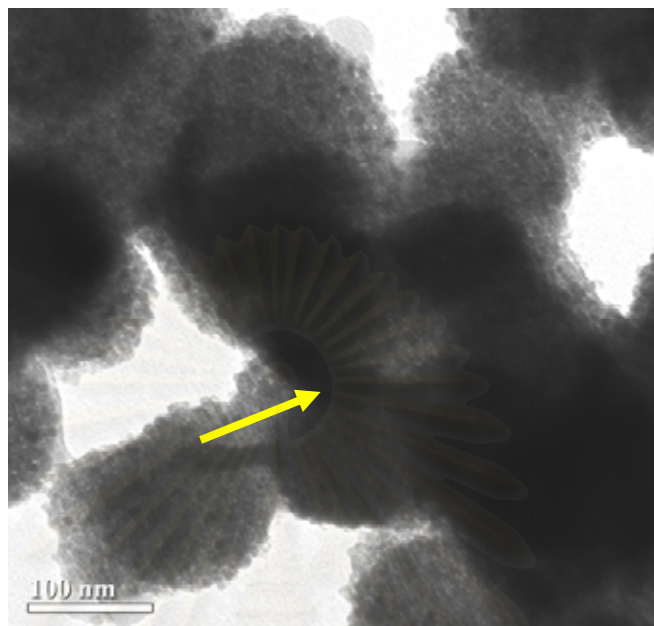


Figure 4.44 TEM image of TiO₂ hollow spheres using polyethylene glycol as the surfactant at scale bar 100 nm.

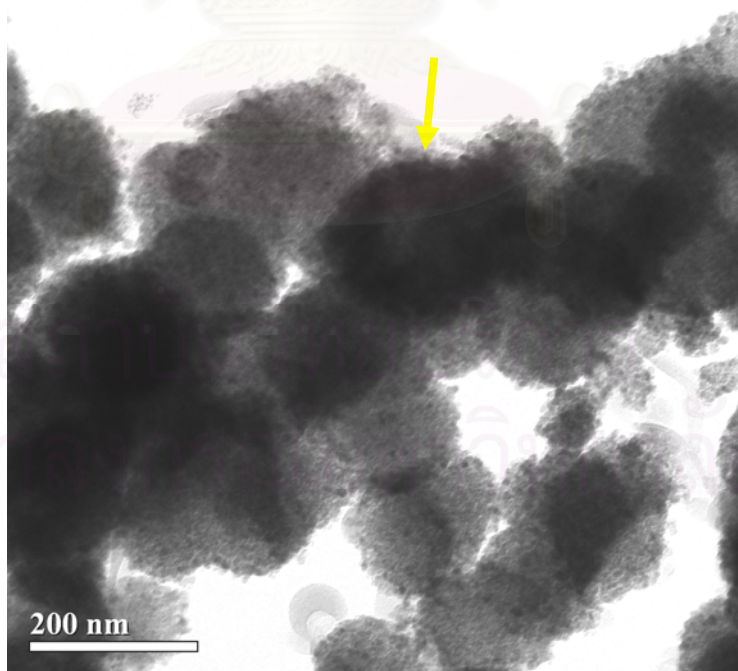


Figure 4.45 TEM image of TiO₂ hollow spheres using polyethylene glycol as the surfactant at scale bar 200 nm.

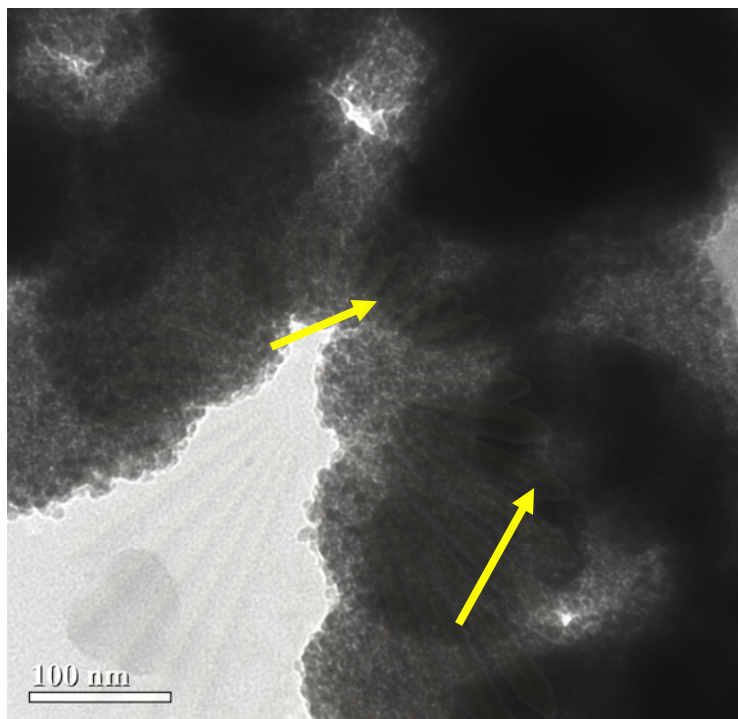


Figure 4.46 TEM image of TiO₂ hollow spheres using polyethylene glycol as the surfactant at scale bar 100 nm.

4.6.3 Average particles size of TiO₂ hollow spheres.

The general information of TiO₂ hollow spheres were determined from SEM and TEM image. By to consist of nozzle-solution distances, spraying flow rate of titanium sulfate solution, concentration of surfactant solution, average particles size, standard deviations (SD) and Z-score respectively. The results are listed in Table 4.7.

Table 4.7 Average particles size of TiO₂ hollow spheres using sodium dodecyl sulfate as a surfactant.

| Distance (cm) | Flow rate (L/h) | Conc (v/v) | Average Particle size (nm) | SD |
|---------------|-----------------|------------|----------------------------|-------|
| 10 | 3 | 0.2% | 131 | 15.03 |
| | | 2% | 125 | 14.56 |
| | 5 | 0.2% | 120 | 10.46 |
| | | 2% | 116 | 14.66 |
| 30 | 3 | 0.2% | 113 | 12.45 |
| | | 2% | 107 | 15.08 |
| | 5 | 0.2% | 108 | 11.84 |
| | | 2% | 96 | 16.56 |

4.6.4 Influence of spraying flow rate titanium sulfate solution.

The influence of spraying flow rate of titanium sulfate solution on the average particle sizes were showed in Figure 4.47, the concentrations of surfactant solution and the nozzle-solution distance were fixed at 0.2% and 2% (v/v) and at 10 cm respectively. The flow rates were varied at 3 and 5 L/h. The results found that the average particle sizes of resultant were decrease from 131 to 120 nm and 125 to 116 nm respectively. However, in Figure 4.48 when changed the nozzle-solution distance was at 30 cm and the concentrations of surfactant solution were fixed at 0.2% and 2% (v/v). The flow rates were varied at 3 and 5 L/h. The result found that the average particle sizes decrease from 113 to 108 nm and 107 to 96 nm respectively, with observed in the same way with the results in Figure 4.47. With the influence of spraying flow rate of titanium sulfate solution on the average particle sizes, the result found that the average particles size decrease 4-10 %.

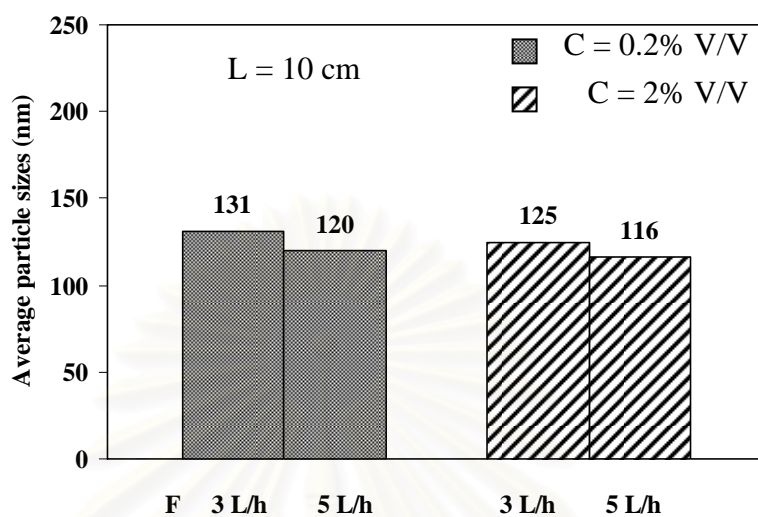


Figure 4.47 The average particle sizes of TiO_2 hollow spheres prepared by spraying titanium sulfate solution the flow rates were varied at F 3 and 5 L/h and fixed concentration C 0.2% and 2% (v/v) of nozzle-solution distance L 10 cm

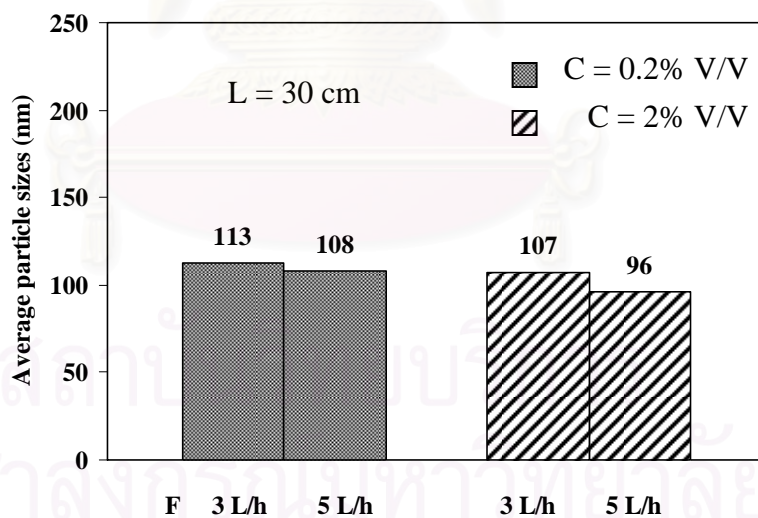


Figure 4.48 The average particle sizes of TiO_2 hollow spheres prepared by spraying titanium sulfate solution the flow rates were varied at F 3 and 5 L/h and fixed concentration C 0.2% and 2% (v/v) of nozzle-solution distance L 30 cm.

4.6.5 Influence of concentration of surfactant solution.

The influence of concentration of surfactant solution on the average particle sizes were showed in Figure 4.49, the flow rate and the nozzle-solution distance were fixed at 3 and 5 L/h and 10 cm respectively. The concentration of surfactant solution was varied 0.2% and 2% (v/v). The result found that the average particles size of resultant were decrease from 131 to 125 nm and 120 to 116 nm respectively. However, in Figure 4.50 when change the nozzle-solution distance was at 30 cm and the flow rates were fixed at 3 and 5 L/h. The concentrations of surfactant solution were varied 0.2% and 2% (v/v). The result found that the average particles size decrease from 113 to 107 nm and 108 to 96 nm respectively, with observed in the same way with the results in Figure 4.49. With the influence of concentration of surfactant solution on the average particle sizes, the result found that the average particles size decrease 3-11 %.

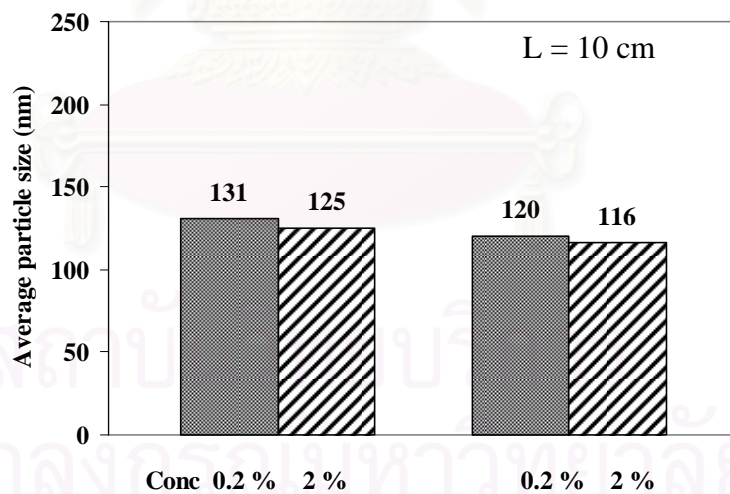


Figure 4.49 The averages particle sizes of TiO₂ hollow spheres by varied concentration C 0.2% and 2% (v/v) and fixed flow rate F 3 and 5 L/h of nozzle-solution distances L 10 cm

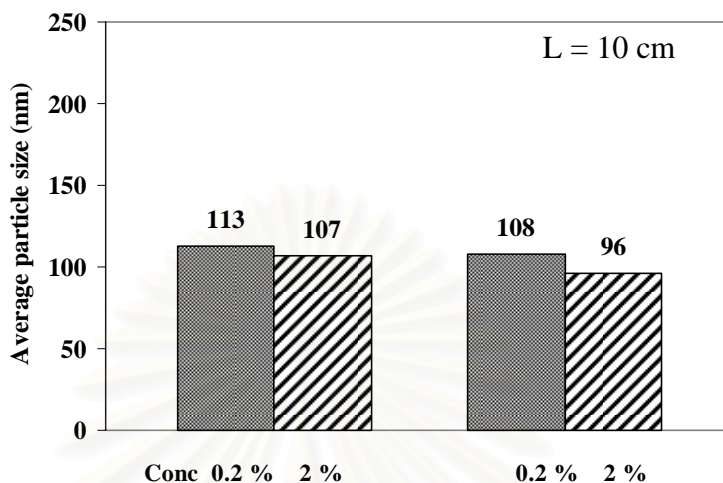


Figure 4.50 The averages particle sizes of TiO₂ hollow spheres by varied concentration C 0.2% and 2% (v/v) and fixed flow rate F 3 and 5 L/h of nozzle-solution distances L 30 cm.

4.6.6 Influence of distance from nozzle to liquid surfactant.

The influence of distance from nozzle to liquid surfactant on the average particle sizes were showed in Figure 4.51, the spraying flow rate of titanium sulfate solution and concentration of surfactant solution were fixed at 3 L/h and at 0.2% and 2% (v/v) respectively. The nozzle-solution distance was varied at 10 and 30 cm. The result found that the average particles sizes of resultant were decrease from 131 to 113 nm and 125 to 107 nm respectively. However, in Figure 4.52 when change the flow rate was at 5 L/h and concentrations of surfactant solution was fixed at 0.2% and 2% (v/v). The nozzle-solution distance was varied at 10 and 30 cm. The result found that the average particles size decrease 120 to 108 nm and 116 to 96 nm respectively, with observed in the same way with the results in Figure 4.51. With the influence of distance from nozzle to liquid surfactant on the average particle sizes, the result found that the average particles size decrease 10-17 %.

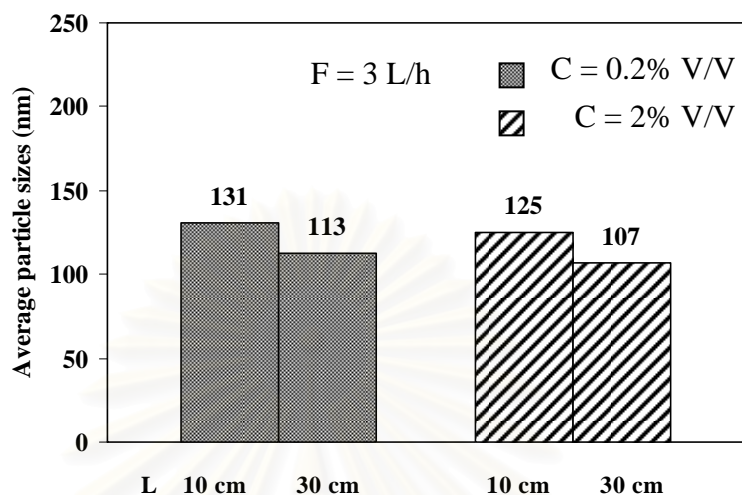


Figure 4.51 The averages particle sizes of TiO₂ hollow spheres by the nozzle-solution distances varied at L 10 and 30 cm and fixed concentration C 0.2% and 2% (v/v) and flow rate F 3 L/h

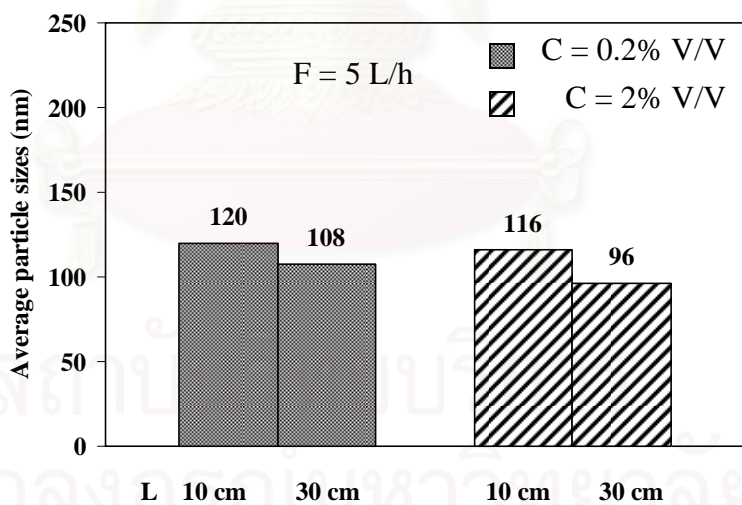


Figure 4.52 The averages particle sizes of TiO₂ hollow spheres by the nozzle-solution distances varied at L 10 and 30 cm and fixed concentration C 0.2% and 2% (v/v) and flow rate F 5 L/h.

4.7 The analysis from program Minitab.

By default, Minitab randomizes the run order of all design types. Randomization helps to ensure that the model meets certain statistical assumptions and can also help reduce the effects of factors not included in the study. The analysis information of 2^4 full factorial designs of experiments was studied. The results are listed in Table 4.8.

Table 4.8 The 2^4 full factorial designs of experiments

| 4 factors | High + | Low - |
|--|-----------------------|------------------------|
| 1. Type of surfactant | Anionic surfactant | Nonionic surfactant |
| 2. Concentration of surfactant solution | 2.0 %(V/V) | 0.2 %(V/V) |
| 3. Flow rate of titanium sulfate solution | 5 (L/hr) | 3 (L/hr) |
| 4. Distance from nozzle to liquid surfactant | 30 (cm) | 10 (cm) |

The full model, which includes the effects on the average particle sizes of TiO_2 hollow spheres were showed in Figure 4.53, and 4.54. The p-values (P) were used to Estimate Effects and Coefficients table to determine which effects are significant (see Appendix C).

Table 4.9 The 2⁴ full factorial designs of experiments on the average particle sizes of TiO₂ hollow spheres of two surfactants were sodium dodecyl sulfate and tween 20. By to consist type of surfactant, spraying flow rate of titanium sulfate solution, nozzle-solution distances, concentration of surfactant solution, average particles size, standard deviations (SD) and number particles respectively.

| Surfactant | Flow rate (L/h) | Distances (cm) | Concentration (V/V) | Average Particle size (nm) | SD | N |
|------------|-----------------|----------------|---------------------|----------------------------|-------|----|
| SDS | 3 | 10 | 0.2 | 131 | 15.03 | 67 |
| | 3 | 10 | 2 | 125 | 14.56 | 55 |
| | 3 | 30 | 0.2 | 113 | 12.45 | 82 |
| | 3 | 30 | 2 | 107 | 15.08 | 55 |
| | 5 | 10 | 0.2 | 120 | 10.46 | 58 |
| | 5 | 10 | 2 | 116 | 14.66 | 63 |
| | 5 | 30 | 0.2 | 108 | 11.84 | 65 |
| | 5 | 30 | 2 | 96 | 16.56 | 57 |
| Tween 20 | 3 | 10 | 0.2 | 151 | 14.33 | 54 |
| | 3 | 10 | 2 | 120 | 12.08 | 51 |
| | 3 | 30 | 0.2 | 133 | 12.19 | 53 |
| | 3 | 30 | 2 | 112 | 10.37 | 54 |
| | 5 | 10 | 0.2 | 138 | 13.45 | 65 |
| | 5 | 10 | 2 | 111 | 17.94 | 53 |
| | 5 | 30 | 0.2 | 118 | 13.36 | 63 |
| | 5 | 30 | 2 | 99 | 11.34 | 63 |

The information from table 4.9 show the response data, If can generate graphs to evaluate the effects. Use the results from graphs to see which factors are important on the average particle sizes of TiO₂ hollow spheres. The analysis information from program minitab of two surfactants were sodium dodecyl sulfate and tween 20 in the figure 4.53(see Appendix C). The p-values (P) was using $\alpha = 0.05$ which mean 95% significant effect to experiment design level or 2.571 of standardized effect, which for the main effects for order flow rate of titanium sulfate solution, concentration of surfactant solution, the distance from nozzle to liquid surfactant and type of surfactants, their p-

values are less than 0.05 or more than 95% significant effect to experiment design level and be the statistically significant effects. Moreover, term of AD had standardized effect more than 2.571 which showed a significant interaction effect of concentration of surfactant solution and type of surfactants in experiment design.

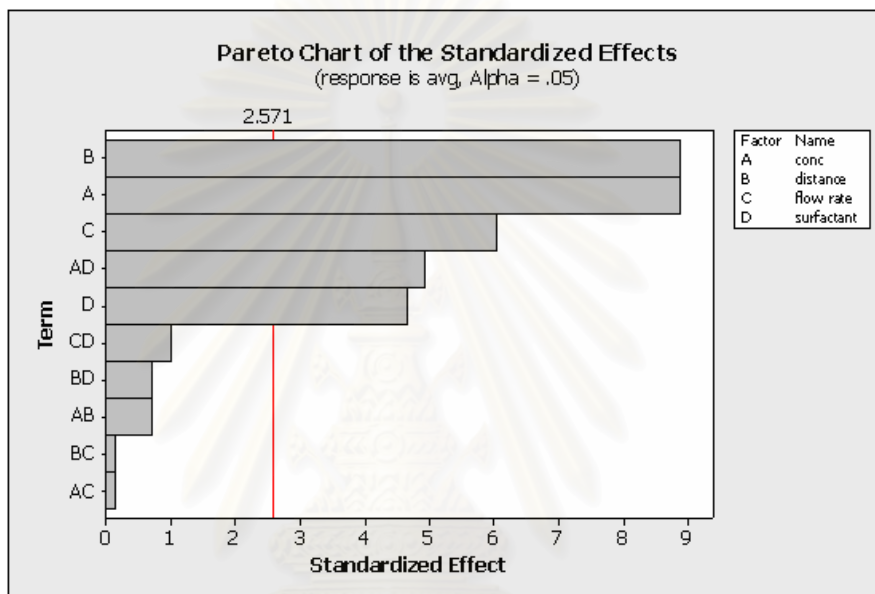


Figure 4.53 The effects on the average particle sizes of TiO₂ hollow spheres of two surfactants were sodium dodecyl sulfate and tween 20.

สถาบันวิทยบริการ
จุฬาลงกรณ์มหาวิทยาลัย

Table 4.10 The 2⁴ full factorial designs of experiments on the average particle sizes of TiO₂ hollow spheres of two surfactants were sodium dodecyl sulfate and polyethylene glycol. By to consist type of surfactant, spraying flow rate of titanium sulfate solution, nozzle-solution distances, concentration of surfactant solution, average particles size, standard deviations (SD) and number particles respectively.

| Surfactant | Flow rate (L/h) | Distances (cm) | Concentration (V/V) | Average Particle size (nm) | SD | N |
|------------|-----------------|----------------|---------------------|----------------------------|-------|----|
| SDS | 3 | 10 | 0.2 | 131 | 15.03 | 67 |
| | 3 | 10 | 2 | 125 | 14.56 | 55 |
| | 3 | 30 | 0.2 | 113 | 12.45 | 82 |
| | 3 | 30 | 2 | 107 | 15.08 | 55 |
| | 5 | 10 | 0.2 | 120 | 10.46 | 58 |
| | 5 | 10 | 2 | 116 | 14.66 | 63 |
| | 5 | 30 | 0.2 | 108 | 11.84 | 65 |
| | 5 | 30 | 2 | 96 | 16.56 | 57 |
| PEG | 3 | 10 | 0.2 | 177 | 36.97 | 55 |
| | 3 | 10 | 2 | 168 | 18.37 | 53 |
| | 3 | 30 | 0.2 | 139 | 21.37 | 51 |
| | 3 | 30 | 2 | 132 | 16.93 | 56 |
| | 5 | 10 | 0.2 | 156 | 21.16 | 62 |
| | 5 | 10 | 2 | 147 | 18.33 | 55 |
| | 5 | 30 | 0.2 | 126 | 20.06 | 56 |
| | 5 | 30 | 2 | 115 | 15.55 | 57 |

The information from table 4.10 show the response data, If can generate graphs to evaluate the effects. Use the results from graphs to see which factors are important on the average particle sizes of TiO₂ hollow spheres. The analysis information from program minitab of two surfactants were sodium dodecyl sulfate and polyethylene glycol in the Figure 4.54(see Appendix C). The p-values (P) was using $\alpha = 0.05$ which mean 95% significant effect to experiment design level or 2.571 of standardized effect, which for the main effects for order flow rate of titanium sulfate solution, concentration of surfactant solution, the distance from nozzle to liquid surfactant and type of surfactants, their p-

values are less than 0.05 or more than 95% significant effect to experiment design level and be the statistically significant effects. Moreover, term of BD and CD had standardized effect more than 2.571 which showed a significant interaction effect of distance from nozzle to liquid surfactant with type of surfactants and flow rate of titanium sulfate solution with type of surfactants in experiment design.

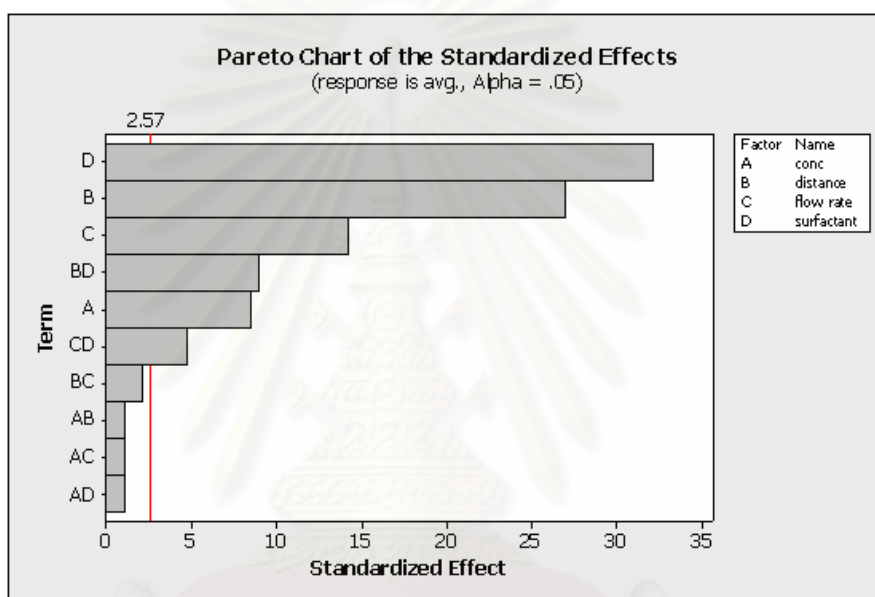


Figure 4.54 The effects on the average particle sizes of TiO₂ hollow spheres of two surfactants were sodium dodecyl sulfate and polyethylene glycol.

4.8 Influence of spraying flow rate titanium sulfate solution.

The influence of spraying flow rate of titanium sulfate solution on the average particle sizes. The result found that the average particle sizes of resultant were decreased, when the flow rate of titanium sulfate solution is increased from 3 L/h to 5 L/h. The result found that from number of size droplets increase. The laser diffraction was chosen as a size droplets of sprayed exist nozzle measurement technique.

4.9 Influence of concentration of surfactant solution.

The influence of concentration of surfactant solution on the average particle sizes. The average particle sizes of TiO₂ hollow spheres appears to be controlled by the concentration of surfactant solution, increasing concentration of surfactant solution with respect to the titania precursor results in the a larger number of smaller spheres. The result found that the average particle sizes of resultant were decreased, together with a concomitant increase in surfactant concentration. This result agrees with reported of T. Prozorov et al., 1998 and Elizabeth A. et al., 2005.

4.10 Influence of distance from nozzle to liquid surfactant.

The influence of distance from nozzle to liquid surfactant on the average particle sizes. It is expected that the average particle size can be controlled by adjusting the distance from the tip of the nozzle to the surface of surfactant solution. The average particle size at various nozzle-solution distances were showed in Fig. 4.21, 4.22, 4.36, 4.37, 4.51 and 4.52. The average particle sizes were systematically decreased, when the distance from the nozzle to the solution is increased from 10 cm to 30 cm. This tendency is in agreement with our expectation and demonstrates the possibility of controlling the particle size by setting the nozzle-solution distance.

4.11 Influence of types of surfactant.

The average particle sizes of TiO₂ hollow spheres were varied from different physical properties of anionic surfactant and nonionic surfactant, especially size and structure of surfactants that major effected by molecular weight. Therefore, nonionic surfactant which has the largest molecular weight of all surfactants gave the largest average particle sizes of TiO₂ hollow spheres also and the smallest molecular weight, anionic surfactant gave the smallest one also.

CHAPTER V

CONCLUSIONS AND RECOMMENDATIONS

5.1 Conclusion

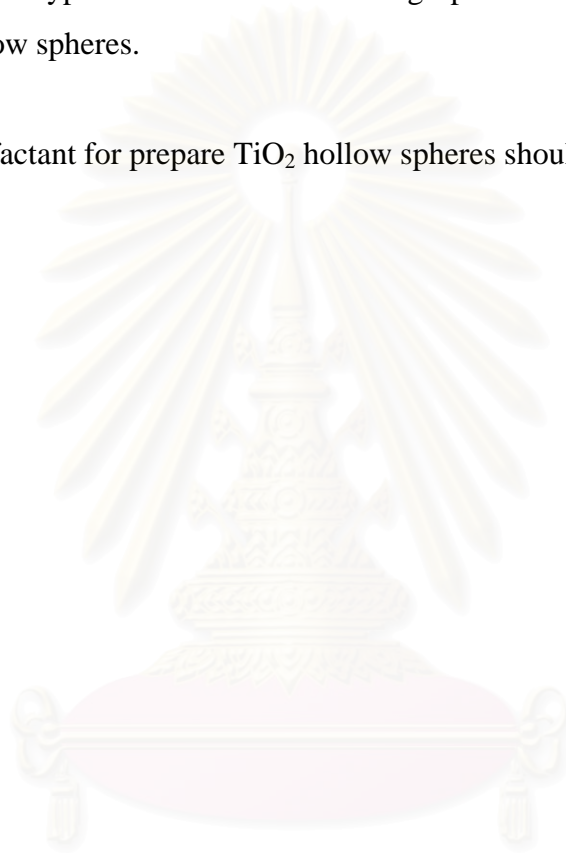
In this study, synthesis TiO₂ hollow spheres by spraying technique and the effects of spraying conditions and surfactant on physical properties of TiO₂ hollow spheres were investigated. The conclusions of the study are summarized as follows:

1. Anatase-TiO₂ hollow spheres were successfully synthesized by spraying technique.
2. The average particle size of TiO₂ hollow spheres decreased if the flow rate of titanium sulfate solution, concentration of surfactant and the distances from the nozzle to the surfactant solution were increased.
3. There were no influences of the flow rate of titanium sulfate solution, concentration of surfactant and distances from the nozzle to the surfactant solution on the crystal size of TiO₂ hollow spheres.
4. The average particle size of the synthesis TiO₂ hollow spheres was in the range of 100-170 nm.
5. The influence on the average particle sizes were flow rate, concentration, distances and surfactant type.

6.2 Recommendations for future research

From the previous conclusions, the following recommendations for the future study are propose.

1. Investigated type of nozzle on the average particle size and morphology of TiO_2 hollow spheres.
2. Other surfactant for prepare TiO_2 hollow spheres should be tried.



สถาบันวิทยบริการ
จุฬาลงกรณ์มหาวิทยาลัย

REFERENCES

- Aba, Priev., Samuel, Zalipsky., Rivka, Cohen., and Yechezkel, Barenholz. (2002). Determination of Critical Micelle Concentration of Lipopolymers and Other Amphiphiles. Comparison of Sound Velocity and Fluorescent Measurements 18: 612-617
- Arabatzis, I.M., Bernard, M.C., Falaras, P., Kontos, A.I., Kontos, A.G., Tsoukleris, D.S., and Petrakis, D.E. (2005). Efficient photocatalysts by hydrothermal treatment of TiO₂. Catalysis. Today 101: 275-281.
- Bahnmann, D.W., Choi, W., Hoffmann, M.R., and Martin, S.T. (1995). Environmental applications of semiconductor photocatalysis. Chem. Reviews 95: 69-96.
- Calza, P., Minero, C., and Pelizzetti, E. Photocatalytically assisted hydrolysis of chlorinated methanes under anaerobic conditions. Environmental Science and Technology 31: 2198-2203.
- Cao, J., Chang X., Liu, Jinsong, Ma., Wang, J., Xian, jia., and Zheng, M. (2006). Preparation of oxide hollow spheres by colloidal carbon spheres Preparation of oxide hollow spheres by colloidal carbon spheres. Materials Letters 60: 2991–2993.
- Dodge, Y. (2003). The Oxford Dictionary of Statistical Terms, OUP, ISBN 0-19-920613-9.
- G.H. Li., T. Xiea., Y.X. Zhang., and Y.C., Wu. (2005). Sol–gel synthesis of titania hollow spheres. Materials Research Bulletin, 40: 1993–1999.

- Han, G., and Nam, W. Characterization and photocatalytic performance of nanosize TiO₂ powders prepared by the solvothermal method. Korean Journal of Chemical Engineering 20: 1149-1153.
- Hong, B.Y., Su, C., and Tseng, C.M. (2004). Sol-gel preparation and photocatalysis of titanium dioxide. Catalysis. Today, 96: 119-126.
- Iwamoto, H., Konishi, Y., Nagamine, S., and Sugioka, A. (2007). Formation of TiO₂ hollow microparticles by spraying water droplets into an organic solution of titanium tetraisopropoxide (TTIP) — Effects of TTIP concentration and TTIP-protecting additives. Powder Technology.
- John, Bibby. (1974). An axiomatic approach to averages is provided Axiomatisations of the average and a further generalization of monotonic sequences. Glasgow Mathematical Journal vol. 15: pp: 63–65.
- Konishi, Y., Nagamine, S., and Sugioka, A. (2007). Preparation of TiO₂ hollow microparticles by spraying water droplets into an organic solution of titanium tetraisopropoxide. Materials Letters 61 4: 44–447.
- Linsebigler, A.L., Lu, G., and Yates, Jr. J. T. (1995). Photocatalysis on TiO₂ surfaces: principles, mechanism, and selected results. Chem. Reviews, 95: 735-758.
- Mills, A., and Wang, J. Photomineralisation of 4-chlorophenol sensitized by TiO₂ thin films. Zeitschrift fur Physikalische Chemie 213: 49-58.
- Pearson, K. (1894). On the dissection of asymmetrical frequency curves. Phil. Trans. Roy. Soc. London 185 7: 19–810.

Ren, Tie-Zhen., Yuan, Zhong-Yong., and Su, Bao-Lian. (2003). Surfactant-assisted preparation of hollow microspheres of mesoporous TiO₂. Chemical Physics Letters 374: 170–175.

Richard J, Larsen., and Morris, L. Marx: An Introduction to Mathematical Statistics and Its Applications, Third Edition, p.: 282.

Symon, Keith. (1971). Mechanics, Third Edition, Addison-Wesley.

Wang, G., and Yua, J. (2008). Hydrothermal synthesis and photocatalytic activity of mesoporous titania hollow microspheres. Journal of Physics and Chemistry of Solids.

Wang, Y., Yang, Z., and Zhou, A. (2008) Preparation of hollow TiO₂ microspheres by the reverse microemulsions. Materials Letters 62: 1930–1932.

Y, ling Cao Y., Li, Z., Ding, J., Liu, Jun-song., Chi, Yuan-bin., and zheng, zhu. (2007) Synthesis and photonic band calculations of NCP face-centered cubic photonic crystals of TiO₂ hollow spheres. Journal of Colloid and Interface Science, 306: 133–136



APPENDICES

สถาบันวิทยบริการ
จุฬาลงกรณ์มหาวิทยาลัย

APPENDIX A

CALCULATION OF THE CRYSTALLITE SIZE

Calculation of the crystallite size by Debye-Scherrer equation

The crystallite size was calculated from the width at half-height of the diffraction peak of XRD pattern using the Debye-Scherrer equation.

From Scherrer equation:

$$D = \frac{K\lambda}{\beta \cos \theta} \quad (\text{A.1})$$

- where
- D = Crystallite size, Å
 - K = Crystallite-shape factor = 0.9
 - λ = X-ray wavelength, 1.5418 Å for CuK α
 - θ = Observed peak angle, degree
 - β = X-ray diffraction broadening, radian

The X-ray diffraction broadening (β) is the pure width of a powder diffraction, free of all broadening due to the experimental equipment. Standard α -alumina is used to observe the instrumental broadening since its crystallite size is larger than 2000 Å. The X-ray diffraction broadening (β) can be obtained by using Warren's formula.

From Warren's formula:

$$\beta^2 = B_M^2 - B_S^2 \quad (\text{A.2})$$
$$\beta = \sqrt{B_M^2 - B_S^2}$$

- Where
- B_M = The measured peak width in radians at half peak height.
 - B_S = The corresponding width of a standard material.

Example: Calculation of the crystallite size of titania

$$\begin{aligned} \text{The half-height width of 101 diffraction peak} &= 0.93125^\circ \\ &= 0.01625 \text{ radian} \end{aligned}$$

$$\text{The corresponding half-height width of peak of } \alpha\text{-alumina} = 0.004 \text{ radian}$$

$$\begin{aligned} \text{The pure width} &= \sqrt{B_M^2 - B_S^2} \\ &= \sqrt{0.01625^2 - 0.004^2} \\ &= 0.01577 \text{ radian} \end{aligned}$$

$$\beta = 0.01577 \text{ radian}$$

$$2\theta = 25.56^\circ$$

$$\theta = 12.78^\circ$$

$$\lambda = 1.5418 \text{ \AA}$$

$$\begin{aligned} \text{The crystallite size} &= \frac{0.9 \times 1.5418}{0.01577 \cos 12.78} = 90.15 \text{ \AA} \\ &= 9 \text{ nm} \end{aligned}$$

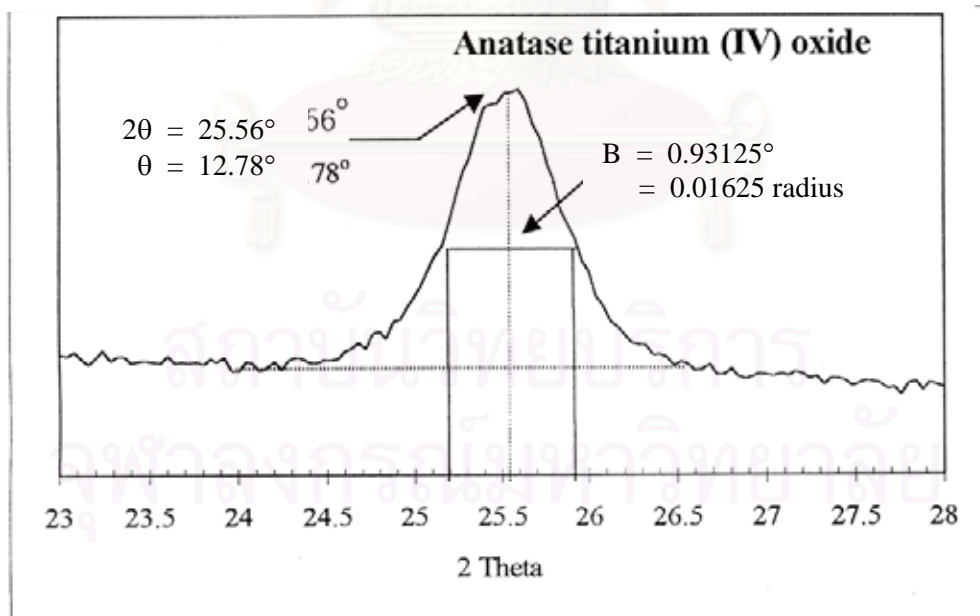


Figure A.1 The 101 diffraction peak of titania for calculation of the crystallite size

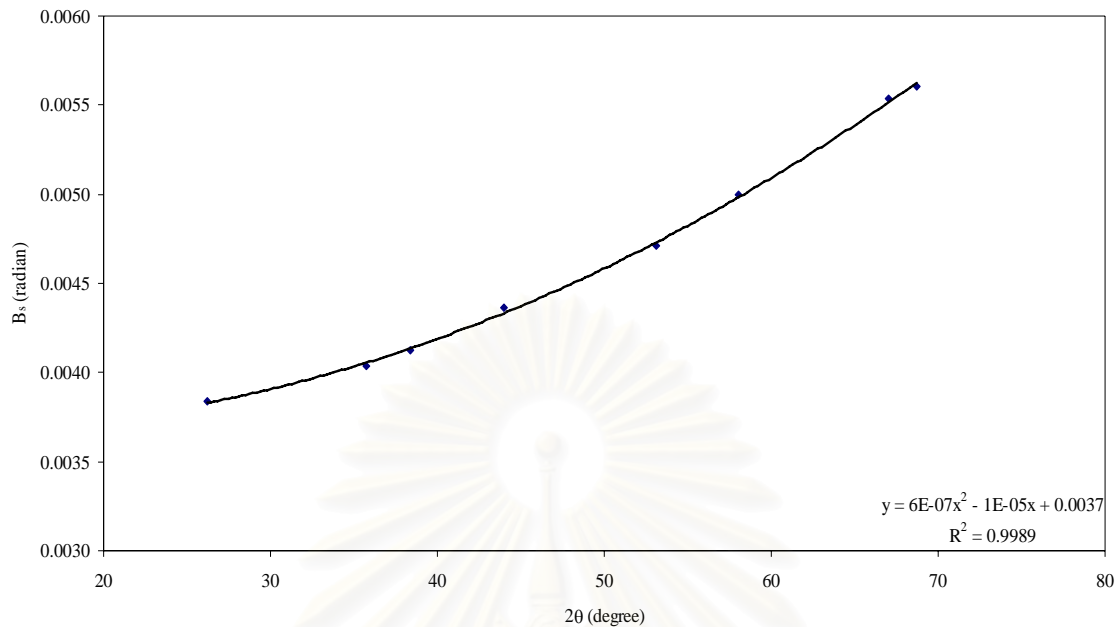


Figure A.2 The plot indicating the value of line broadening due to the equipment. The data were obtained by using α -alumina as standard.

สถาบันวิทยบริการ
จุฬาลงกรณ์มหาวิทยาลัย

APPENDIX B

PARTICLE SIZES DISTRIBUTION AND CALCULATION OF SEM AND TEM RESULTS

Particle sizes distribution of titanium dioxide

The particle sizes distribution of titanium dioxide nanoparticles are show in Table B1 of TiO₂ hollow spheres

Table B1 Particle sizes distribution of titanium dioxide

| No | Particle sizes (nm) |
|----|---------------------|
| 1 | 124 |
| 2 | 109 |
| 3 | 133 |
| 4 | 156 |
| 5 | 139 |
| 6 | 124 |
| 7 | 148 |
| 8 | 127 |
| 9 | 154 |
| 10 | 138 |
| 11 | 167 |
| 12 | 139 |
| 13 | 157 |
| 14 | 132 |
| 15 | 163 |
| 16 | 149 |
| 17 | 179 |
| 18 | 125 |
| 19 | 147 |
| 20 | 126 |
| 21 | 160 |
| 22 | 131 |
| 23 | 136 |
| 24 | 127 |
| 25 | 154 |

Table B1 Particle sizes distribution of titanium dioxide (Cont.)

| No | Particle sizes (nm) |
|----|---------------------|
| 26 | 156 |
| 27 | 115 |
| 28 | 170 |
| 29 | 159 |
| 30 | 132 |
| 31 | 138 |
| 32 | 148 |
| 33 | 134 |
| 34 | 176 |
| 35 | 178 |
| 36 | 120 |
| 37 | 125 |
| 38 | 145 |
| 39 | 136 |
| 40 | 162 |
| 41 | 158 |
| 42 | 147 |
| 43 | 132 |
| 44 | 153 |
| 45 | 149 |
| 46 | 137 |
| 47 | 142 |
| 48 | 138 |
| 49 | 114 |
| 50 | 136 |
| 51 | 133 |
| 52 | 150 |
| 53 | 117 |
| 54 | 194 |
| 55 | 164 |
| 56 | 168 |
| 57 | 146 |

Average particle size = 147 nm

Standard deviation = 18.33 nm

Calculation of SEM and TEM results

Average particle size

The average particle size was calculated from the equation:

$$\bar{d} = \frac{\sum_{i=1}^n d_i}{n} \quad (\text{B1})$$

Where d_i = the diameter of each particles (nm)
 n = the number of appeared in the SEM and TEM images

Standard deviation

The standard deviation of particle size was calculated from the equation:

$$s.d. = \sqrt{\frac{1}{n-1} \sum_{i=1}^n (d_i - \bar{d})^2} \quad (\text{B2})$$

Where d_i = the diameter of each particles (nm)
 \bar{d} = the average particle sizes (nm)
 n = the number of appeared in the SEM and TEM images

สถาบันวิทยบริการ
 จุฬาลงกรณ์มหาวิทยาลัย

APPENDIX C

CALCULATION OF THE AVERAGE PARTICLE SIZES

Calculation of the average particle sizes by program minitab

The analysis information from program minitab of two surfactants were tween 20 and sodium dodecyl sulfate.

Full Factorial Design

Factors: 4 Base Designs: 4, 16
Runs: 16 Replicates: 1
Blocks: 1 Center pts (total): 0

All terms are free from aliasing.

Factorial Fit: average particle sizes versus concentration, distance, flow rate, surfactant

Estimated Effects and Coefficients for average particle sizes (coded units)

| Term | Effect | Coef | SE Coef | T | P |
|-----------------|---------|---------|---------|--------|-------|
| Constant | | 118.625 | 0.7437 | 159.50 | 0.000 |
| Conc | -15.750 | -7.875 | 0.7437 | -10.59 | 0.000 |
| distance | -15.750 | -7.875 | 0.7437 | -10.59 | 0.000 |
| flow rate | -10.750 | -5.375 | 0.7437 | -7.23 | 0.000 |
| surfactant | -8.250 | -4.125 | 0.7437 | -5.55 | 0.000 |
| conc*surfactant | 8.750 | 4.375 | 0.7437 | 5.88 | 0.000 |

S = 2.97489 R-Sq = 97.16% R-Sq(adj) = 95.74%

Analysis of Variance for average particle sizes (coded units)

| Source | DF | Seq SS | Adj SS | Adj MS | F | P |
|--------------|----|---------|---------|---------|-------|-------|
| Main Effects | 4 | 2719.00 | 2719.00 | 679.750 | 76.81 | 0.000 |

| | | | | | | |
|--------------------|----|---------|--------|---------|-------|-------|
| 2-Way Interactions | 1 | 306.25 | 306.25 | 306.250 | 34.60 | 0.000 |
| Residual Error | 10 | 88.50 | 88.50 | 8.850 | | |
| Total | 15 | 3113.75 | | | | |

The analysis information from program minitab of two surfactants were sodium dodecyl sulfate and polyethylene glycol.

Full Factorial Design

| | | |
|------------|---------------------|-------|
| Factors: 4 | Base Designs: | 4, 16 |
| Runs: 16 | Replicates: | 1 |
| Blocks: 1 | Center pts (total): | 0 |

All terms are free from aliasing.

Factorial Fit: average particle sizes versus concentration, distance, flow rate, surfactant

Estimated Effects and Coefficients for average particle sizes (coded units)

| Term | Effect | Coef | SE Coef | T | P |
|----------------------|--------|--------|---------|--------|-------|
| Constant | | 129.75 | 0.5652 | 229.57 | 0.000 |
| conc | -8.00 | -4.00 | 0.5652 | -7.08 | 0.000 |
| distance | -25.50 | -12.75 | 0.5652 | -22.56 | 0.000 |
| flow rate | -13.50 | -6.75 | 0.5652 | -11.94 | 0.000 |
| surfactant | 30.50 | 15.25 | 0.5652 | 26.98 | 0.000 |
| distance*surfactant | -8.50 | -4.25 | 0.5652 | -7.52 | 0.000 |
| flow rate*surfactant | -4.50 | -2.25 | 0.5652 | -3.98 | 0.003 |

S = 2.26078 R-Sq = 99.40% R-Sq(adj) = 99.01%

Analysis of Variance for average particle sizes (coded units)

| Source | DF | Seq SS | Adj SS | Adj MS | F | P |
|--------------------|----|---------|---------|---------|--------|-------|
| Main Effects | 4 | 7307.00 | 7307.00 | 1826.75 | 357.41 | 0.000 |
| 2-Way Interactions | 2 | 370.00 | 370.00 | 185.00 | 36.20 | 0.000 |

| | | | | |
|----------------|----|---------|-------|------|
| Residual Error | 9 | 46.00 | 46.00 | 5.11 |
| Total | 15 | 7723.00 | | |

The analysis information from program minitab of two surfactants were tween 20 and polyethylene glycol.

Full Factorial Design

| | |
|------------|-----------------------|
| Factors: 4 | Base Designs: 4, 16 |
| Runs: 16 | Replicates: 1 |
| Blocks: 1 | Center pts (total): 0 |

All terms are free from aliasing.

Factorial Fit: average particle sizes versus concentration, distance, flow rate, surfactant

Estimated Effects and Coefficients for average particle sizes (coded units)

| Term | Effect | Coef | SE Coef | T | P |
|---------------------|--------|--------|---------|--------|-------|
| Constant | | 133.88 | 0.8427 | 158.87 | 0.000 |
| conc | -16.75 | -8.38 | 0.8427 | -9.94 | 0.000 |
| distance | -24.25 | -12.12 | 0.8427 | -14.39 | 0.000 |
| flow rate | -15.25 | -7.63 | 0.8427 | -9.05 | 0.000 |
| surfactant | 22.25 | 11.12 | 0.8427 | 13.20 | 0.000 |
| conc*surfactant | 7.75 | 3.87 | 0.8427 | 4.60 | 0.001 |
| distance*surfactant | -9.75 | -4.88 | 0.8427 | -5.79 | 0.000 |

S = 3.37062 R-Sq = 98.56% R-Sq(adj) = 97.60%

Analysis of Variance for average particle sizes (coded units)

| Source | DF | Seq SS | Adj SS | Adj MS | F | P |
|--------------------|----|--------|--------|---------|--------|-------|
| Main Effects | 4 | 6385.0 | 6385.0 | 1596.25 | 140.50 | 0.000 |
| 2-Way Interactions | 2 | 620.5 | 620.5 | 310.25 | 27.31 | 0.000 |
| Residual Error | 9 | 102.2 | 102.2 | 11.36 | | |
| Total | 15 | 7107.7 | | | | |

LIST OF PUBLICATIONS

Eakasit Namkaeo and Akawat Sirisuk. Synthesis and characterization of TiO₂ hollow spheres using spraying technique, 2nd SUT Graduate Conference, Suranaree University of Technology, Nakhon Ratchasima, Thailand, January 21-22, 2009.



สถาบันวิทยบริการ
จุฬาลงกรณ์มหาวิทยาลัย

VITA

Mr. Eakasit Namkaeo was born on October 26 1984, in Lopburi, Thailand. He received the Bachelor Degree of Chemical Engineering from Faculty of Engineering, Burapha University, in 2007. He continued his Master's study at Chulalongkorn University in June, 2007.



สถาบันวิทยบริการ
จุฬาลงกรณ์มหาวิทยาลัย